CHALMERS

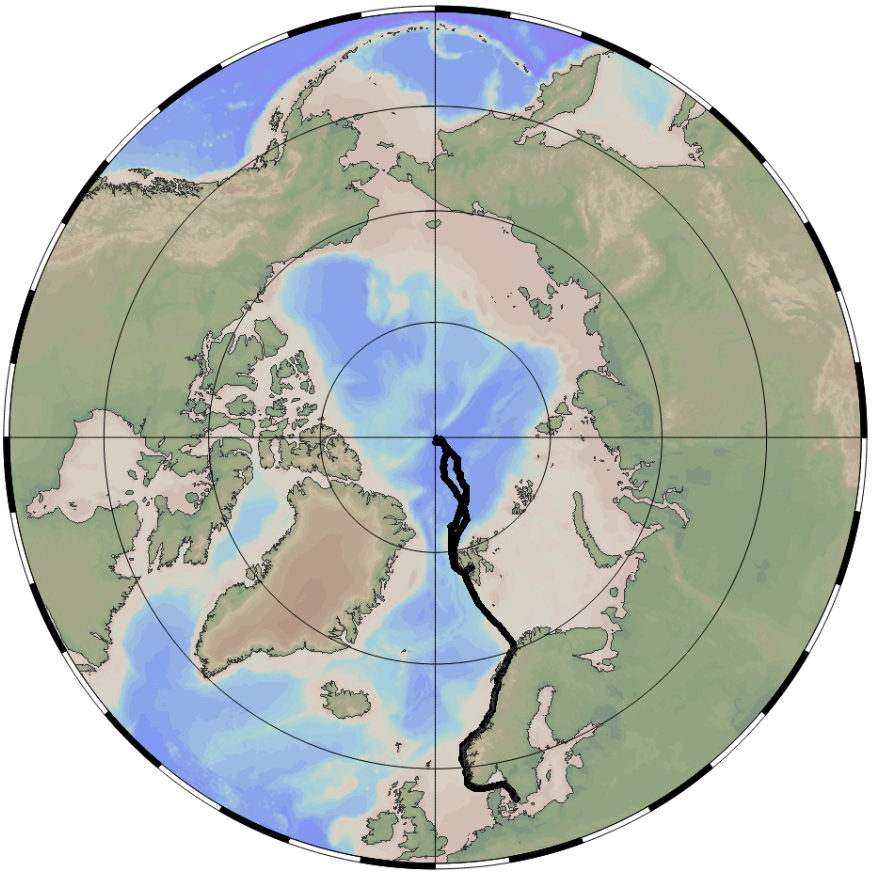

Evaluation of airborne mercury

Measurements taken during the expedition Arctic Ocean 2018 and at the transit from Svalbard to Helsingborg

Master's thesis in Environmental Inorganic Chemistry

JOSEFIN GUNNARSSON
LISA GUSTAFSSON

Department of Chemistry and Chemical Engineering
CHALMERS UNIVERSITY OF TECHNOLOGY
Göteborg, Sweden 2019

MASTER'S THESIS IN ENVIRONMENTAL INORGANIC CHEMISTRY

Evaluation of airborne mercury

Measurements taken during the expedition Arctic Ocean 2018 and at the transit from Svalbard to Helsingborg

JOSEFIN GUNNARSSON
LISA GUSTAFSSON

Department of Chemistry and Chemical Engineering
Division of Environmental Inorganic Chemistry
CHALMERS UNIVERSITY OF TECHNOLOGY

Göteborg, Sweden 2019

Evaluation of airborne mercury
Measurements taken during the expedition Arctic Ocean 2018 and at the transit from Svalbard to Helsingborg
JOSEFIN GUNNARSSON
LISA GUSTAFSSON

Department of Chemistry and Chemical Engineering
Division of Environmental Inorganic Chemistry
Chalmers University of Technology
SE-412 96 Göteborg
Sweden
Telephone: +46 (0)31-772 1000

Cover:
Map over the gaseous elemental mercury sampling route in the North Pole and the transit south from Svalbard to the west coast of Sweden.

Chalmers Reproservice
Göteborg, Sweden 2019

Evaluation of airborne mercury
Measurements taken during the expedition Arctic Ocean 2018 and at the transit from Svalbard to Helsingborg
Master's thesis in Environmental Inorganic Chemistry
JOSEFIN GUNNARSSON
LISA GUSTAFSSON
Department of Chemistry and Chemical Engineering
Division of Environmental Inorganic Chemistry
Chalmers University of Technology

Abstract

Mercury is a toxic pollutant that can cause severe effects such as mercury poisoning when it bio-accumulate and biomagnify in the food chain. It is released from natural and anthropogenic activities and from re-emission of past deposited mercury. The main form emitted to the atmosphere is gaseous elemental mercury (GEM), which is subjected to long range transport and thus travels all over the world and reach remote areas such as the Arctics. During the summer of 2018, the Swedish icebreaker *Oden* was used as a platform for sampling GEM in the arctic environment (expedition *Arctic Ocean 2018*) and during the transit south from Svalbard to west coast of Sweden. The instrument Tekran 2537A was used for measuring GEM concentrations in ambient air. The GEM data were evaluated in regard to meteorological parameters, oxidants (BrO), and trajectories were conducted for tracing air masses backward in time to find potential mercury sources. A contamination mask was constructed for minimising the risk of evaluating measurements that possibly could have been influenced by contamination.

The overall average concentration of GEM was found to be 1.412 ± 0.38 ng/m^3. The highest observed GEM concentrations were found over continuous ice and reached a maximum level of 3.86 ng/m^3. A half atmospheric mercury depletion event (AMDE) was also found over continuous ice, where the GEM concentration dropped to 0.57 ng/m^3. Elevated and depleted concentrations of GEM were found to correlate with high solar radiation and changes in air pressure. The majority of the observed elevated GEM concentrations found in the Arctic region were suggested to not be directly linked to anthropogenic activities, but rather originate from re-emission of earlier deposited mercury at Arctic surfaces. However, observed elevated GEM concentrations further south were more likely related to anthropogenic activities. The observed depleted concentrations of GEM were proposed to be caused by the introduction of new air masses containing already depleted GEM levels.

Keywords: Mercury, gaseous elemental mercury, long range transport, Arctic region, west coast of Norway and Sweden, mapping of GEM levels, depletion, geographical regions, meteorological parameters

Acknowledgements

We would like to thank Katarina Gårdfeldt at the Swedish Polar Research Secretariat for making this master thesis possible by generating measurements and introducing us to our supervisor Sofi Jonsson at Stockholm's University. Sofi has provided invaluable support, guidance and contributed with valuable input and competence. Special thanks should be given to the researches Paul Zieger, Linn Karlsson, Julia Schmale and Ian Brooks for contributing with data and valuable expertise. Further, we would also like to express a thank to Lars Lehnert, technical specialist at *IB Oden*, for contributing with data. Our grateful thanks are also extended to Mark Cohen at NOAA for his helpfulness and enthusiasm. Finally, we would like to thank our examiner Ulf Jäglid at Chalmers University of Technology for valuable inputs and for his engagement in the project.

Josefin Gunnarsson and Lisa Gustafsson 2019-05-21

Nomenclature

Abbreviations

Hg	Mercury
GEM	Gaseous Elemental Mercury
GOM	Gaseous Oxidised Mercury
HgP	Particulate Mercury
RGM	Reactive Gaseous Mercury
TGM	Total Gaseous Mercury
THg	Total Mercury
THg*	Total Mercury except for GEM
THg**	Total Mercury except for Me2Hg
MeHg	Methylmercury
Me2Hg	Dimethylmercury
BC	Black Carbon
AMDE	Atmospheric Mercury Depletion Event
PBL	Planetary Boundary Layer
IB	Ice Breaker
ODV	Ocean Data View
HYSPLIT	Hybrid Single-Particle Lagrangian Integrated Trajectory
MIZ	Marginal Ice Zone
GMA	Global Mercury Assessment
NOAA	National Oceanic and Atmospheric Administration
AMAP	Arctic Monitoring and Assessment Programme
ASGM	Artisanal Small scale Gold Mining

Contribution Report

In this master's thesis literature review, data sorting, evaluation and discussion of measurements were performed by both authors. The master thesis was characterised by a close team work, where the introduction was written by both authors. The writing of theory part was divided between the authors. Lisa was in charge of writing the sections: Properties of mercury, The Minamata Convention, The global mercury cycle, The air-ocean interaction and the software tools. Josefin was in charge of writing the sections: The Arctic environment, The Arctic mercury cycle, Climate change affecting the mercury cycling in the Arctics and mercury sampling - Tekran 2537A. The methodology was written by Josefin with input from Lisa. Both authors provided critical feedback on the parts written by the other author. The result and discussion, conclusion and future research were written jointly by the two authors.

Contents

1 Introduction

Mercury is a toxic pollutant that exists naturally at small quantities in Earth's crust.[1] Mercury can be released to the atmosphere through natural and anthropogenic activities or re-emitted from past natural and anthropogenic activities. Anthropogenic activities accounts for 30 % of the total mercury emissions, 10 % of the total emissions originate from natural activities and the remaining 60 % is re-emissions of past deposited mercury.[2]

Natural releases of mercury to the atmosphere arise from weathering of rocks, geothermal activities, and volcanic eruptions. There are several anthropogenic activities that release mercury to the atmosphere, for instance metal and cement production, coal and wood combustion, artisanal small-scale gold mining (ASGM), oil refining and the chlor-alkali process. Mercury used in consumer products such as lamps, batteries and dental fillings, result in emissions to air, mainly from the disposal. Re-emissions of mercury to the atmosphere arise from mercury that has previously been deposited onto soils, waters and vegetation.[3]

The three major forms of mercury in the atmosphere are gaseous elementary mercury (GEM or Hg^0), gaseous oxidised mercury (GOM or Hg^{2+}) and particulate mercury (HgP). GEM is the most abundant form of mercury in the atmosphere and it has a residence time of 0.5 to 1 year, and it is subjected to long range transport. GOM and HgP have a shorter residence time in the atmosphere and therefore deposits rapidly, often close to the emission source.[4]

When GOM and HgP are deposited into aquatic and terrestrial ecosystems it can be methylated by bacteria and algae into organic forms of mercury such as methylmercury ($MeHg$) and dimethylmercury (Me_2Hg). Methylated mercury bio-accumulate and biomagnify through the food chain, reaching dangerous concentrations that can cause severe effects for humans relying on upper trophic level species as their main food source. Through history, catastrophic events of mercury poisoning have occurred, for instance in the Japanese city of Minamata. The city of Minamata suffered from mercury poising for several decades. An industry producing acetaldehyde released mercury contaminated industrial freshwater into the bay of Minamata. Mercury accumulated in fish, which resulted in devastating consequences for the local people relying on seafood from the bay. People died or came to suffered from different kind of disabilities.[5] Public health disasters like the one in Minamata have resulted in the establishment of *The Minamata Convention*. The Convention is a global agreement for limiting anthropogenic mercury releases, with the purpose of protecting humans and the environment from the toxic properties of mercury. It was agreed on in January 2013 and entered into force in August 2017.[6]

As a consequence of GEM being subjected to long-range transport, enhanced levels of mercury are found all over the world, even at remote areas such as the Arctics, far away from anthropogenic activities. Within the Arctic region the mercury cycling is complex with several unique processes and phenomenons. One unique phenomenon is called atmospheric mercury depletion event (AMDE). It takes place mainly during spring when enhanced levels of halogens are released from the sea salt to the atmosphere. A photochemical reaction produces halogen radicals, which has shown to be able to oxidise GEM into GOM. Further, bromine oxide (BrO) has shown to be another potential oxidising agent of GEM. These oxidations results in reduced levels of GEM in the atmosphere during springtime and the mechanisms is thought to be one of the reasons behind the high levels of methylmercury found in Arctic marine mammals.[7]

Other unique features affecting the Arctic mercury cycle are also related to seasonality. Seasonality contributes to variations in sea ice coverage, solar radiation, air temperature and fresh water input to the ocean from riverine. Climate change is predicted to affect the seasonality in the Arctic environment with increased temperature and increased fresh water input to the ocean, while the sea ice coverage is decreasing.[7]

Understanding the mercury cycling in the Arctic region is a critical part of mapping the global mercury cycling and the biomagnification of mercury in the food chain, therefore it is important to perform Arctic mercury research. During the summer of 2018, *IB Oden* travelled from Helsingborg in Sweden to Svalbard for conducting a research expedition, *Arctic Ocean 2018*, at the North Pole (see figure 1.1). At the expedition and during the transit south from Svalbard to Helsingborg, continuous measurement of airborne mercury (GEM) was conducted.

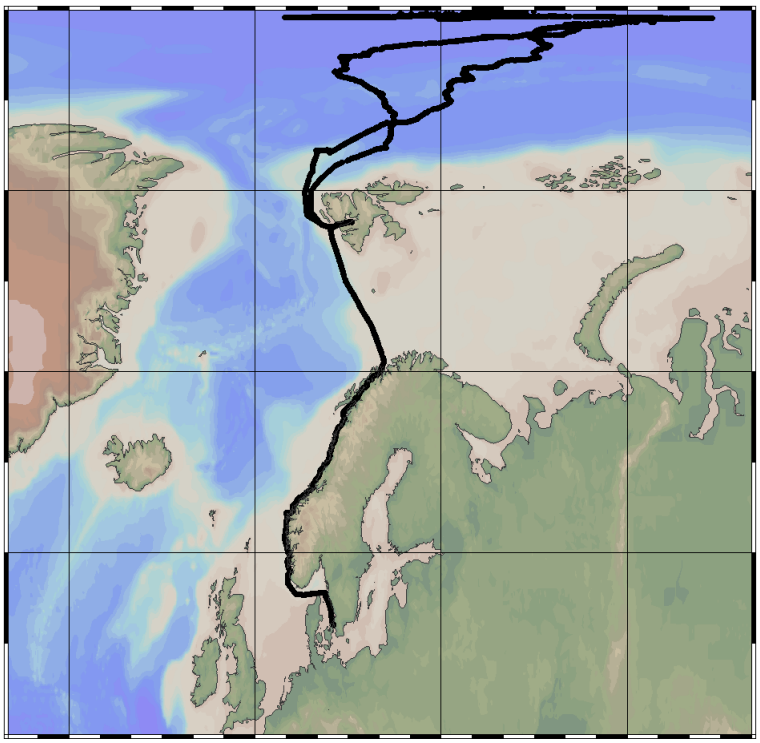

Figure 1.1: *Travel and sampling route during the expedition Arctic Ocean 2018 and during the transit south from Svalbard to Helsingborg*

1.1 Aim

The aim with this master thesis is to evaluate concentrations of airborne mercury (GEM) during the expedition *Arctic Ocean 2018* and the transit south from Svalbard to the west coast of Sweden. Identified concentrations clearly deviating from background concentration, will be further analysed with respect to meteorological parameters (air pressure, relative humidity, visibility, air temperature and solar radiation), anthropogenic point sources, the presence of oxidants such as bromine oxide and ice concentrations. Backward trajectories of air masses will be generated in the purpose of finding potential explanations for the identified elevated and depleted GEM concentrations. Furthermore, the GEM measurements taken in the Arctic region will be evaluated in order to identify trends through time and possible effects of climate change.

1.2 Research hypotheses

The GEM measurements in relation to the factors mentioned in the aim will be analysed by testing the hypotheses described below. We predict that:

- Similar meteorological conditions will be present when elevated GEM concentrations will be observed.
- If anthropogenic sources have an impact on the measured GEM concentrations, then elevated concentrations of GEM will be identified when air masses originates from areas with high mercury releasing anthropogenic activities.
- Periods with high atmospheric concentrations of oxidants will result in decreased concentrations of GEM in the atmosphere.
- Areas with continuous ice limits the exchange of mercury between the ocean and the atmosphere, result in lower concentrations of GEM in the atmosphere compared to areas with the open sea.

- Changes in the environment caused by climate change will affect the Arctic mercury cycle by increasing the interactions between the ocean and the atmosphere.

1.3 Limitations

This master thesis is limited to evaluate ship-based measurements of mercury concentrations obtained during the expedition *Arctic Ocean 2018* and the transit south from Svalbard to the west cost of Sweden.

The instrument *Tekran 2537A* used during the sampling generates measurements of total gaseous mercury (TGM), which is the sum of both GEM and GOM.[8][9] However, GEM makes up 90-99% of the total atmospheric mercury and thus the measured concentrations are assumed to be GEM.[4] No other forms of mercury in the atmosphere, such as HgP and Hg^{2+}, are studied in the project since filters are installed in the instrument.[8] Therefore, this master thesis is limited to study gaseous elementary mercury, GEM. Additionally, no measurements of mercury concentrations in water, ice and snow were taken during the sampling route.

When back tracing the origin of the mercury emissions only anthropogenic activities that result in emissions to air is considered. The backward trajectories were limited to be performed at three different levels above sea ($0.3, 0.5$ and $0.7 \cdot PBL$) and to trace 5 and 28 days back in time.

2 Theory

In this chapter, background information necessary for understanding and analysing measurements of GEM is introduced. The chapter begins with general information about mercury and its toxicity. Secondly, information about *The Minamata Convention* is presented. Thirdly, the cycling of mercury on a global scale is explained. Thereafter, information about the Arctic environment and the cycling of mercury within it are presented. The chapter ends with information about the mercury sampling and the software tools used for conducting the evaluation.

2.1 Properties of mercury

Mercury can exist in a number of different forms, where each form has its own chemical, physical and ecotoxicological properties. The specific properties are of central importance for how the specific species of mercury will behave in the environment. The main types of mercury known to exist in the environment are elemental mercury (Hg^0), divalent mercury (Hg^{2+}), monomethylmercury ($MeHg$) and dimethylmercury (Me_2Hg).[10]

Elemental mercury is stable due to its low reactivity in the atmosphere, it has low solubility in water and high vapour pressure. In the atmosphere, elemental mercury is often referred to as gaseous elemental mercury (GEM). GEM is the main form of mercury emitted to the atmosphere, from both natural and anthropogenic activities.[11] With an atmospheric residence time of 0.5 to 1 year, GEM is subjected to homogeneous mixing within the hemispheres and long range transport. GEM is the predominant form of mercury in the atmosphere, making up 90-99 % of the total atmospheric mercury (TGM).[4] Background concentration of GEM within the Northern Hemisphere ranges between 1.5-1.7 ng/m^3. GEM can be converted to gaseous oxidised mercury (GOM) through a sequence of oxidation reactions.[3]

Oxidised forms of mercury such as divalent mercury are more water soluble than GEM and have a high affinity to both organic and inorganic ligands. In the atmosphere, oxidised mercury is often referred to as gaseous oxidised mercury (GOM), or when adsorbed to particles, particle-bound mercury (HgP). GOM and HgP deposits fast onto soils, waters and plants and often close to the emission source.[12] When mercury has been deposited, either as GEM or as any of its oxidised forms, it can either be transported further in the environment or be re-volatilised into the atmosphere again.[3]

When mercury ends up in oceans, lakes and terrestrial ecosystems it can be methylated in to the organic form, $MeHg$, by microbial metabolism performed by algae or bacteria.[12] Me_2Hg is another organic form of mercury and both the organic forms are toxic. $MeHg$ can bio-accumulate in organisms and is subjected to biomagnification in the food chain, whether this is true also for Me_2Hg is still unknown.[10] $MeHg$ makes up only a minor fraction of the total amount of mercury present in the environment.[3]

The amount of mercury that is present in the environment depends on several different sources. Mercury is a naturally occurring element found in Earth's crust and it is released to the environment both through natural and anthropogenic activities. A mixture of historical anthropogenic releases and historical natural inputs together with current anthropogenic and natural releases hold the responsibility for the today present mercury concentrations in different environmental compartments.[3] Natural processes like volcanic eruptions, weathering of rocks and forest fires release mercury to the environment. Moreover, anthropogenic processes like burning of fossil fuels especially coal, cement production, metal smelting, the chlor-alkali process, waste handling of mercury-containing products, cremation of bodies containing dental amalgam, mining and artisanal small-scale gold mining (ASGM), also result in mercury emissions to the environment. In 2013, *The Global Mercury Assessment (GMA) 2018* estimated that anthropogenic activities over the last decade have increased anthropogenic mercury levels by 300-500 %, and during the same period a doubling of mercury was observed in surface water.[3] The limited knowledge regarding historical anthropogenic emissions together with a limited understanding of the oceanographic processes makes it difficult to assess how the oceans will respond to changes in anthropogenic mercury emissions in the future.[3]

Different models for estimating the concentration of mercury in both terrestrial and aquatic systems diverge widely in their concluded estimates. Major risks associated with mercury contamination originate from the

marine food web and therefore a lot of work is put into understanding how anthropogenic emissions of mercury affect the oceans.[10] Understanding global emissions and how they travel around the globe is of critical importance in order to develop strategies and introduce policies to reduce the global impact of mercury.[7]

2.1.1 Toxicity of mercury

All the different forms of mercury are in fact toxic, and could cause severe health effects. The degree of toxicity and the effects they can cause varies between the different chemical structures, the dose and the rate of exposure. Mercury is binding to the sulfhydryl and selenohydryl groups of proteins alternating their tertiary and quaternary structure, poisoning cellular functions.[13] Mercury poisoning cause severe effects to the brain but it can also effect the nervous-, immune- and digestive systems, as well as cause severe effects on lungs, eyes, kidneys and skin. Severe poisoning can result in death.[14]

Exposure to inorganic forms of mercury (GEM) usually occurs through inhalation of mercury vapour, either as a result of humans occupation or due to outgassing of mercury from dental amalgam.[13] While exposure to organic forms of mercury mostly take place through dietary intake of primarily fish.[7] When mercury vapour enters the body it can easily bond to sulfur-containing aminoacids because of its high affinity to sulfhydryl groups. It passes easily through the blood barrier and in to the placenta. Elemental mercury deposits readily in the brain and other organs. However, a part of the elemental mercury that is entering the blood stream is oxidised.[13] Oxidised forms of mercury are often found bound to form salts like mercuric chloride ($HgCl_2$). These mercury complexes adhere to sulfhydryl groups in the bloodstream in a similar manner as elemental mercury but they can not efficiently cross the blood-brain barrier. Mercury salts mainly damage the kidney and the gut lining.[13]

Methylation of GOM into organic forms of mercury ($MeHg$ and Me_2Hg) can be performed both in abiotic and biotic conditions. Biotic formation takes place mainly in the aquatic ecosystems and it is thought to be the primary process generating organic mercury.[12] The organic forms are believed to be the most toxic forms of mercury existing in the environment. However, Me_2Hg is not found at high concentrations in the environment and thus $MeHg$ is seen as the major threat. $MeHg$ bio-accumulates and biomagnifies in the food chain.[12] Studies estimate that during the last 150 years, a ten-fold increase of mercury concentrations in the bodies of marine animals higher up in the food chain has taken place.[3] When $MeHg$ is entering the blood stream it adheres to sulfhydryl groups, especially to those found in cyestein and deposit throughout the body. Concentration of $MeHg$ is eventually occurring in the brain, kidneys, liver, placenta and fetus.[13]

The fact that different forms of mercury target and affects different organs in the body results in difficulties in diagnosing mercury poisoning.[13] Public health disasters have through history taken place due to the toxic properties of mercury. In Minamata, Japan, between 1932 and 1968, a factory producing acetaldehyde discharged large amounts of mercury containing waste into the river of Minamata, which resulted in contamination of a large amount of fish. Eventually, the contamination caused a local disaster in the community with more than 50 000 people affected by symptoms of mercury poisoning and at least 2000 cases of the so-called Minamata disease.[14] Similar events of mercury poisoning have also taken place in Iraq, Pakistan and Guatemala.[15]

2.2 The Minamata Convention

The toxic properties of mercury and the disasters described in the section above have resulted in a global treaty, called *The Minamata Convention*, was agreed on in January 2013. The convention addresses a wide range of mercury related activities, among them, bans on new mercury mines, phase out and phase down (gradually reduce) mercury containing products and processes, control measures on emissions of mercury to air, water and land and new regulations regarding informal ASGM. Further, waste handling issues, contaminated sites and health issues related to mercury are addressed in the convention.[5]

The purpose of the convention is, according to *The United Nations for Environment*, "to protect human health and the environment from the adverse effects of mercury". *The Minamata Convention* helps countries to adapt to better and safer alternatives that already exists by tracing the life cycle of mercury. With the goal of reducing health-related and environmental risk for humans, animals and communities around the world.[6]

On the 18th of May 2017, the *European Union* and seven of its Member States, ratified the convention, making the parties that had ratified exceeding the minimum limit of 50 nations. 90 days later, on the 16th of August 2017, the convention entered into force. The convention is thought to have concrete impact relatively fast. Already by 2020, all countries that have ratified the agreement shall have phased out mercury containing products and phased down (gradually reduce) the use of dental amalgam. Over time the convention will hopefully result in an overall reduction of anthropogenic mercury emissions to the environment.[6]

2.3 The global mercury cycle

The circulation and transformation of different forms of mercury in the environment can be described in a serie of reactions taking place to govern the distribution among the different environmental compartments. Mercury is, as described above in section 2.1, emitted to the different environmental compartments from a number of sources: natural, anthropogenic and re-emission of earlier deposited concentrations.[10] In the atmosphere mercury can, depending on its form, either deposit relatively close to the emission source (GOM) or be subjected to long range transport (GEM). An illustration of the flows of mercury taking place in the environment has been complied based on several studies, [16], [3], [17], [12], [18], [7] and [10], see figure 2.1.

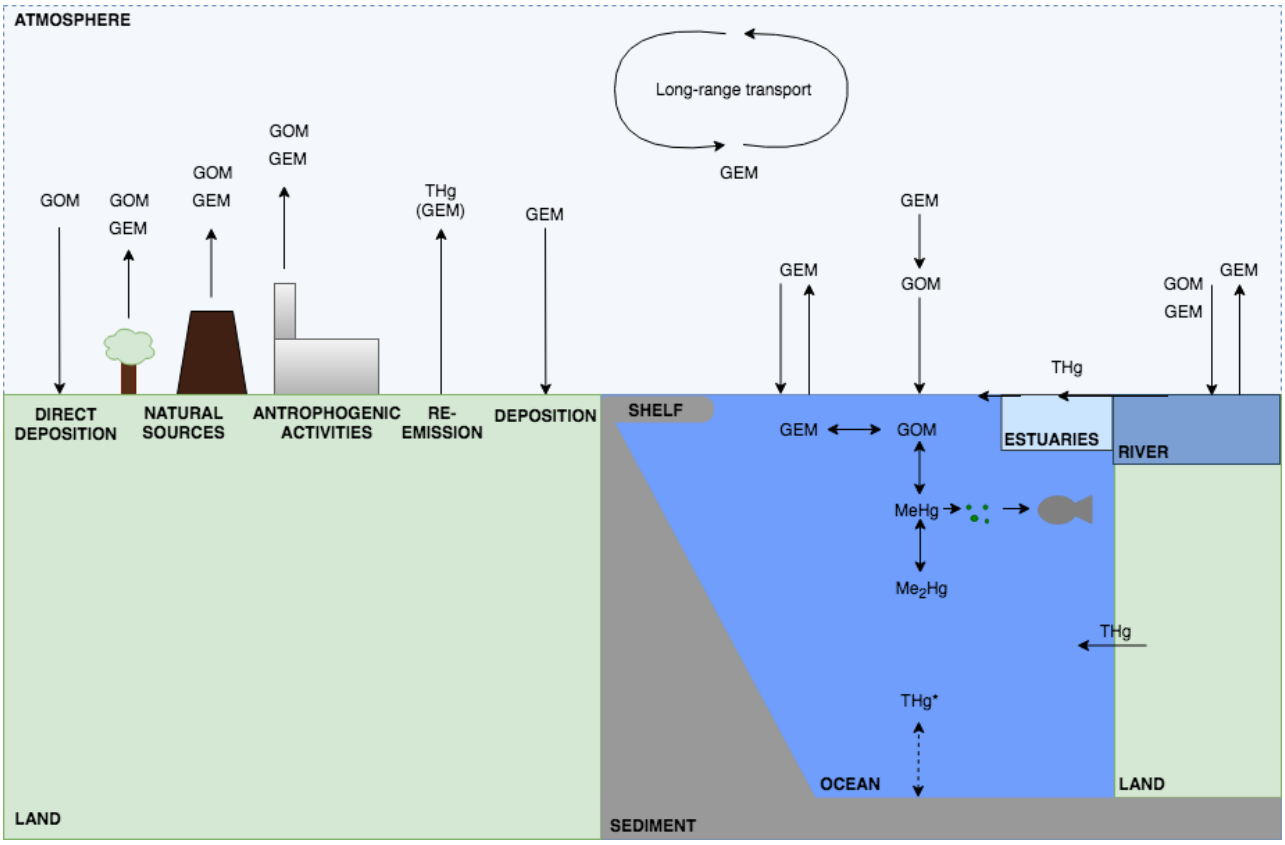

Figure 2.1: *Mercury cycling in the global environment. The boxes specifies the different compartments in the environment. Arrows illustrate flows of mercury between different sources and compartments. GEM is referring to gaseous elemental mercury, GOM to gaseous oxidised mercury including particulate mercury, $MeHg$ and Me_2Hg to mono- and dimetylmercury and THg is used at the flows where all of the mercury forms are known to be present. $THg*$ represents all forms of mercury except GEM.*

Air-ocean modelling shows that global oceans have not yet reached an equilibrium with the today present mercury levels in the atmosphere. Thus, concentrations of mercury in oceans are predicted to keep increasing for decades, or even centuries, even if there is no further increase in mercury emissions to the atmosphere.[7] GEM can be transported around the world but is eventually deposited into soils, oceans and terrestrial ecosystems.

Mercury can be removed from the atmosphere by wet or dry deposition. Wet deposition is the dominant process taking place. Dry deposition is the process of GEM being removed from the atmosphere into oceans or terrestrial ecosystems in the absence of precipitation, while wet deposition is defined as the air to surface flux taking place in snow, rain, fog or ice.[16] Wet deposition is mainly taking place with GOM and HgP. GOM and HgP are generally either deposited into terrestrial and aquatic ecosystems close to the emission source, or deposited into oceans as a consequence of GEM being oxidised to GOM.

Deposited mercury can either be re-emitted to the atmosphere, transported into the ocean or lake sediments and deposited onto surface soils. Within the aquatic and terrestrial ecosystems, mercury can be transformed into organic forms and eventually undergo bio-accumulation and biomagnification.[3] Methylation of inorganic forms of mercury mainly takes place in lakes, rivers, wetlands and oceans.[17] Re-emission of mercury takes place mainly as GEM due to its volatile character. GEM can be re-emitted into the atmosphere either following direct deposition or when GOM undergoes photochemical reduction back to GEM. Mercury is eventually removed from the global cycle by being deposited into the deep ocean. Deep ocean sediments are making up the main sink for mercury.[12]

Most of the mercury released to the atmosphere is inorganic mercury, but organic mercury is also released into the air. The total annual mercury emissions to the atmosphere were in 2013 estimated to be somewhere between 5500 tonnes to 8900 tonnes.[12] The *GME 2018* estimate that around 10 % of the total mercury emissions to air originate from natural processes like volcanic eruptions. 60 % of the emissions to air is due to environmental processes that involve re-cycling of earlier deposited anthropogenic mercury and 30% originates from today active anthropogenic emissions. As mentioned in section 2.1, there are several different anthropogenic activities that result in mercury emissions. Among them stationary combustion of coal and ASGM, these are according to the *GMA 2018* responsible for 60 % of the anthropogenic emissions to air.[3]

As for emissions to air, mercury emissions to water and terrestrial ecosystems originate from several different sources. In the terrestrial ecosystems, the main mercury reservoir is the soil. The distribution and concentration of mercury in the soil are thought to depend on several factors such as: soil organic matter, precipitation, latitude, vegetation index, and leaf area index. Mercury is entering oceans and lakes from the terrestrial ecosystem as a result of coastal erosion. Mercury is transported with rivers from land to oceans and is stored in continental shelves and estuaries. Mercury levels in the oceans are considered to be substantial and have a large effect on the air-ocean exchange.[18] Divalent mercury that ends up in the soils and waters can further be methylated into $MeHg$ or even Me_2Hg by methylating bacteria. Organic forms of mercury can bioaccumulate in algae and eventually biomagnify in the food chain.[7]

High levels of mercury have been observed at remote areas, such as the polar region, even though there are few natural and anthropogenic activities that releases mercury at these latitudes. Long range transport of GEM emitted at low or mid-latitudes brings mercury with air masses to the pristine environments at the poles.[10]

2.4 The Arctic environment

A large amount of mercury enters the Arctic environment and a majority of the flow is a result of released mercury in the Northern Hemisphere. In this section, the special features of the Arctic environment are described, followed by information about the Arctic climate and weather.

2.4.1 The Arctic ecosystem

The Arctic region entails the *Arctic Ocean*, which is mainly covered by 2-3 meters thick frozen seawater, and the nearby land area surrounding the ocean. The nearby land area includes the northern landmasses of Alaska, Canada, Norway, Russia, Greenland and Spitsbergen. Parts of the Arctic land area are covered by ice meanwhile others have lush tundra.[7][19]

The inputs of GEM to the Arctic environment are caused by long range transport of GEM and emissions of GEM from the oceanic surface. The cycling within the region is controlled by mercury processes, such as photochemical and methylation processes. The mercury processes are not unique for the Arctic environment and studies have shown that they occur at other locations as well. However, the Arctic region has several

unique features that contributes to an increase transformation of GEM to other more toxic forms of mercury.[7] One of the unique features with the Arctic region is the large variations in seasonality. During the winter, the solar radiation decreases and the North Pole faces total darkness for some weeks. While reverse condition, total sunlight, is present during the summer. The number of days of total darkness/light decreases with decreasing latitude. Based on the seasonality in the Arctic region, no photochemical reactions take place when the Arctic region undergoes total darkness resulting in that the mercury cycling undergoes exceptional seasonality.[7]

Another unique feature with the Arctic region is the change in ice cover. The sea ice acts as a barrier and limits the exchange of mercury, heat and gases between the atmosphere and the ocean. During springtime, the sea ice starts to melt which contributes to an increased exchange of elements and energy between the atmosphere and the ocean. Halogens (Cl, Br, I) are elements that exist in sea salt and during springtime, they are emitted from the ocean and the melting sea ice and influence the mercury cycling, through chemical reactions that affect the air and water exchange.[7] Sea ice is classified by its age and is often divided into multi-year and first-year ice.[20] Climate change is causing a shift in the type of ice present and contributing to a decrease in the ice cover. The multi-year sea ice is melting and being replaced by seasonal sea ice, which is younger and more saline. Young ice is more saline because sea salt is trapped in the ice and the drainage takes time.[21] This transition is predicted to have extensive effects on the Hg cycling.[7]

The extension of the sea ice is often determined using the factor sea ice concentration. The edge of the sea ice is called the *Marginal Ice Zone* (MIZ). The MIZ is defined as the area going from open sea (0 % ice concentration) to continuous sea ice, which is often defined as approximately 80 % sea ice concentration. The MIZ area change during the year due to the spring and summer melt, ocean currents, wind patterns and when the re-freeze takes place in September.[22] The input of fresh water to the *Arctic Ocean* is 11 % of total global runoff, making this physical link between the land and the ocean unique.[7] The input of fresh water to the *Arctic Ocean* is accelerated due to degrading permafrost caused by climate change and due to melting of snow/ice on land. The flow of fresh water to the ocean causes stratification in the upper part of the ocean. The stratification creates a layer of fresh water melt, which disconnects the deep ocean from the upper ocean and limits the exchange between the deep ocean and the atmosphere.[7] The water exchange between the *Arctic Ocean* and other oceans is minor, meaning that the *Arctic Ocean* can be seen as a semi-enclosed reservoir. However, the air mixing is not restricted meaning that the Arctic region can retrieve and redistribute pollution from and to other continents.[7]

The mixing and exchange of heat, gases and particles between the Earth's surface and the atmosphere are controlled by surface and boundary processes. These processes operate within the lower troposphere in the region called the atmospheric boundary layer, also referred to as the planetary boundary layer (PBL). The PBL is defined as the region between the Earth's surface and around 1-2 km up in the atmosphere. The height of the PBL changes due to variation in the topography, magnitude of heating on the Earths' surface and the amount of water that evaporates from surfaces on Earth into the atmosphere.[23][24] This means that more heating leads to increased convection, which result in a thicker PBL. During day-time, the PBL is thicker and results in higher mixing, meanwhile during night the PBL is more shallow, which results in lower mixing ratios. Over ocean surfaces, the PBL is usually lower compared to land surfaces because of the vertical mixing of water in the ocean.[24]

2.4.2 The Arctic climate and weather

The Arctic climate and weather are influenced by a number of variables such as latitude, sunlight, pressure, wind, temperature, humidity and clouds.[25] As mentioned in the section above, the intensity of solar radiation changes with season and latitude. The other parameters are described in the sections below.

Air pressure is the weight of air molecules on a specific point on Earth. Air moves from regions with high pressure to a regions with low pressure and this is usually referred to as wind. The direction of the wind is further determined by the Coriolis force, caused by Earths rotation and surface friction. Within the polar cell the surface winds are easterly. High-pressure systems usually result in clear and dry conditions, meanwhile, low-pressure systems cause cloudy and wet conditions.[25]

The typical average winter temperature in the Arctic region is around – 1°C and during summer the temperature can reach up to 10°C.[26] When warmer air is found higher up in the atmosphere and cold air is located near the ground, a phenomena known as inversion layer appears and separates the warm and cold air from

each other, which limits the air exchange. The inversion layer could possibly trap mercury near the ground and/or high up in the atmosphere.[25] Earlier observations have indicated that inversion layers could have an effect on the mercury cycling.[27] The relative humidity is the amount of water vapour in air relative to the saturated amount of water in air. During summer, over the ocean area, the temperature rises and leads to more evaporation from the water reservoir, which results in high humidity. The humidity is usually low in the Arctic region during the winter, when the temperature is low and the ocean is covered with ice. Nevertheless, open oceans during the winter can cause a lot of evaporation to the atmosphere due to higher temperature in the oceans compared to the air temperature. Additionally, fog can be formed during these circumstances.[25] Cloud formation depend on the season and the amount of open water. During summer, the sea ice melts and the area of open water expands leading to increased release of moisture to the atmosphere. The increased amount of moisture in the atmosphere result in cloud formation.[25] In addition, the supersaturated air that is created above open leads of sea water during spring and summer results in increased halogen transport from the melting sea ice to the atmosphere and promotes the growth of ice and snow crystals. These crystals are often referred to as frost flowers.[10]

2.5 The Arctic mercury cycle

Gaseous elemental mercury (Hg^0) released in the Northern Hemisphere travels long distances with air masses and brings mercury to the Arctic environment. In the Arctic region, mercury species can deposit, react and transform in all of the environmental compartments (atmosphere, ocean, and terrestrial). In figure 2.2, based on several studies a detailed illustration of the mercury cycling within the Arctic environment is shown [7], [18], [28], [12], [29], [10], [11], [27], [30], [31] and [32]. In the figure, the boxes illustrate different reservoirs in the Arctic region, the black arrows visualise the flows of mercury and the dotted arrows depict what is thought to be small flows of mercury, due to the character of the mercury specie or due to limited observation of the magnitude of the flow. The red arrows represent flows of halogens (H). The Arctic mercury cycle experience exceptional seasonality and therefore, the magnitude of the interactions between the compartments changes during the year. In the sections below, the interaction between the reservoirs (atmosphere, ocean and terrestrial) are described.

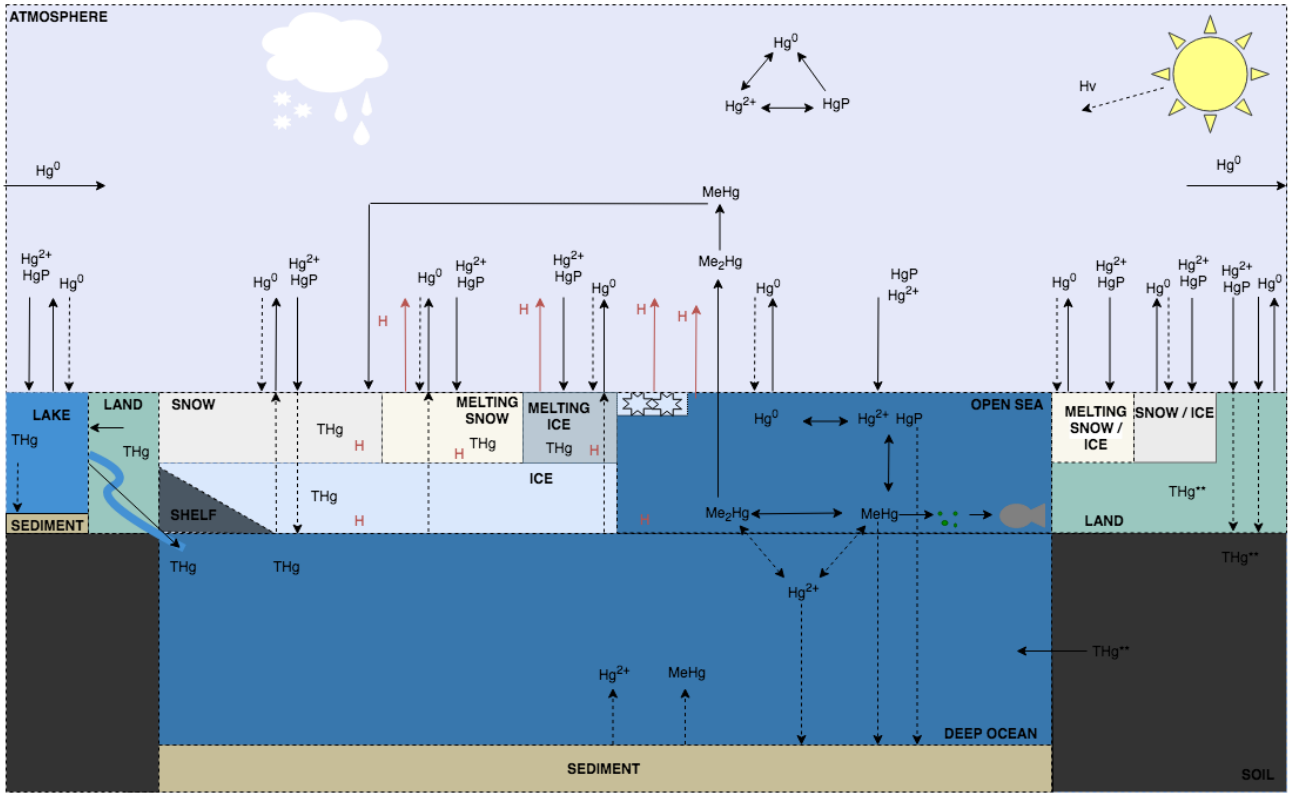

Figure 2.2: *Mercury cycling in the Arctic environment. The rectangular boxes specify the different compartments in the environment, the black arrows refer to mercury flows, the red arrows refer to flows of halogens (H) such as Br, Cl and I and the dotted arrows points out smaller flows of mercury. THg refer to total mercury, meaning all of the forms noted in the picture. The abbreviation (THg) is used at the flows where all of the mercury forms are known to be present. THg^{**} refers to all forms of mercury except for Me_2Hg.*

2.5.1 The air - ocean interactions

The exchange of mercury between the upper ocean and the atmosphere is considered to be the most important pathway in the Arctic mercury cycling. The air-ocean exchange regulates the magnitude of the transformation between different forms of mercury. Only a small fraction of the mercury that is taken up by the oceans is removed to the deep ocean sediment. Consequently, the surface layers will reach equilibrium faster than the deep ocean.[7]

The dominant form of mercury present in the atmosphere is GEM (Hg^0). Hg^0 is brought to the Arctic environment by long range transport from southward latitudes, but can also originate from evasion from oceans,

sea ice and melting snow.[18] Prior deposition, Hg^0 is commonly oxidised into Hg^{2+} and HgP. However, a small fraction of Hg^0 is deposited, this fraction is often re-emitted back in to the atmosphere, due to the volatile character of Hg^0. Further, unreacted Hg^0 can be transported out of the Arctic region with the movement of air masses.[7]

Atmospheric oxidation of Hg^0 into Hg^{2+} in the Arctic region is often referred to as atmospheric mercury depletion event (AMDE). AMDEs result in changing the distribution of mercury species in the environment temporarily. These events are frequently observed during Arctic spring when a large amount of halogens are being released from the melting sea ice and snow. The halogens are, when in the atmosphere, acting as a reactant for initiating the oxidation of Hg^0 into Hg^{2+}, a more detailed description is found in the section below.[7] The exact way reactive species of mercury are formed in the atmosphere remains a key question that needs to be investigated further to fully understand the atmospheric chemistry of mercury. However, what is known is that the reactivity of mercury is linked to radical reactions initiated by photolysis.[7] Following AMDE, the oxidised forms of mercury can deposit into oceans, snow or ice either by wet or dry deposition. Wet and dry deposition of the oxidised forms of mercury are thought to be the major pathways for mercury removal from the Arctic atmosphere. However, also a small fraction of Hg^0 is removed from the atmosphere and deposited into the oceans by dry deposition. The amount of Hg^0 that is being removed by wet deposition is thought to be insignificant, mainly due to the very low water solubility of Hg^0.[12]

The exchange of mercury between the snow located on sea ice and the atmosphere, as a consequence of AMDEs, is a complex and dynamic flow. The *Arctic Monitoring and Assessment Program (AMAP)* estimated 2011 that 80 % of the Hg^0 deposited to snow following AMDEs is re-emitted as Hg^0 within a few days.[7] The relationship becomes even more complex due to the phenomena of frost flowers. Frost flowers are thought to contribute to increased scavenging of mercury from the atmosphere. Observations by Douglas et al. (2018) showed that frost flowers contain high levels of mercury and frost flowers formed on brine rich sea ice is suggested to be an important source of halogens that potentially can initiate AMDEs.[29] However, more research needs to be put into validating the mercury scavenging effects of frost flowers.[10]

The dominant forms of mercury in the surface ocean are Hg^{2+} and Hg^0. Hg^{2+} is either transported to the ocean from the atmosphere through deposition, or created within the ocean through chemical reactions. Within the ocean, there are several chemical reactions that can form Hg^{2+}. It can be formed by oxidation of Hg^0 or by reduction of Me_2Hg and $MeHg$. However, Hg^{2+} can also be methylated by bacteria or algae to form $MeHg$ and possibly further transformed to Me_2Hg. $MeHg$ can bio-accumulate in aquatic organisms and biomagnify through the food chain. Mercury attached to particles (HgP, $MeHg$) and Hg^{2+} have further been observed to sink to the ocean sediment.[33] Within the ocean sediment, Hg^{2+} can undergo methylation by bacteria and form $MeHg$. Me_2Hg on the other hand, is suggested to easily evade from the ocean to the atmosphere. When in the atmosphere it is thought to rapidly undergo photolytic decomposition to $MeHg$, which deposits on snow and meltwater ponds.[7]

The unique features of the Arctic environment, with the sea ice acting as a semipermeable cover and the large difference in solar radiation during different times of the year, results in strong seasonal variations of mercury fluxes. At wintertime, the large sea ice cover is preventing mercury from being released from the oceans but at the same time, the sea ice acts like a cover for mercury to deposit into the ocean. Deposited mercury then ends up in the ice- and snowpacks. At summertime, when a large amount of open water is present, the atmosphere-ocean exchange is large and the ocean acts as a net source of mercury to the atmosphere. Earlier deposited mercury present in snow, sea ice and oceans is during this season re-emitted back to the atmosphere.[28]

Atmospheric mercury depletion event (AMDE)

A sudden drop in gaseous elemental mercury (GEM) concentrations in the lower atmosphere during springtime at the polar regions are, as mentioned above, is often referred to as atmospheric mercury depletion events (AMDEs). These events are commonly suggested to depend on a sunlight-induced atmospheric reaction where halogen radicals like bromine ($Br\cdot$), chlorine ($Cl\cdot$), or bromine oxide molecules (BrO) are produced and act as the primary oxidising agent of GEM. Hg^0 is thus oxidised in two steps to produce gaseous oxidised mercury (Hg^{2+}) as either can stay in gaseous form (GOM) or bound to a particle (HgP).[7] These oxidation reactions mainly take place within the troposphere.[34]

The reaction initiating AMDEs is often suggested to be induced by a photolytic step where $Br\cdot$ are produced from Br_2. Br_2 is released from sea salt when ice and snow packs start to melt during early spring, see reaction 2.1.[7] In the reaction below $h\nu$ refers to sunlight.

$$Br_2 + h\nu \longrightarrow 2Br\cdot \tag{2.1}$$

The $Br\cdot$ formed in reaction 2.1 are highly reactive and will oxidise Hg^0 to Hg^{1+} and/or Hg^{2+} according to 2.1a,2.1d. Reaction 2.1a and 2.1d are competing with 2.1b and 2.1c to fulfil the complete oxidation of Hg. X is considered to be the first stage Hg^0 oxidant, Y is the second stage Hg^{1+} oxidant and M represent a molecule of air. First stage oxidants are typically suggested to be halogen radicals or BrO molecules, which obviously also can act as a second stage oxidant.[11] The second stage oxidation could also be preformed by other molecules such as the $OH\cdot$.

$$Hg^0 + X + M \longrightarrow Hg^{1+}X + M \tag{2.1a}$$
$$Hg^{1+}X + M \longrightarrow Hg^0 + X + M \tag{2.1b}$$
$$Hg^{1+}X + Y \longrightarrow Hg^0 + XY \tag{2.1c}$$
$$Hg^{1+}X + Y + M \longrightarrow Hg^{2+}XY + M \tag{2.1d}$$

Simultaneously when oxidising Hg, $Br\cdot$ is also acting as an oxidant of O_3 and thus depletion of O_3 is often seen in correlation with oxidation of Hg^0, the overall reaction can be seen as seen in equation 2.2.[12]

$$Hg^0 + 2Br\cdot + O_3 \longrightarrow Hg^{1+}Br + BrO + O_2 \tag{2.2}$$

The above described reaction is, except from solar radiation and halogen-containing sea ice, believed to be dependent on cold temperatures to occur. There are several studies that have shown a clear correlation between cold temperatures and the amount of AMDEs that takes place. However, the temperature limit for when AMDEs start to occur is still ambiguous. Skov et al. (2004) proposed a temperature limit of $\leq$ -4°C.[35]These favourable conditions causing AMDEs are generally present in the Arctic region during springtime and thus these events are sometimes referred to as springtime AMDEs.

The dark mechanism

Despite the fact that AMDEs are suggested to depend on the sunlight-induced photolytic reaction there has been evidence for that AMDEs also occur in the absence of sunlight. During the winter expedition to Antarctica, *ANTX-XIX/6*, several events of AMDEs were observed even during Antarctic winter and similar observations were also made by Spicer et al. (2002) and Bottenheim et al. (2002).[36][37] An additional dark mechanism was proposed by Nerentorp et al. (2016), where Br_2 is assumed to directly oxidise Hg to form $HgBr_2$, see reaction 2.3.

$$Hg^0 + Br_2 \longrightarrow HgBr_2 \tag{2.3}$$

The suggested reaction above would be dependent on very high Br_2 concentrations for the oxidation of GEM to take place and cause mercury depletion. Levels of around 200 to 40 000 times more Br_2 than $Br\cdot$ or BrO present in the atmosphere has been suggested to be needed for the reaction to take place.[27]

Other oxidants

OH and O_3 were for a long time considered as the main oxidants of Hg^0 in the atmosphere. The $OH\cdot$ is a very important oxidant present in the troposphere and a key player for oxidation of trace compounds in the atmosphere. The $OH\cdot$ is present in the atmosphere during the day time since it is generated from a photolytic reaction.[30] However, results from recent laboratory trails have shown that the products generated from the

OH and O_3 oxidations are too thermodynamically unstable to enable oxidation of Hg^0 under atmospheric conditions.

In addition to $OH\cdot$ and O_3, several different atoms and molecules have been proposed as oxidants for Hg^0 in the atmosphere, one of them is NO_3. During night time and Arctic winter, i.e when no solar radiation is present, the $OH\cdot$ concentration in the atmosphere is close to zero and the NO_3 radical takes over as the main oxidant in the atmosphere.[30] NO_3 is generated through a reaction between NO_2 and ozone. NO_3 can oxidise Hg^0 to form HgO according to equation 2.4. However, this reaction has been shown to not have any significant impact in the atmosphere, not even at night in highly polluted areas.[11]

$$Hg^0 + NO_3 \longrightarrow HgO + NO_2 \tag{2.4}$$

Other proposed oxidation agents for Hg^0 have been; I, I_2, Br_2, Cl_2, BrO, ClO, HCl and HO_2. However, none of the above described reactants have shown to play a significant role for the oxidation of GEM during atmospheric conditions. Though, O_3 and $OH\cdot$ could though still be important oxidants on aerosol surfaces.[11]

2.5.2 The air - terrestrial interactions

In figure 2.2, seen above, the interactions between the atmosphere and the terrestrial reservoir (land) are shown. The magnitude of the bidirectional flows between the atmosphere and the terrestrial system are uncertain and it is highly debated whether the terrestrial system is a sink or a source of mercury.[18] However, the largest reservoir of mercury known is the surface soil.[7]

All the major forms of mercury found in the atmosphere (Hg^0, Hg^{2+} and HgP) can deposit into lakes and rivers. Mercury species connected to particles (HgP) will settle in the river sediments.[18] As mentioned in the air – ocean interactions, Hg^0 and Hg^{2+} can be deposited from the atmosphere to ice and snow reservoirs. These mechanisms also takes place in the terrestrial reservoir.[7] Additionally, Hg^0 can evade from the terrestrial reservoir to the atmosphere. Hg^{2+} can enter the terrestrial reservoirs through wet deposition, meanwhile Hg^0 can enter the system through dry deposition on soil and vegetation.[18] Hg^0 has been observed to be the largest input of mercury to the terrestrial system and the input has shown to be around 70 % of the mercury in the Arctic Tundra is Hg^0. Litter fall is the major pathway for Hg^0 to deposit from the atmosphere into the Arctic soils.[31][18] GEM can be released through volatilisation from natural occurring mercury in the soil, or from soils enriched with mercury due to anthropogenic activity.[18] Within the soil, bacteria can methylate Hg^{2+} into $MeHg$.[7][32] The soil can therefore contain Hg^0, Hg^{2+}, $MeHg$. Within the permafrost, frozen land, the major form of mercury is Hg^{2+}, however a small fraction of $MeHg$ also exits.[7]

The seasonality in the Arctic environment influences the exchange of mercury between the air-vegetation-soil reservoirs. During wintertime, the majority of the vegetation is covered by ice and snow, which results in deposition of Hg^0 on the snow/ice-pack. In the snow and ice-covered soil, mercury is protected from the heat caused by sunlight, which limits the release of mercury to the air.[32] The mechanism of Hg^0 uptake in soils is not known, but earlier observations have shown that the soil acts as a sink during wintertime.[31]

2.5.3 The ocean - terrestrial interactions

There are several pathways for mercury to be transported between the terrestrial system and the ocean, see figure 2.2. River flows introduce inorganic and organic compounds containing mercury into the ocean. The mercury compounds can be subjected to sequestration and become buried in the ocean sediment or occur in compounds as a organic ligands. However, the magnitude of the mercury flow to the ocean is uncertain resulting in an unquantified mercury budget for the *Arctic Ocean*.[7] Coast erosion is another pathway for mercury in the terrestrial reservoir to enter the ocean. The pathway introduces mainly Hg^{2+}, but also *methylmercury* and dissolved Hg^0.[7]

During the transportation between the two reservoirs, a majority of the mercury in the flows becomes trapped and stored in estuaries and on continental shelves. Within estuaries and continental shelves, mercury can either react with sulfide and form sulfide divalent mercury that can be sequestrated, or it can be transformed into $MeHg$. The higher level of sequestration results in less formation of $MeHg$. Nonetheless, the mechanism can

result in that sediments, estuaries and shelves acts as sources of $MeHg$ to the ocean.[7] During spring and summer, the interaction between the terrestrial and the ocean reservoirs amplifies due to the melting of snow and ice on land and permafrost.[7]

2.6 Climate change affecting the mercury cycle in the Arctics

Climate change is predicted to cause changes in the Arctic environment and these changes will most likely have significant effects on the transportation and transformation of mercury globally, regionally and locally.[7][18] Changes in the physical compartments, such as changed precipitation patterns, are better understood compared to changes in the biological system. Therefore, it is easier to model and understand how an alteration of physical parameters such as temperature, precipitation and ice coverage will affect the cycling of mercury in the Arctic region. The insufficient knowledge about how climate change will affect biological systems makes it hard to model and predict the effects on the mercury cycling. This section will present the current knowledge of how changes in the Arctic climate will affect the mercury cycling within the region.[7]

The most obvious change in the Arctic environment is the loss of sea ice cover. Another major change within the reservoir is the loss of multi-year ice, which is being replaced by first-year ice. These changes are predicted to potentially affect the mercury cycling. Wind mixing and heating are two of the parameters that will be affected by the decline in sea ice and this will further affect the mercury exchange between the ocean and the atmosphere. Concerning shrinking of sea ice, mercury deposition is likely to be affected in two major ways. The first course is that a majority of GOM will deposit on open ocean surfaces instead of on ice and snow. Secondly, the air-sea interaction will possibly happen more easily and result in enhanced exchange of GEM between the reservoirs. The increased air temperature in the Arctic region, caused by climate change, makes the weather more unstable and harder to predict. When the air temperature is rising and the sea ice cover is decreasing, the flux between the upper ocean and the atmosphere will increase and thus more heat will be stored in the ocean.[7]

Mercury oxidation in the atmosphere could possibly be influenced by the rise in air temperature.[18][7] As mentioned in the section *Atmospheric mercury depletion event (AMDE)*, AMDE is more likely to occur in cold temperatures. Based on this, it is suggested that climate change could lead to less oxidation of GEM and slow down the deposition. However, how the oxidants will be affected by climate change is not known. The current knowledge about the reaction of GEM to GOM and the deposition mechanism is not certain and there could exist other mechanisms leading to oxidation of mercury that are not yet known. The unknown mechanisms could potentially have a temperature dependency and therefore be affected by a rise in temperature.[7]

Additionally, changes in precipitation and temperature may influence the magnitude and seasonal variation of mercury deposition to the Arctic environment.[7][18]. Changes in precipitation patterns will especially affect wet deposition of GOM. Therefore, the magnitude and distribution of mercury in snow and ice-packs will change.[28] Atmospheric pressure patterns have, during the past decades, been characterised by abnormal high and low sea-level pressures in the North American and Eurasian parts of Arctic, respectively. This pattern has resulted in more southerly winds being introduced to the Arctic environment, which affect the cycling of mercury in and out of the arctic system.[7]

The effects of climate change could also be seen in the terrestrial compartments (snow and ice, permafrost, vegetation and rivers) and the changes happens at different rates and in diverse ways. Therefore, the effects caused by climate change in the terrestrial compartments together with the seasonality in the Arctic environment make the system highly complex. Changes in the terrestrial systems are predicted to have effects on the mercury cycling, both spatially and temporally.[7]

Glaciers and permafrost are shrinking and the temperature within the permafrost is increasing, causing enhanced releases of mercury to the atmosphere and to the river compartment. The higher flow of mercury to the river compartment in combination with higher temperature in the fresh water could result in higher $MeHg$ concentrations.[38][7] Additionally, climate change results in decreased ice cover in lakes and rivers, which result in that more solar radiation reaches the open fresh waters causing increased primary production. The effects of increased productivity is uncertain but could possibly result in bio-dilution, meaning that mercury concentration decreases through the food chain or that $MeHg$ will demethylate due to increased exposure to

light. At the same time, the increased amount of carbon supply caused by the enhanced productivity could increase the formation of $MeHg$ and counteract the demethylation.[39][7]

As mentioned in the section 2.4, the *Arctic Ocean* has a freshwater enriched layer in the upper ocean. The freshwater originate mostly from sea ice melt and from the *Arctic Ocean* ice shelves. This mechanism is predicted to stop within years to a decade because of the limited supply of freshwater, which will leave the *Arctic Ocean* less stratified and more saline.[7] Another effect caused by climate change is acidification in the ocean, lower pH in the ocean has been shown to result in enhanced production of $MeHg$.[7]

2.7 Mercury sampling - Tekran 2537A

Tekran 2537A is an instrument commonly used for measuring mercury in ambient air. The 2537A model used for sampling mercury during the expedition is one of the oldest mercury analysers.[40] The *Tekran 2537A* is a mercury vapour analyser, measuring total gaseous mercury (TGM) concentrations (ng/m^3) in air. TGM is defined as the sum of both GEM and GOM. As mentioned in section 2.1, air mainly consist of GEM and the instrument has a particulate filter sorting out particles larger than 0.2 μm and therefore, it is assumed that *Tekran 2537A* mainly measures GEM.[8][9]

A schematic picture of the instrument is seen in figure 2.3. The instrument collects air through the sample air inlet. Within the inlet the particulate 0.2 μm filter is used for the purpose of removing particles, such as HgP. The sampled air enters either cartridge A or B. The air sampling is conducted continuously for five minutes per cartridges. For measuring the flow rate of sampled air through the cartridges a mass flow meter (MFM) is used. The cartridges consists of an ultra-pure gold adsorbent. Mercury is absorbed to the cartridge, followed by exposure to heat in the presence of argon gas (the carrier gas) and therefore desorbs thermally. The carrier gas comes from the argon carrier inlet and the flow is determined by the mass flow controller (MFC). The desorbed mercury flow enters the detector which uses a Cold Vapour Fluorescence Spectrometry (CVAFS) to identify the concentration of mercury in the air. In the detector, mercury is exposed to illumination created by a low pressure mercury vapour lamp. Mercury atoms present in the air will be excited when exposed to radiation with a wavelength of 253.7 nm. The excited mercury atoms will re-radiate fluorescence at a specific wavelength, and the intensity of the fluorescence is detected by a photomultiplier tube (PMT). The concentration of mercury is identified because the intensity of the fluorescence is directly proportional to the amount of mercury present. The cartridges do not sample air at the same time. When one of the cartridges samples the other one is heated in the presence of argon gas and become analysed.[8]

During the calibration period, zero air is collected from the zero air inlet and a charcoal filter is used to produce the zero air. The calibration is performed in 3 steps. Each of the steps are conducted in the cartridges separately before moving on to the next step.[8] First, the cartridges are exposed to zero air in the purpose of removing residual mercury and cleaning the cartridges before calibrations begins. Secondly, zero air is again introduced to the cartridges to examine the instrument for possible contamination and check possible mercury levels in the zero air. In the last step, the cartridges are exposed to a known amount of mercury for the purpose of checking the sensitivity of the instrument. The use of the permeation source inlet and injection port is an alternative to the automatic calibration conducting manual injections instead. However, the inlet and port was not used for calibration during the sampling.[8]

The gold cartridges have large surfaces that mercury can absorbed onto. One problem with the use of this old model is that other species possibly also can be absorbed onto the gold surface causing passivation. Signs of passivation during occasional periods have been observed by the first generation Tekran users. During Arctic and Marin expedition, passivation have been seen in one or both of the cartridges. Passivation in one of the cartridges is identified if one of the cartridges shows unexpected low values compared to the other cartridge. The recommendation from the first generation Tekran users is to remove the data point from the passivated cartridge. Passivation on both of the cartridges, simultaneously, is very unlikely and technically difficult to observe.[40][41]

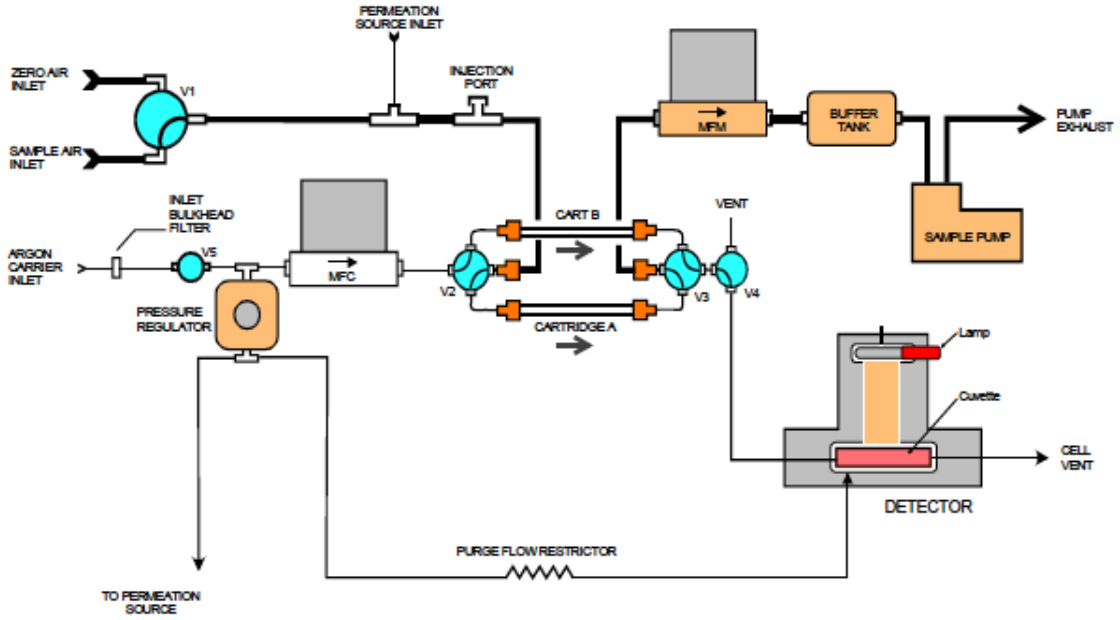

Figure 2.3: *Schematic picture of the mercury instrument Tekran 2537A.[8] MFC refers to mass flow controller, MFM stands for mass flow meter and V refers to valves.*

2.8 Software tools

2.8.1 Ocean data view

Ocean Data View (ODV) is a software used to visualise and analyse data sets of: oceanographic, atmospheric and geographical profiles. *ODV* was developed under the SeaDataNet program at the *Alfred Weneger Institute*. It is a freely available software package that can be downloaded from the website.[42]

The software includes two "fast weighted-averaging gridding algorithms" as well as the "DIVA gridding software". Data from a large set of different sources such as: *Argo, GTSPP, CCHDO, World Ocean Database, World Ocean Atlas*, can easily be imported into the ODV software. *ODV* displays gridded fields based on original data or the actual original data.[42] Various plots can be produced such as; stations maps, property-property plots, scatter plots and iso-surfaces of property distributions.[43]

2.8.2 Hybrid Single-Particle Lagrangian Integrated Trajectory

The Hybrid Single-Particle Lagrangian Integrated Trajectory (HYSPLIT) is a modelling tool that can be used for calculating simple air parcel trajectories as well as more complex airborne transport trajectories. It can be used for looking at dispersion, deposition or transformation of atmospheric pollutants. It is one of the most used models in the atmospheric science community and widely used by scientist all over the world.[44] When using the *HYSPLIT* model for creating backward trajectories, an uncertainty emerges of approximately 10 % of the travel distance.[45]

The *HYSPLIT* model is developed by the *National Oceanic and Atmospheric Administration (NOAA) Air Resources Laboratory (ARL)*. The model has evolved over more than 30 years and it applies a calculation model that is a hybrid between the Lagrangian approach and the Eulerian methodology.[46] The model can either run online or be installed on a local computer. It requires meteorological data, which can be found on the ARL-Hysplit website.[44]

3 Methodology

In this chapter, the methodology of the master thesis is described. The first section, GEM sampling, describes how the GEM concentrations were sampled and where the sampling took place. The following section, data sorting, present how the data set was processed and arranged. Thereafter, the method used during the evaluation of the data set is described.

3.1 GEM sampling

The sampling of GEM concentrations were performed on board the Swedish ship Oden during the *Arctic Ocean Expedition 2018* and during the transit south from Svalbard to the west coast of Sweden. Oden has a length of 107 meters, is 31 meters wide and is used for breaking ice in Luleå during the winters in Sweden.[47] Furthermore, *IB Oden* works as a research platform and is often used during expeditions in the Arctic and Antarctic regions. The ship is equipped with a geographical information system, as well as meteorological and oceanographic monitoring systems that reports data every minute. GEM concentrations were measured using the automatic instrument *Tekran 2537A*. The instrument was calibrated every day at 11 am for about 40 minutes. The instrument was stationed in front of the bridged on second deck in a laboratory container at a height of approximately 10 m above sea surface and the air inlet was placed on the outside of the container making continuous sampling of air.

The expedition and GEM sampling began the 1 of August 2018 at Longyearbyen in Svalbard. The ship travelled towards the North Pole, but stopped for some days at the MIZ. The ship passed the MIZ and entered into the area with continuous ice on the 6th of August. The expedition continued further north and *IB Oden* was docked to a ice sheet during the time period 14th of August - 14th of September. During this period, the ship was re-positioned to facilitate air sampling from the front of the ship without potential influence from the chimney. *IB Oden* started to travel south and reached the MIZ the 18th of September. The expedition and GEM sampling ended the 22 of September 2018 at Longyearbyen in Svalbard. GEM sampling began again in the 22 of September 2018 at Longyearbyen Svalbard when IB Oden started to travel south along the west coast of Norway. The sampling ended when the ship reached the port in Helsingborg, Sweden, on the 5th of October.

Information about the expedition cruise and the route from Svalbard to Helsingborg is presented in table 3.1. The position of the MIZ, contiguous ice and open ocean were determined using ice maps obtained from European Organization for the Exploitation of Meteorological Satellites (EUMETSAT). Pictures of ice concentrations in the Northern Hemisphere are found in Appendix A.4.

Table 3.1: Information about the expedition cruise and the route from Svalbard to Helsingborg.

Start Position	Start [yy-mm-dd]	Stop Position	Stop [yy-mm-dd]	Geographical Region
Longyearbyen	18-08-01	MIZ	18-08-02	Open ocean
MIZ start	18-08-02	MIZ end	18-08-06	MIZ
End of MIZ	18-08-06	Begin of MIZ	18-08-14	Contiguous ice
MIZ start	18-09-18	MIZ end	18-09-20	MIZ
MIZ	18-09-20	Longyearbyen	18-09-21	Open ocean
Longyearbyen	18-09-22	Helsingborg	18-10-05	Open Ocean

3.2 Data sorting

The sorting of the data set started with removing measurements with multiple peaks (measurements that resulted in several peaks at different wavelengths) from the data set obtained from *Tekran 2537A*. The measurements from cartridge A were removed from the data set due to signs of passivation, see information about passivation in the theory section about *Tekran 2537A*. After the removal of the measurements from cartridge A, the data

set consisted of data measured every 10th minute, with exceptions during the calibration period and when measurements with multiple peaks were found. The data were sorted using Microsoft Excel.

Ancillary data obtained from *IB Odens* ship data included coordinates, wind direction and wind speed relative to the ships position, air temperature, humidity and air pressure. The ancillary data were obtained every minute and therefore 5-minute averages were taken, and every second value was then used to fit the GEM data. The 5-minute average were extracted using Matlab R2017b.

Additional data were obtained from other research projects performed during the *Arctic Ocean 2018* expedition. Paul Zieger at Stockholm University and Bolin Centre for Climate Research and Linn Karlsson at Stockholms University contributed with data on visibility, concentrations of particles and black carbon (BC) in the atmosphere. Particle concentration was derived from measurements of aerosols larger than 8 nm in diameter. Concentration of BC was derived by collecting particles on a filter and measure the particles light absorption at one wavelength. By applying an assumed mass adsorption coefficient, the concentration of black carbon was obtained.[48] Julia Yvonne Schmale at Paul Scherrer Institut in Schweiz contributed with data on ozone in the atmosphere. The ozone concentrations are initial/raw data, which implies that a calibration factor must be applied to the data set for more accurate values. However, in this study the data were only used for investigating trends and the initial/raw data works for the purpose.[49] The measurements of particles, BC and ozone were conducted on the fourth deck at IB Oden. Ian Brooks at the University of Leeds contributed with data on solar radiation, i.e down welling short wave radiation. The additional data were also aggregated into 5-minute averages and every second value was used to fit the *GEM* data.

3.3 Evaluation of GEM concentrations

The evaluation of the data set of GEM concentration was divided into two steps, subsequent sorting of the data set for evaluation of contamination risks and analysis of GEM concentrations and regional/temporal trends. The methodologies used in each step are described in this section.

3.3.1 Subsequent sorting of the data set and evaluation of contamination risks

The first step of the evaluation aimed to analyse and validate the data set by making plots against time, the ships coordinates, wind speed and wind direction both relative to the ships position. The data on particles and BC were used for evaluating possible contamination of the data set. The program *Ocean Data View* (ODV), version 5.1.5, was used for plotting. Furthermore, literature research was performed with the purpose of finding other studies of GEM that dealt with the risk of contamination.

Contamination

One part of the analysis was to assess the data set and examine if exhaust gas from *IB Oden's* chimney possibly could have influenced the measurements of mercury. The risk of contamination was assessed by analysing the wind direction and wind speed relative to the position of the ship.

As mentioned above, the wind directions and wind speeds were obtained as 5-minutes averages and these values were further analysed in this step. When obtaining the averages of wind direction a cos-function was used, in the purpose of examining the wind direction relative to the boat. A wind that enters the boat from the stern ($180° \pm 90°$) resulted in negative values and winds that enters the boat from the fore ($0° \pm 90°$) resulted in a positive value. However, the average values could be positive even though the wind at some point during the interval was coming from the stern. To eliminate this risk the minimum cos-value during an interval was extracted and if it was negative GEM data was sorted out.

The risk of evaluating contaminated measurements were minimised by removing data points from the data set. The data points that were chosen to be removed were when the wind speed was below 4 m/s and the minimum wind direction, in the 5-minutes averages, was in the interval ($180° \pm 90°$), meaning that the wind was coming from the stern. Furthermore, if the wind fluctuated (shifted wind direction between the fore and the stern) in a time period less then 1 h then these data points were removed from the data set. Moreover, other activities such

as the use of a helicopter and surrounding ships could also possible contribute to contamination of the data set. The logbook at Oden was analysed with the purpose of finding activities that possibly could contribute to contamination.

3.3.2 Analysis of GEM concentrations and regional/temporal trends

The final analysis of the data set involved evaluation of the GEM concentrations that remained in the data set after the removal of data point possibly influenced by the exhaust gas from *IB Odens* chimney. The purpose of this evaluation step was to analyse possible depleted and/or elevated GEM concentrations. Further, the evaluation aimed at analysing possible trends over the geographical regions marginal ice zone, contiguous ice and open ocean during the expedition. In this step, ODV version 5.1.5 was used for making plots of GEM concentrations against time, cruise coordinates, air temperature, air pressure, humidity, visibility, radiation and wind speed. Alongside evaluating the data set in ODV, literature research was performed in the purpose of understanding trends, abnormal high and/or low concentrations, atmospheric chemistry and analysing the data. Furthermore, the data set was evaluated by looking at the GEM measurements of the different geographical regions. A comparison of earlier conducted studies in the Arctic region were conducing for analysing GEM concentrations though time and possible effects of climate change.

Analysis using HYSLPIT

The National Oceanic and Atmospheric Administrations Hybrid Single-Particle Lagrangian Integrated Trajectory (NOAA HYSPLIT) tool was used to create back trajectories to find the origin of both depleted and elevated air masses. The Windows Public (unregistred) version was used and the meteorology data were obtained from the Gridded Meteorological Data Archives at NOAA. The meteorological data used was Global Data Assimilation System (GDAS), 1 °, global, Dec 2004 - present.[50] The HYSPLIT model was used for calculating 5 and 28 days backward trajectories at three different vertical heights: 0.3, 0.5 and $0.7 \cdot PBL$. Further, HYSPLIT was used for creating cluster analyses at the height of 0.5*PBL, for trajectories going back 5 days in time and for trajectories going back 28 days in time. The clusters were generated by creating trajectories every 4th hour for 5 days back in time from the time of the measurement of interest.

A study by Radke et al. (2007) evaluated the vertical profile of GEM by taking measurements of mercury at different altitudes using air planes. The authors findings showed that the vertical profile of GEM is approximately constant or somewhat decreasing at low altitudes (0-3 km).[51] Based on these findings, it was assumed that the measured concentration of GEM was vertically constant and therefore different vertical heights could be analysed.

The vertical heights were chosen based on recommendations from Dr. Mark Cohens at NOAA Air Resources Laboratory. If heights near the ground are chosen or the sampling height, the trajectories often reaches the ground and will not give a true result. As mentioned in the theory section, most of the air mixing takes place within the PBL and therefore it is preferable to chose height as fractions of PBL. In this study, three different fractions were used. The purpose of choosing several fractions was to analyse the difference between the trajectories and to find the confidence of the result.[52]

The duration of the trajectories was chosen to 5 days and 28 days since GEM undergoes long range transport. The reason for the 5 days trajectories was to capture local sources of mercury, meanwhile 28 days could capture regional and global sources. However, the uncertainty of the trajectories increases with increased distance. The clusters were generated by creating trajectories, 5 days long and 28 days long, every 4th hour during 120 hours back in time. The generated trajectories were then grouped into four different groups to indicate how many percentages of the trajectories that originated from different directions. The cluster analysis was performed for the height of $0.5 \cdot PBL$.

Depleted GEM concentrations

When depleted GEM concentrations were detected, the analysis continued with trying to find the reason behind the identified low concentrations. The HYSPLIT model was used for back tracing the origin of the depleted air

masses and cluster analysis was conducted. Furthermore, possible correlations between GEM depletion, ozone depletion and high concentration of bromine oxide (BrO) were examined. BrO maps were obtained from the GOME-2 / SCIAMACHY DOAS nadir data browser, institute of Environmental Physics at The University of Bremen. The maps illustrates the total concentration of BrO present at the specific geographical region. When using the method for determining the BrO concentration, the vertical origin (boundary layer, troposphere, stratosphere) of the concentration can not easily be determined. Therefore, only changes in the whole BrO column will be analysed.

Elevated GEM concentrations

Concentrations above observed background concentrations were further analysed in the purpose of finding activities that might contributed to these elevated concentrations. First, the HYSPLIT model was used for making backward trajectories of the elevated air masses and cluster analysis. When the origin of the air masses were detected, literature research was performed in order to find the reasons behind the identified high concentrations.

4 Results and discussion

In this chapter, the results of the study are presented. First, the result of the evaluation of the data set obtained during the expedition *Arctic Ocean 2018* is presented, followed by the result of the evaluation of the data set obtained during the travel route from Svalbard to Helsingborg through the Norwegian coastline. The result of the trend analysis over the geographical regions (open ocean, MIZ and continuous ice) is presented in the third section, followed by an comparison of mercury levels in the Arctic region through time and the effects of climate change. Finally, a comprehensive discussion about the result is held.

4.1 GEM concentrations in the Arctic region

This section begins by presenting the result from the initial analysis of the data set obtained in the Arctic region. The analysis aimed at evaluating the risk of contamination by examining GEM concentration in relation to BC concentration, particles concentration, relative wind direction, and relative wind speed. Followed by the final analysis, where the result of the evaluation of the remaining data set are presented. The data points in the final data set are those that remained after having eliminated the measurements that possibly could be influenced by contamination. Finally, the results from the analysis for the specific events considered to be of interest (elevated and depleted concentration of GEM) will be shown. The parameters assessed in the analysis were air pressure, relative humidity, visibility, air temperature, O_3 concentration, BrO concentration and solar radiation. As mentioned in the methodology, the meteorological and oceanographic monitoring system on *IB Odens* measured air pressure, humidity and air temperature. Data on concentration of BC and particles, and visibility were provided by Paul Zieger at Stockholm University and Bolin Centre for Climate Research and Linn Karlsson at Stockholm's University. Ozone data were provided by Julia Yvonne Schmale at the Paul Scherrer Institut Schweiz and Ian Brooks at the University of Leeds contributed with data on incoming shortwave solar radiation. BrO maps were obtained from the GOME-2 / SCIAMACHY DOAS nadir data browser, institute of Environmental Physics at The University of Bremen.

4.1.1 Analysis of the initial Arctic GEM-data set and possible contamination

The result of the GEM measurements taken during the expedition *Arctic Ocean 2018* is found in figure 4.1. A majority of the observed concentrations throughout the expedition were characterised by concentrations in the interval $1.5 - 1.8\ ng/m^3$. In *AMAP* 2011, it was reported that the Arctic background concentration of GEM is about $1.6\ ng/m^3$ and in *GMA* 2018, it was reported that background concentration in the Northern Hemisphere ranges from $1.5 - 1.7\ ng/m^3$.[7][3] When comparing the Arctic data set in this study with previously reported background concentrations, it was found that the majority of the GEM concentrations were within or just above the reported range. Regardless, a somewhat decreasing trend in the background concentrations could possibly be observed from the 20th of August and forward. Several periods were characterised by elevated concentrations in the data set and some of the peaks became suddenly high. The suddenly high peaks were considered to be a sign of possible contamination, meanwhile, some of the peaks had a gradually build up and where thus not thought to be created by contamination.

In the 18th of September, a period of suddenly high concentrations of GEM were observed. The instrument measured concentrations above $8\ ng/m^3$ and the peak was considered to be a typical case of contamination. This peak showed a correlation with particles and BC concentration, which further was considered to strengthen the evidence for possible contamination. Figures of particles and BC concentrations against time are found in Appendix, see figures A.1 and A.2. Other events of suddenly high concentrations were observed, for instance, on the 26th of August and on the 5th and 6th of September

Gradual build up peaks were for example observed on the 23rd of August and the 6th of September. The peak observed on the 23rd of August reached a concentration of $5.19\ ng/m^3$ and elevated concentrations were found from 22nd of August at 10:25 am to 23rd of August 16:00 pm. The peak observed the on 6th of September reached a maximum concentration of $2.31\ ng/m^3$ and elevated concentrations were found from 5th of October 06:00 am to 6th of September 12.25 pm. One period of large fluctuations in the GEM concentrations were found between the 6th of August until the 15th of August, see figure 4.1.

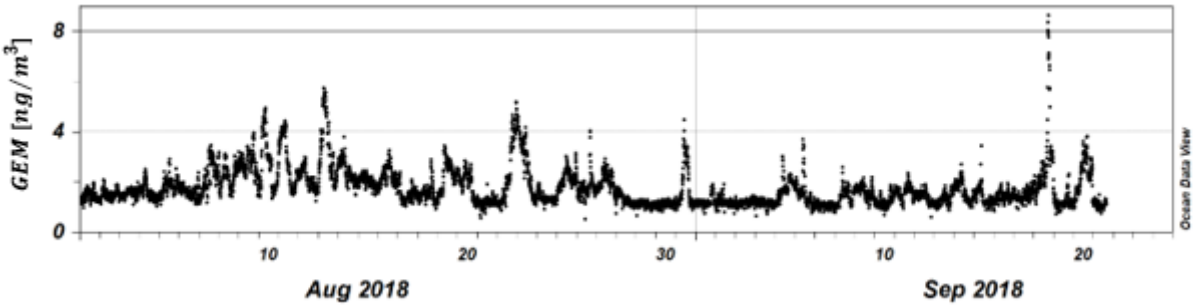

Figure 4.1: *Concentration of GEM against time for the initial data set. The measurements were taken during the expedition Arctic Ocean 2018 (1 of August to 21st of September).*

In figure 4.2, graphs of BC, particles and GEM concentrations against the relative wind direction are shown. As can be seen in the graphs 4.2a and 4.2b, higher concentrations were found when the wind entered the ship from the stern (90°to 180°and -90°to -180°). Similar trends were found in the data set of BC and particles. This trend was not that obvious in the data set of GEM, see figure 4.2c. Elevated concentrations of GEM above background concentrations were observed when the wind was entering the ship from all wind directions. However, concentrations of GEM above 6 ng/m^3 were observed when the wind entered the ship at the stern from the port side (between -180°and -90°). These high concentrations could be caused by the fact that the wind captured smoke from *IB Odens* chimney and transported the smoke to the ships fore, where the sampling took place.

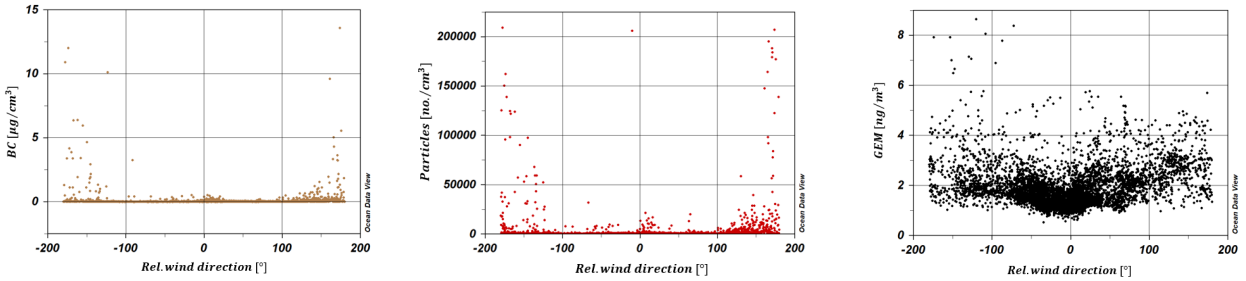

(a) (b) (c)

Figure 4.2: *BC, particles and GEM concentrations against the relative wind direction for the initial data set. Data on BC and particles provided by Paul Zieger and Linn Karlsson. When the wind comes in over the right side of the ship, starboard, the wind direction is between 0° to 180°. When the wind comes in over the left side of the ship, port, the wind direction is between 0° to -180°. The data points are 5-minute averages.*

Concentration of GEM plotted against wind speed and particles concentration are found in figure 4.3. It was observed that remarkably high concentrations of GEM were found at low wind speeds (< 4 m/s), see figure 4.3a. GEM concentrations around background concentrations were found at both high and low wind speeds. At the expedition, the wind speed ranged between $0.3 - 20.1$ m/s. Further, both high and low concentrations of GEM were found at low concentrations of particles, as depicted in figure 4.3b. When high concentrations of particles were observed, low concentrations of GEM (around background concentrations) were found. This observation indicated that the data set contained elevated concentrations that probably had not been influenced by smoke from *IB Odens* chimney.

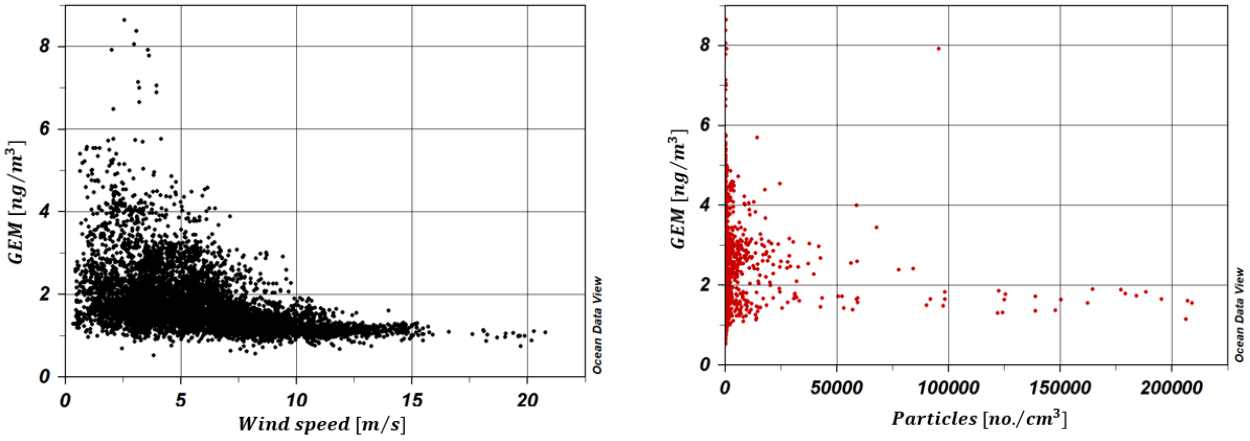

(a) (b)

Figure 4.3: *Concentration of GEM plotted against wind speed and concentration of particles for the initial data set. Wind speed and concentration of particles are 5-minute averages. Data on BC were provided by Paul Zieger and Linn Karlsson.*

The risk of contamination during ship-based measurements of mercury have been assessed in other studies. Summar et al. (2008) evaluated the risk of contamination from the exhaust gas from *IB Odens* by studying data point when the wind entered the Ship's bow at $180° \pm 60°$ or when the wind speed was less than 3 m/s. However, the authors concluded that no measurement had been influenced by the ships exhaust gas, and thus no data points were excluded from the evaluation.[53] Aspmo et al. (2006) analysed the risk of contamination during the summer expedition in the Arctic using the German ship RV Polarstern. The authors removed measurements from the data set when the wind was below 5 m/s and entered the ship at the bow between $180° \pm 45°$.[54] With regard to the initial results together with the knowledge from the past studies, it was determined to remove data points when the wind speed was lower than 4 m/s, the wind entered the ships bow at $180° \pm 90°$ or when the wind direction shifted between the port and the fore within 1 hour, see detailed description in the methodology. The settings used for removing measurements are further in the text referred to as the contamination mask. The data set remained after the removal is shown and described in the next section (4.1.2).

4.1.2 Analysis of the final Arctic GEM-data set

In figure 4.4 seen below, the remaining *GEM* measurements after the removal of data points due to the risk of contamination are plotted against time. A large number of data points have been removed, however, *GEM* concentrations above background concentrations still exist in the data set. The period 6th to 15th of August, when large fluctuation in the *GEM* concentrations were observed have been removed from the data set. The gradual build-up peak found the 23rd of August partly remains in the data set, whereas a part of the peak has been removed due to the use of the contamination mask. The gradually built up peak observed the 6th of September was found to be removed, however, elevated concentrations of *GEM* above background concentrations still exists in the data set. A majority of the data points in the suddenly high peak observed the 18th of September were removed when using the contamination mask. However, the remaining data points in the peak were still above background concentration, and these measurements were marked to be caused by contamination. A part of the other suddenly elevated peak mentioned in the initial analysis was removed and the remaining data points were marked as well to be caused by contamination. Therefore, these elevated *GEM* concentrations were determined to be excluded from the resumed evaluation.

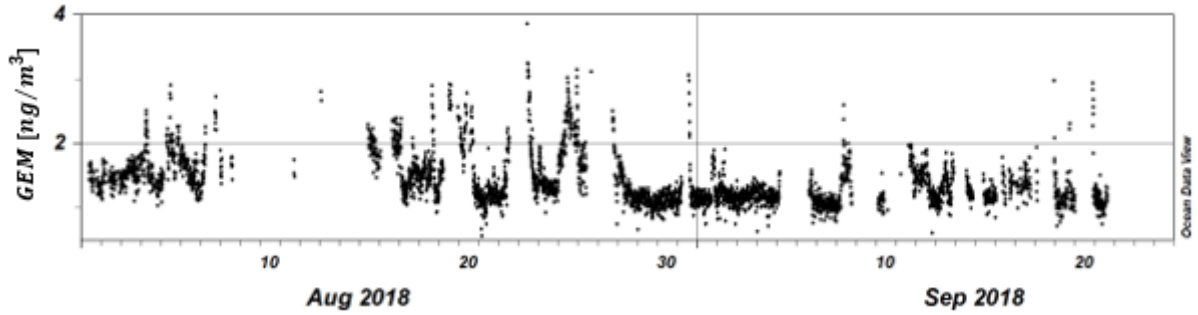

Figure 4.4: *Concentration of GEM plotted against time for the final data set. The measurements were taken during the expedition Arctic Ocean 2018 (1 of August to 21st of September).*

In figure 4.5, concentration of BC, particles, and the remaining GEM measurements in the data set are plotted against the relative wind direction. It could be observed that the high concentrations (above 6 ng/m^3) found in the initial data set, see figure 4.2, were removed, see figure 4.5. The majority of the elevated concentrations of BC in the finial data set were found when the relative wind direction entered the ship from the starboard side close to the fore, see figure 4.5a. This trend was also observed for particles, see figure 4.5b. Considering the GEM concentration, it could be observed that the measurements were distributed over all wind directions. However, the majority of the GEM concentrations around background levels were found close to 0°, that is when the wind entered the ship at the fore, see figure 4.5c.

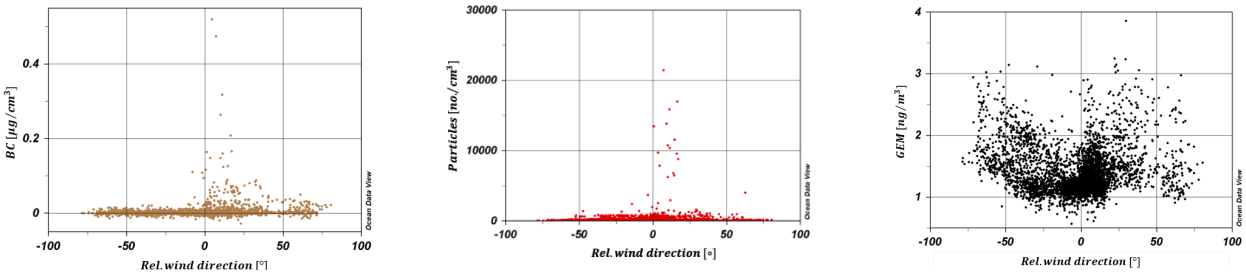

(a) (b) (c)

Figure 4.5: *BC, particles and GEM concentrations plotted against the relative wind direction for the final data set. Data on BC and particles provided by Paul Zieger and Linn Karlsson. When the wind comes in over the right side of the ship, starboard, the wind direction is between 0 to 90°. When the wind comes in over the left side of the ship, port, the wind direction is between 0 to -90°. The data on BC, particles and relative wind direction are 5-minute averages.*

In figure 4.6, the GEM concentrations in the final data set are plotted against wind speed and against the concentration of particles. In comparison with the observation seen in figure 4.3a, it was observed that a large amount of the high concentrations had been removed (see figure 4.6a). However, the same trends regarding wind speed and concentration of particles were observed as in the initial data set, low and high concentrations of GEM were found at wind speed between 4 and 8 m/s and low and high concentrations of GEM still existed at low concentrations of particles, see figure 4.6b.

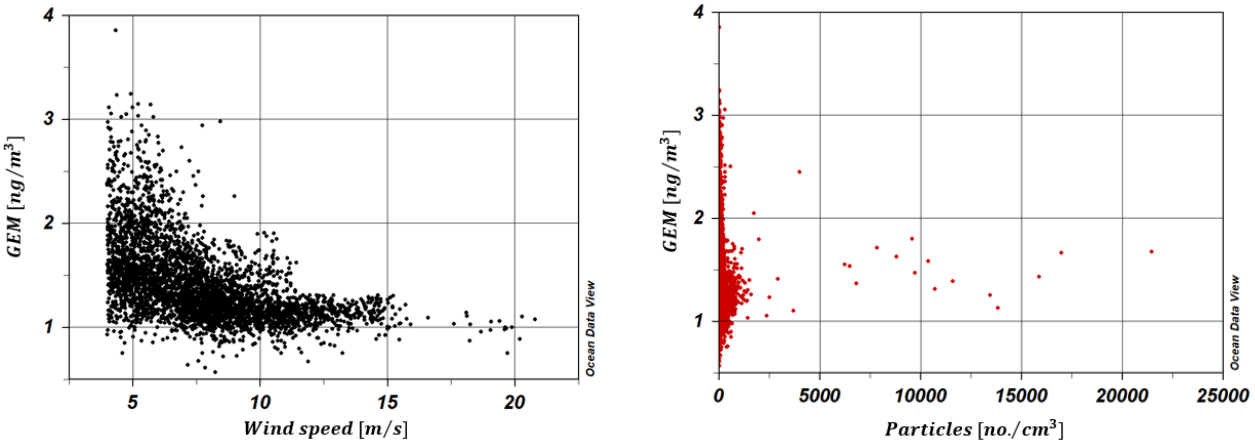

(a) (b)

Figure 4.6: *Concentration of GEM against wind speed and concentration of particles for the final data set. Wind speed and concentration of particles are 5-minute averages. Data on BC were provided by Paul Zieger and Linn Karlsson.*

When applying a contamination mask, like the one used in this study, there is a risk that too few or too many measurements are removed. Summer et al. (2008) concluded in their study that their data set did not seem to have been influenced by contamination caused by smoke from *IB Odens* chimney, and thus they choose to keep all the data in their initial data set. Sometimes this seemed to be the case in this study as well, or at least it could be argued that the contamination mask used were too strict and removed too many measurements. For instance, the gradual build up peak observed on the 6th of September was found to be removed when applying the contamination mask, as well as many measurements in the peak 23ed of August.On the other hand, there is a possibility that too few data points were removed. For instance, the results from the final data set showed that only some parts of the suddenly high peak observed on the 18th of September have been removed when applying the contamination mask. It could be argued that a more elaborated contamination mask should have been able to completely eliminate this kind of peak. A solution to both of the problems could thus possibly be to use another type of contamination mask, which is further discussed in section 4.5.3 below.

4.1.3 Analysis of elevated and depleted GEM concentrations in the Arctics

The evaluation and discussion performed for the observations of high and low *GEM* concentrations during the expedition *Arctic Ocean 2018* are found in the following section. The events considered to be of special interest are named: **A**-**H** and can be seen in figure 4.7. Each event has been analysed in relation to the meteorological parameters: air pressure, relative humidity, visibility, air temperature and solar radiation. However, it should be noted that data on solar radiation were not available for the entire expedition. In total, seven events of elevated levels of *GEM* and one event of depleted concentrations were chosen for further evaluation.

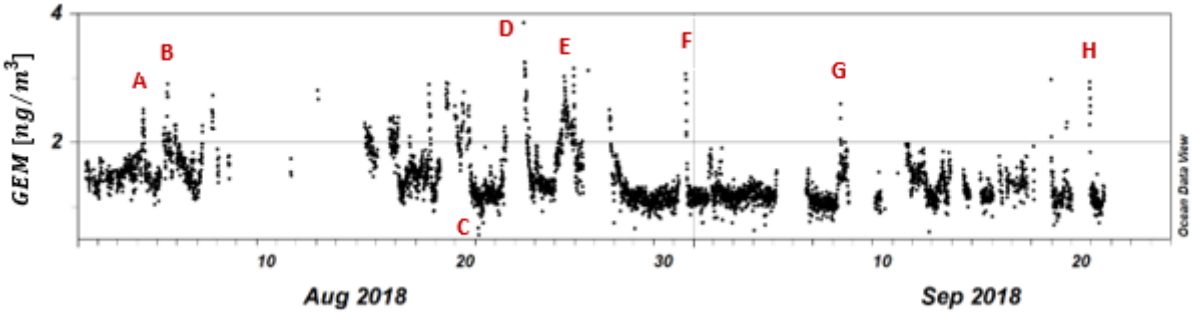

Figure 4.7: *GEM concentrations against time for the final data set with the events, A to H, pointed out, during the expedition Arctic Ocean 2018 (1 of August to 21st of September).*

As can be seen in figure 4.8a, the air pressure varied considerably during the expedition, which indicates that several different air masses were sampled during the expedition. In figure 4.8b, it can be seen that the relative humidity during the expedition was stable and high (around 100 %). This is most likely explained by movements of humid air masses from southern latitudes. Figure 4.8c shows the visibility during the expedition and based on this plot it could be concluded that the visibility was alternating between clear conditions and foggy conditions only a few meters visibility. Regarding the air temperature, see figure 4.8d, a rather stable temperature around 0°C was observed for most of the time at the expedition. Stable temperatures around 0°C is a commonly occurring phenomenon during the summer months in the polar regions as incoming radiation melts ice and snow instead of heating the atmosphere.

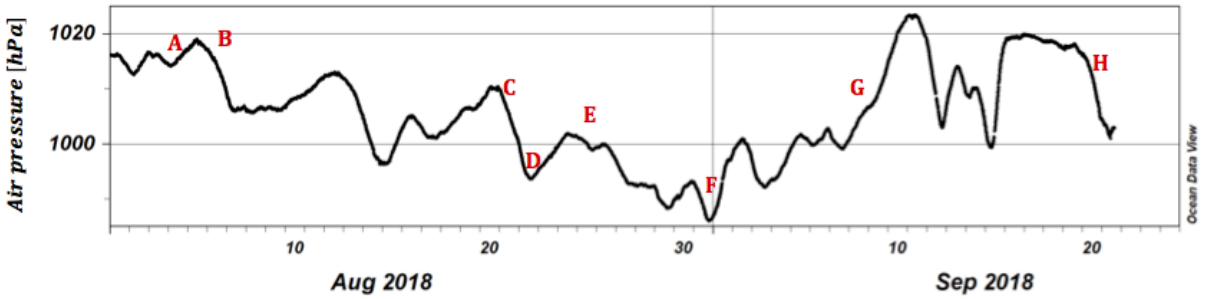

(a)

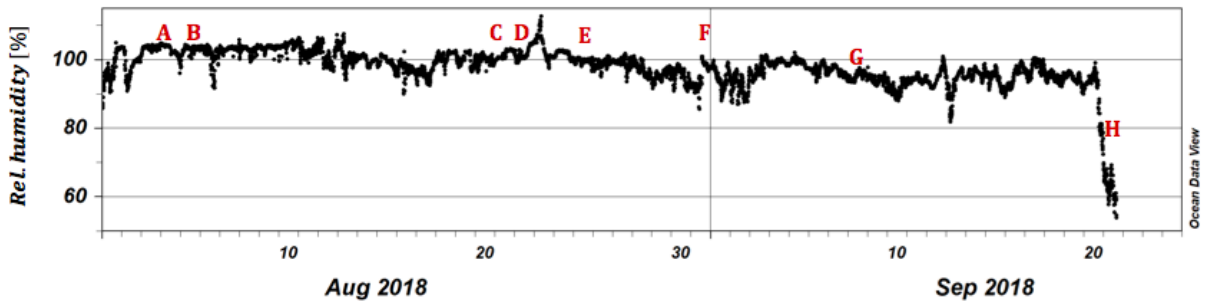

(b)

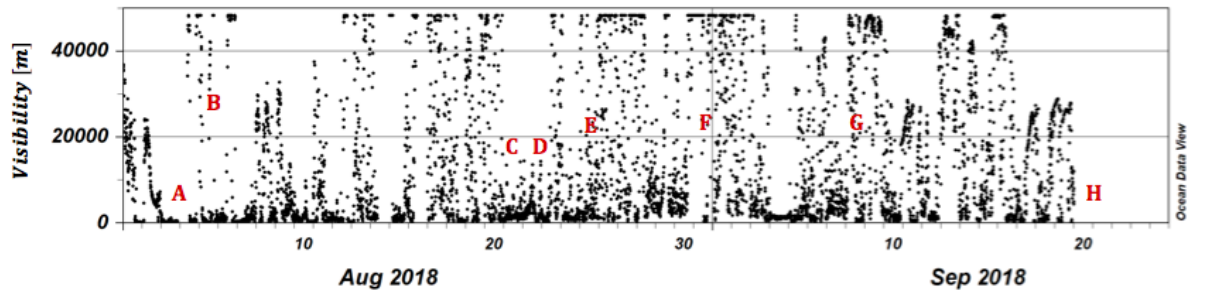

(c)

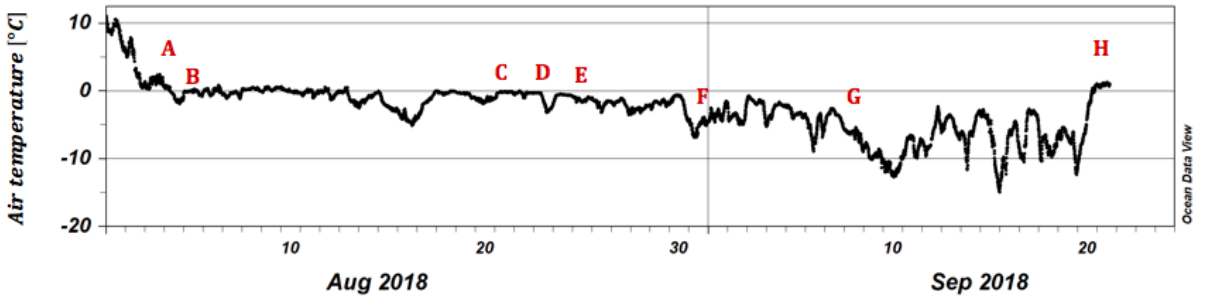

(d)

Figure 4.8: *Air pressure, relative humidity, visibility and air temperature plotted against time during the expedition Arctic Ocean 2018 (1st of August to 21st of September).*

Measurements of incoming shortwave radiation were taken during the time when *IB Oden* was connected to the ice sheet (18 of August - 14 of September), see figure 4.9. Several peaks of incoming solar radiation were observed, with the highest peak reaching a maximum above 300 W/m^2.

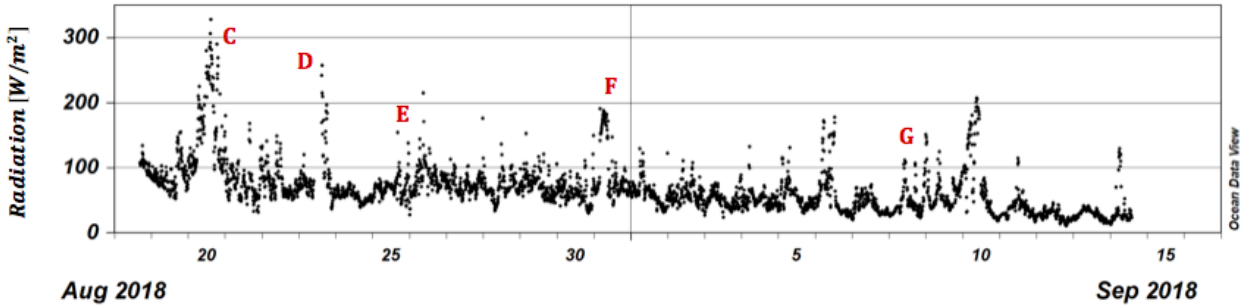

Figure 4.9: *Incoming short-wave radiation provided by Ian Brooks plotted against time, during the time IB Oden was docked to an ice sheet (18 of August - 14 of September).*

For each event, **A**-**H** four types of backward trajectories were generated using the software *HYSPLIT*. 5 days- and 28 days trajectories were preformed for analysing the origin of the air masses and for capturing local and global mercury sources, respectively. Trajectories on different heights of the PBL were constructed for tracing air masses backward in time from the exact time of the elevated measurements. The aim with using these trajectories was to study the specific origin of certain air masses and at the same time get a sense for the uncertainty in the tracing. Cluster analyses were performed to get a wider picture of the origin of the air masses during the time of the events and during the build-up of the elevated and depleted measurements. The figures for the 5-day trajectories are found in connection to each event. The 28-days trajectories are analysed and discussed in section *28-days trajectories for the events A-H* while the pictures are found in Appendix A.

Event A - The 4th of August

The first period of elevated concentrations were observed in the morning on the 4th of August reaching a maximum concentration of 2.52 ng/m^3, see figure 4.7. During this event, a period of low pressure was present and the relative humidity was decreasing. Data regarding visibility was lacking and the temperature was observed to be somewhat above what was considered as typical for the expedition (stable at 0°C), see figure 4.8. No data regarding radiation was available during this event.

The 5-days three-level backwards trajectories suggesed that sampled air masses originated from the ocean south of Svalbard and to have passed over Svalbard before reaching the measurement point at 82.7°N and 15.4°E, see figure 4.10a. The trajectories follow each other, which is an indication for high reliability in the tracing. The cluster analysis showed that the majority of the winds originated from the south or possibly from the west, passing over Greenland before reaching the measurement site, see figure 4.10b. These GEM measurements were taken in the MIZ and since no winds seem to have originated from the north, it was concluded that the winds either originated from open water, land or possibly the MIZ area. Several of the air masses studied seem to have passed over land, see figures 4.10a and 4.10b, indicating a possibility that anthropogenic activities could have been responsible for the elevated levels of mercury observed. However, it should be noted that these land areas have very few human activities and almost no industrial sites. They mostly consists of snow and ice covered tundra. Thus, releases of mercury from melting snow- and ice-packs would be a possible explanations to the observed elevated levels of GEM concentrations at this time of the year. Also, evaporation from the open ocean or the MIZ could be other possible explanation to the elevated GEM concentrations observed.

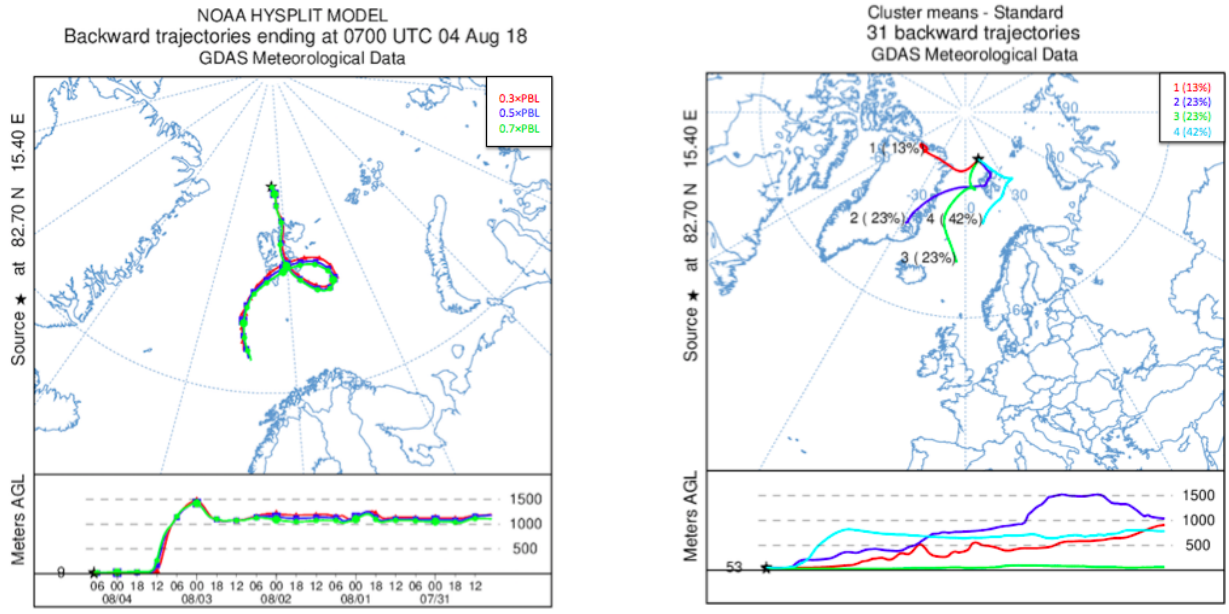

(a) (b)

Figure 4.10: *5-day backward trajectories and cluster analysis for the elevated GEM measurements found the 4th of August. In (a), trajectories for 3 different heights, 0.3, 0.5 and 0.7*PBL, are shown, and in (b) cluster analysis is shown for the height of 0.5*PBL. Meters AGL refers to meters above ground level. The percentages in the cluster analysis does not add up because of round-off error.*

Event B - The 5th of August

A second *GEM* peak was observed at midday on the 5th of August. This peak reached a maximum of 2.9 ng/m^3, see figure 4.7. During this event, the air pressure first peaked followed by a rapid decrease. At the same time, a stable relative humidity just above 100 % and a stable temperature around 0°C was observed. An apparent change in visibility was detected, where low visibility was found during the build-up of the peak, meaning foggy conditions, and when *GEM* reached its maximum and started to decrease, visibility increased significantly again, see figure 4.8. During this event no radiation data were available. The meteorological conditions present during the time of the event (**B**), large changes in pressure and visibility, suggests that new air masses were introduced to the area at this time.

Kamp et al. (2018) discussed trends and correlations between meteorological parameters and *GEM* concentrations in their study *Fluxes of gaseous elemental mercury (GEM) in the High Arctic during atmospheric mercury depletion event (AMDEs).*[55] The authors observed a correlation between a rapid increase in *GEM* and a sudden drop in air pressure which then return back to around previous observed levels. Simultaneously, the air temperature seem to first increase before the peak and the decrease again. Some similarities with the observations made by Kamp et al. (2018), a rapid decrase in pressure, were thus found when analysing the air pressure relation to *GEM* during event**B**.

The 5 days trajectories generated for event **B** are shown in figure 4.11. In figure 4.11a, the trajectories generated for the three different heights of the PBL show that air masses seem to have originated from the Canadian Arctic side, passing over a region of continuous ice, before reaching the measurement point at 84.5°N and 28.7°E. The trajectories follow each other closely. However, according to the cluster analysis, see figure 4.11b, only 13 % of all the air masses seem to have originated from the Canadian Arctics. According to the cluster analysis, the majority of the winds should originate from more southern latitudes. Thus the air masses could have originated from all different geographical regions (MIZ, continouns ice, open ocean).

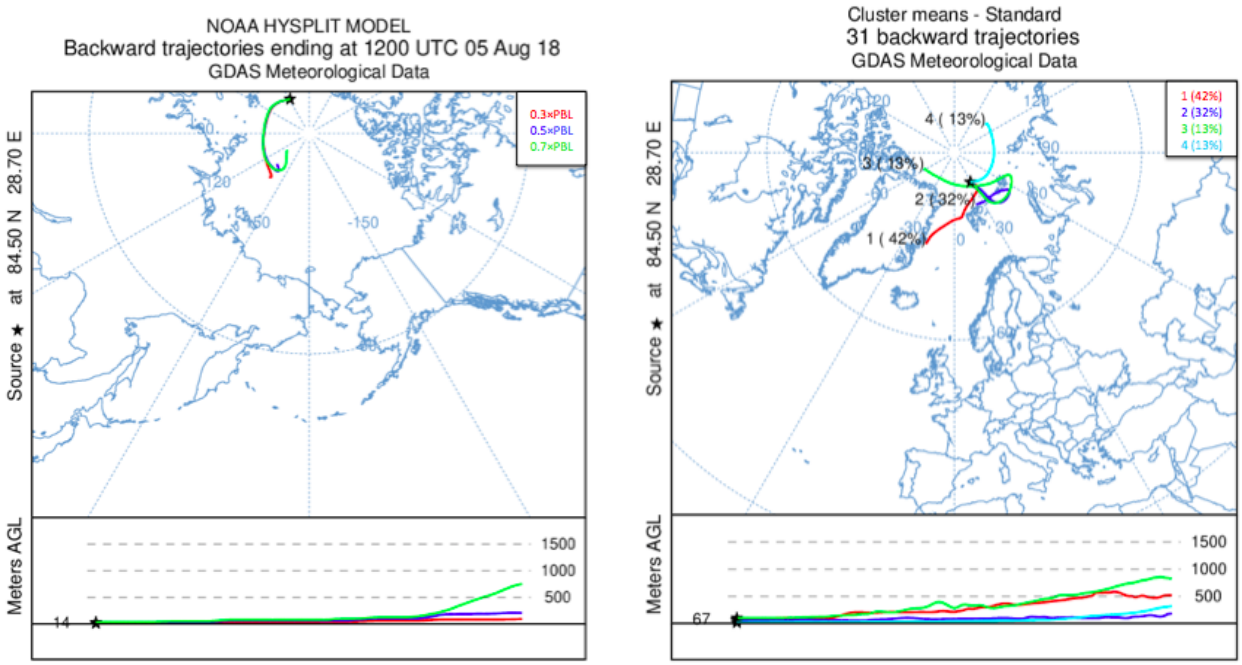

(a) (b)

Figure 4.11: *5-day backward trajectories and cluster analysis for the elevated GEM measurements the 5th of August. In (a), trajectories for 3 different heights, 0.3, 0.5 and 0.7*PBL, are shown, and in (b) cluster analysis is shown for the height of 0.5*PBL. Meters AGL refers to meters above ground level.*

Looking at the 5-days trajectories, the elevated levels of mercury would most likely be explained by evaporation of mercury from open ocean or from the MIZ. Furthermore, it should be observed that three helicopter flights were performed on the 5th of August, which possibly could cause a risk for that contaminated air could have been sampled. However, when looking at the character of the peak, contamination from the helicopter should not be considered as probable explanation to the elevated measurements. Contamination caused by one, or several of the helicopter flights should have resulted in one, or several suddenly high peaks.

Event C - The 21st of August

At early morning on the 21st of August, a section of GEM measurements lower than background concentrations were observed. A minimum concentration of 0.57 ng/m^3 was observed at 04:35 am. These observations of low GEM levels can be referred to as a half atmospheric mercury depletion event, see figure 4.7.

At the time of the event, pressure decreased, humidity and temperature were stable, and visibility was low, see figure 4.8. Incoming shortwave solar radiation was high and stable around 100 W/m^2, see figure 4.9. The usual conditions that, according to previous studies, have been present at this kind of depletion events are described in the theory section 2.5.1. One of the most discussed parameters in earlier studies is the air temperature, a range of different maximum temperatures for when the so called AMDEs can occur have been suggested. For example, Skov et al. (2004) suggested a maximum temperature of $-4°C$, and studies like *Antarctic winter mercury and ozone depletion events over sea ice* observed a clear correlation between the frequency of AMDEs and low air temperatures.[27] The temperature at the moment of the depletion, August 21st, was around 0°C. Thus, higher than earlier suggested maximum air temperatures.

Depletion events are as explained in the theory section often correlated with high halogen levels or BrO levels and low levels of O_3. Br is thought to be the most common first stage oxidant of GEM but since it also acts as an oxidant of O_3 a correlation between low O_3 levels and depletion events of GEM are often seen. O_3 levels measured during the expedition can be seen in figure 4.12. At the time of the depletion event, no decrease in O_3 concentrations were observed, thus no correlation between low GEM and low O_3 levels could be observed.

Neither could unusually high levels of BrO be identified in the Arctic region during this time. *BrO* levels for the time of the depletion event are seen in figure 4.13, and levels for the days before the event are found in Appendix A.5.

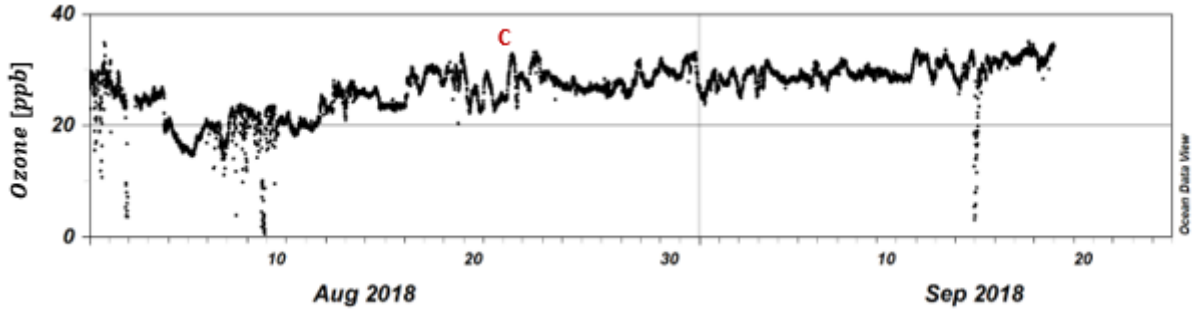

Figure 4.12: *Ozone concentration plotted against time during the expedition Arctic Ocean 2018 (1 of August to 21st of September). Measurements were provided by Julia Yvonne Schmale.*

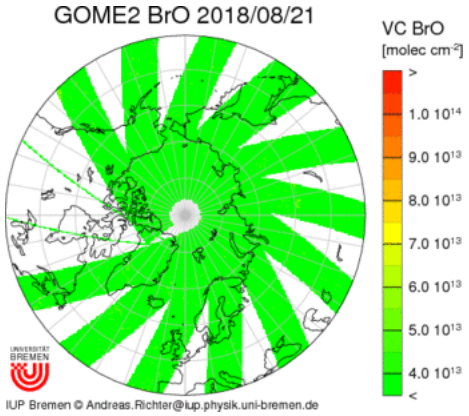

Figure 4.13: *BrO concentrations present during August 21st in the Arctic Environment. The picture was obtained from the University of Bremen.*

The 5-days trajectories generated for event **C** can be seen in figure 4.14. The trajectories on three different heights indicated that air masses originated from the Canadian side of the Arctics and thus from an area mainly consisting of continuous ice, see figure 4.14a. However, when looking at the 5 days cluster analysis, figure 4.14b, a large spread in the origin of the air masses were observed, indicating that air masses possibly could originate from all the different geographical regions.

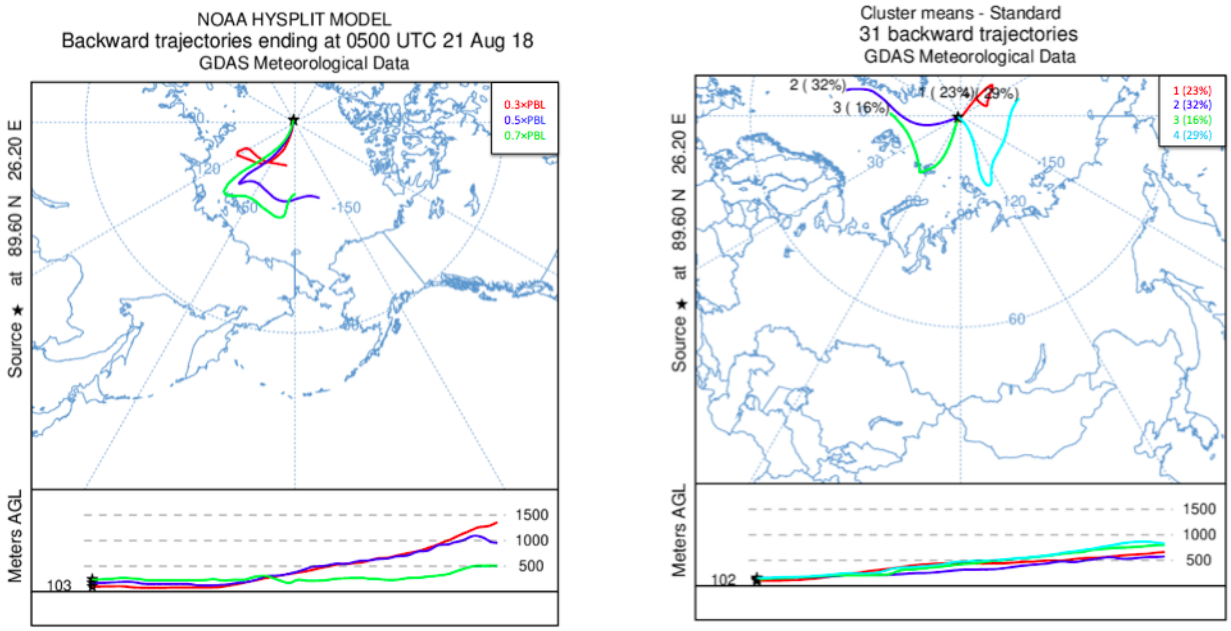

(a) (b)

Figure 4.14: *5-day backward trajectories and cluster analysis for the depleted GEM measurements the 21st of August. In (a), trajectories for 3 different heights, 0.3, 0.5 and 0.7*PBL, are shown, and in (b) cluster analysis is shown for the height of 0.5*PBL. Meters AGL refers to meters above ground level.*

It can be concluded that the typical conditions and correlations earlier seen in relation to AMDEs, cold temperatures, ozone depletion and elevated halogen levels were not observed during the event. Another phenomenon that has been observed in connection to AMDEs is that observations of elevated levels of GEM have been made at the place for the depletion, or in the close surrounding, within days after an event.[56] The peak the 23rd of August (see figure 4.7), or any of the other observed peaks found at this geographical region, would thus support this earlier observed phenomena, further discussed in event **D** below.

Possible explanations to the observed low concentrations of GEM 21st of August could possibly be movements of already depleted air masses. The rather drastic change in pressure during the day of the event, see figure 4.8a, supports the idea that new air masses arrived at the time of the event. Other possible explanations could be oxidation by other agents such as $Cl\cdot$ and $I\cdot$. Yet, this would most likely mean that depletion of O_3 would have taken place.

Event D - The 23rd of August

At forenoon the 23rd of August the highest GEM peak in the final data set was observed. The peak was building up for several hours and reach a maximum of 3.86 ng/m^3, see figure 4.7. Simultaneously with the build up of the high GEM concentrations, a sudden peak in the otherwise stable relative humidity was observed, reaching the highest levels during the expedition, see figure 4.8b. The pressure was increasing during the whole event, visibility was low and temperature dropped, see figure 4.8. In figure 4.9, it can be seen that during the build up of peak, an increase in incoming solar radiation occurred. However, there is a data gap regarding radiation for the remaining part of the peak 23rd of August.

The 5-days trajectories for event **D** are found in figure 4.15. The three-level trajectories generated for the event indicated that the sampled air masses originated from the south of the sampling location (89.5°N and 5.2°E). The 0.5 and $0.7 \cdot PBL$ trajectories reach all the way down to Scandinavia, see figure 4.15a. The 0.7 ·PBL trajectory showed that air masses could have originated from the east coast of Sweden and passed over Finland before heading north. In Finland anthropogenic activities such as coal production and gold mining take place and could thus be possible sources to the elevated GEM concentrations.[57][58]

However, when studying the cluster trajectories in figure 4.15b, it could be be concluded that the majority of the air masses should originate from the Canadian Arctic side. However, some winds were also, according to the cluster analysis, originating from the south relative the measurement point. Consequently, according to the 5-days trajectories, the air masses could possibly have originated from all different geographical regions including land.

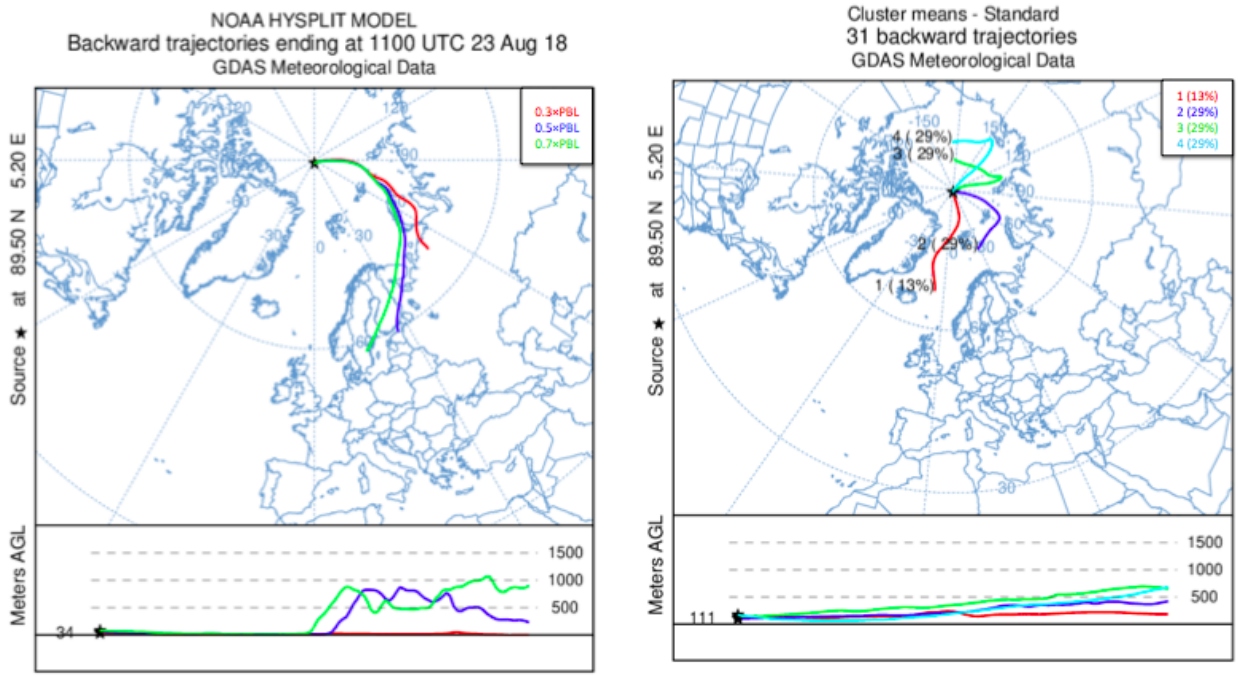

(a) (b)

Figure 4.15: *5-day backward trajectories and cluster analysis for the elevated GEM measurements the 23st of August. In (a), trajectories for 3 different heights, 0.3, 0.5 and 0.7*PBL, are shown, and in (b) cluster analysis is shown for the height of 0.5*PBL. Meters AGL refers to meters above ground level.*

As mentioned in event **C**, 21st of August, earlier observations have shown a correlation between events with depleted GEM concentrations and elevated concentrations in the surrounding area within a few days after the depletion. This trend is believed to be caused by re-emission of previously deposited mercury. GEM that has been oxidised to GOM and deposited is by solar radiation reduced back to GEM and re-emitted to the atmosphere. This phenomenon was for example observed by Kamp et al. (2006).[55]

The rather high radiation (258 W/m^2) and the peak in humidity observed at the time for the event, support the idea that the elevated levels of GEM possibly could originate from re-emission of the earlier observed depletion that took place 21st of August. The elevated levels of GEM observed during event **D** could thus possibly be explained by a combination of re-emission of GEM from ice- and snow-packs around the North Pole and long range transport of GEM from other regions. However, to support this hypothesis measurements of mercury in snow and ice in the area of the event would be necessary, along with measurements of other forms of mercury in the atmosphere. Further, it should be mentioned that one helicopter flight was performed during this day, which possibly could cause contamination. When taking the character of the peak into account, contamination from the helicopter should not be considered as probable explanation to the elevated measurements.

Event E - The 25th of August

A new section of elevated GEM concentrations were observed at midday the 25th of August, with a maximum concentration of 3.02 ng/m^3, see figure 4.7. During this event, pressure first dropped and then increased again in the end of the event. Relative humidity and air temperature remained stable while the visibility was

fluctuating considerably, alternating between high and low values, see figure 4.8. Likewise, a large variation in the solar radiation were observed at this time, however, the solar radiation could be considered as low during this event, see figure 4.9.

The observed behaviour of the pressure during this event have similar characteristics to what was observed by Kamp et al. (2018). With increased *GEM* concentrations, the pressure decreased and when *GEM* started to decrease again pressure increased. Further, Kamp et al. (2018) also observed that temperature increased and then decreased again along with the peak of *GEM*. However, this type of pattern could not be observed during event **E**. The sudden decrease in pressure could indicate that new air masses were temporally introduced at the sampling area.

Trajectories generated for event **E** can be seen in figure 4.16. From the 5-days, three-level trajectories, it can be concluded that these approximations hold a rather high uncertainty since the trajectories only follow each other in the beginning and then turn of in different directions, see figure 4.16a. The cluster analysis seen in figure 4.16b indicated that the majority of the air masses originated from the Canadian Arctic side, mainly from areas of continuous ice. However, as can be seen in figure 4.16b, air masses could possibly also have originated from land area, the MIZ region or open water. The land masses of consideration are areas with few anthropogenic activities.

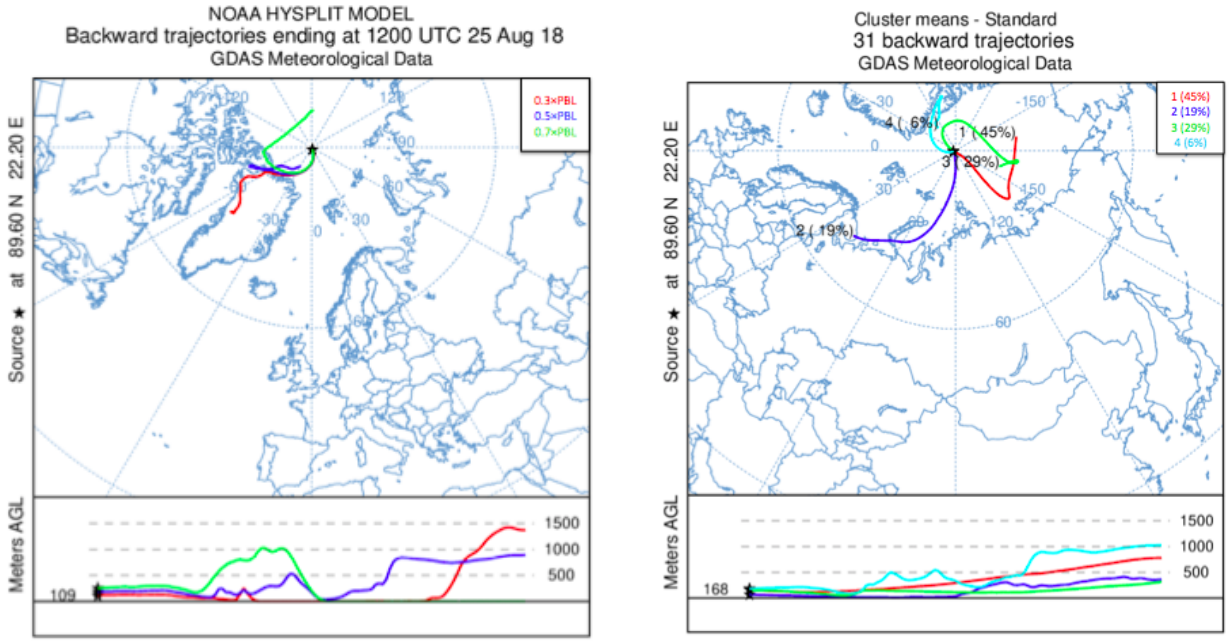

(a) (b)

Figure 4.16: *5-day backward trajectories and cluster analysis for the elevated GEM measruments the 25st of August. In (a), trajectories for 3 different heights, 0.3, 0.5 and 0.7*PBL, are shown, and in (b) cluster analysis is shown for the height of 0.5*PBL. The percentages in the cluster analysis does not add up because of round-off error. Meters AGL refers to meters above ground level.*

Based on the different trajectories it was difficult to find any obvious sources and explanations for the elevated measurements observed on the 25th of August. Air masses could originate from all different geographical regions including land, but the trajectories holds a rather large uncertainty. What possibly could be concluded was that a majority of the air masses originate from the Arctic region. Evaporation of earlier deposited *GEM* from sea ice could possibly be an explanation for the elevated measurements, however the solar radiation at the measurement site was relatively low at this time. Anyhow, the evaporation could have taken place at a different location and by air masses that have been introduced to the sampling area.

Event F - The 31st of August

The *GEM* peak during midday the 31st of August reached a maximum level of 3.06 ng/m^3, see figure 4.7. During this event, the air pressure dropped and reached the lowest level for the whole expedition and then increased again when the *GEM* concentrations started to decrease, see figure 4.8a. The change in pressure indicated that new air masses probably were introduced at the sampling area. Simultaneously, a stable but low for the expedition, relative humidity was observed with a sudden drop in the middle of the *GEM* peak. The visibility was high and air temperature was a bit lower than what could be assumed as standard for the ice sheet floating time of the expedition, see figure 4.8. A peak in solar radiation could also be observed during this event, see figure 4.9. Thus, also during this event similarities with what Kamp et al. (2018) observed regarding air pressure and *GEM* behaviour could be found.[55]

The 5-days trajectories generated for event **F**, can be seen in figure 4.17. In figure 4.17a, the 5-days three-level trajectories showed that air masses originated from the south and travelled along the coast of Greenland before reaching the measurement point (89.5°N and 72.5°E). It can be observed that the trajectories follow each other and thus it can be concluded that the estimation of the origin holds a high confidence. The cluster analysis for the same event showed that air masses originated either from the south or from the north-west relative the measurement point, see figure 4.17b. Thus, the air masses could have originated from all of the different geographical regions, including coastal areas.

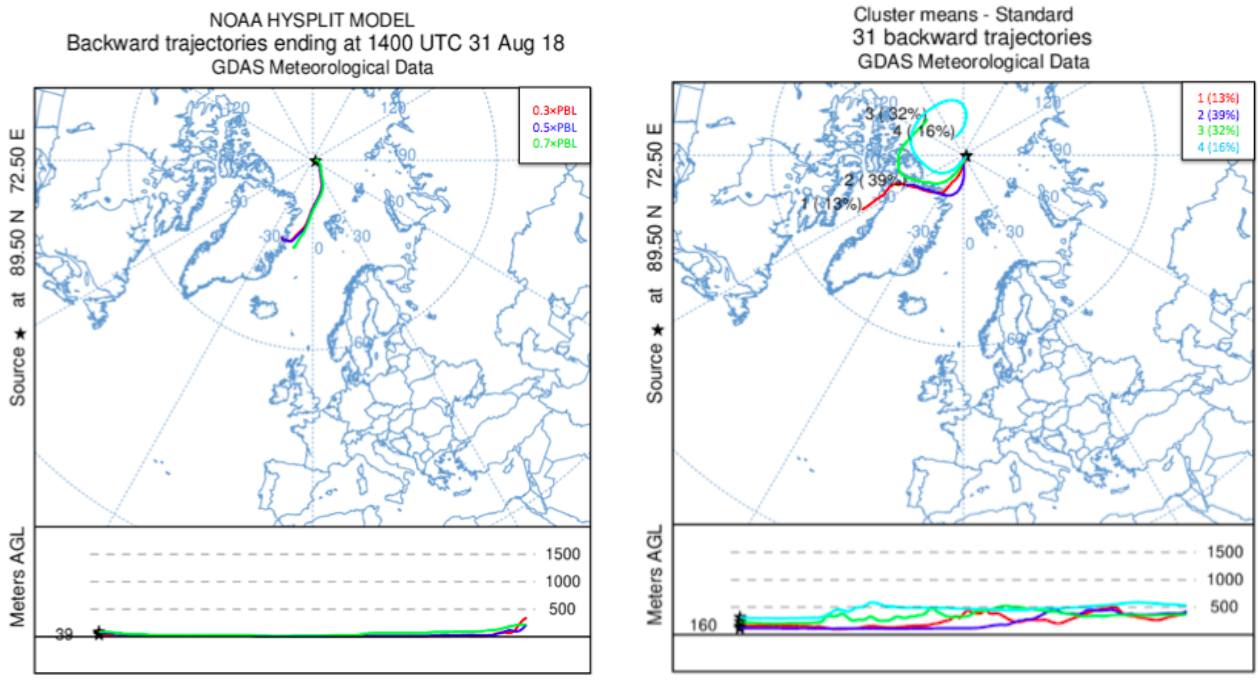

(a) (b)

Figure 4.17: *5-day backward trajectories and cluster analysis for the elevated GEM measurements the 31st of August. In (a), trajectories for 3 different heights, 0.3, 0.5 and 0.7*PBL, are shown, and in (b) cluster analysis is shown for the height of 0.5*PBL. Meters AGL refers to meters above ground level.*

The elevated *GEM* concentrations observed during the event 31st of August could have originated from all of the different geographical regions, including land. Thus explanations to the elevated levels of *GEM* could be found in processes like re-emissions of earlier deposited *GEM* on snow, ice and oceans. Furthermore, a risk for contamination of the sampled air masses arises from the fact that the ship was turned around at 10 am and a helicopter flight was conducted this day.

Event G - The 8th of September

At forenoon the 8th of September elevated *GEM* concentrations were once again observed, reaching a maximum concentration of 2.6 ng/m^3, see figure 4.7. At the time of the peak, the air pressure was building up and reached the highest level observed during the whole expedition, indicating that new air masses were introduced at the area. A small increase in the relative humidity and large fluctuations in visibility were observed. The air temperature was decreasing and reached levels colder than the average for the expedition, see figure 4.8. At the same time, a small peak in solar radiation was observed, see figure 4.9.

The 5-days backward trajectories for the event are found in figure 4.18. Figure 4.18a illustrates the 5-days, three-level trajectories, which indicates that the air masses seem to have originated from the Canadian side of the Arctic. The trajectories follow each other in the beginning but deviates at the end. The cluster analysis seen in figure 4.18b support the idea that air masses could have originated from the Canadian side of the Arctics. However, the air masses seems to have been circulating in the Arctic region and along the Russian coast before reaching the sampling location at 88.7°N and 45.9°E. During this event, the air masses were most likely originating from areas of continuous ice.

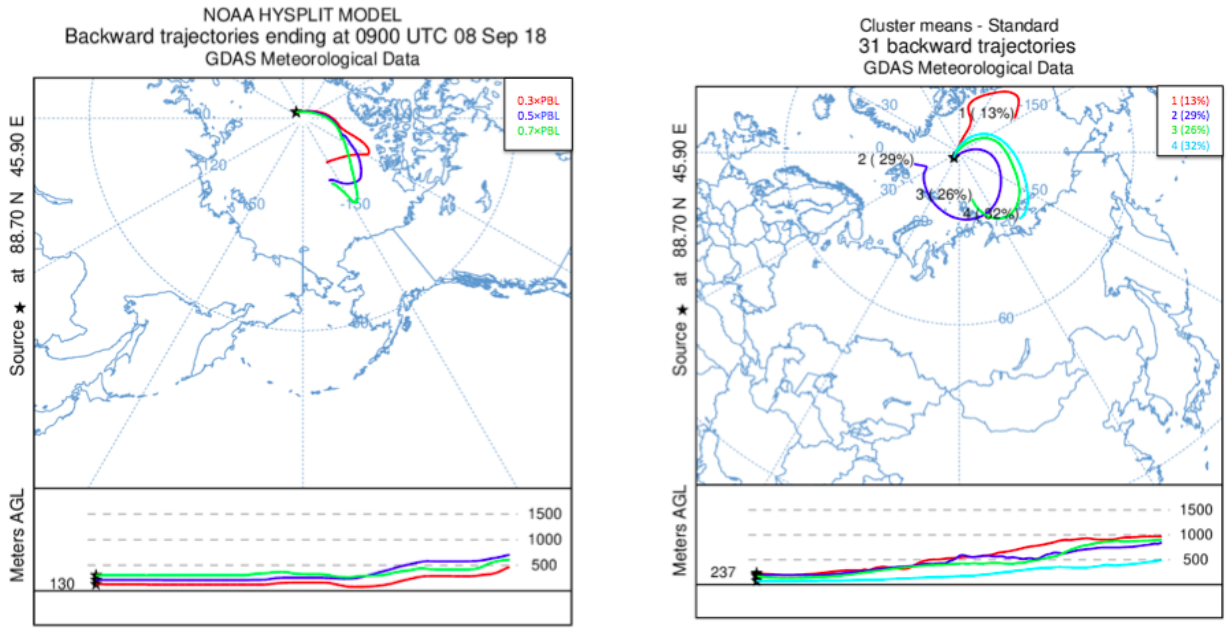

(a) (b)

Figure 4.18: *5-day backward trajectories and cluster analysis for the elevated GEM measurements the 8th of September. In (a), trajectories for 3 different heights, 0.3, 0.5 and 0.7*PBL, are shown, and in (b) cluster analysis is shown for the height of 0.5*PBL. Meters AGL refers to meters above ground level.*

When considering the meteorological parameters together with the trajectories, a possible explanation to the elevated *GEM* concentrations could be that new air masses that contained elevated *GEM* levels were introduced to the sampling area. The elevated levels of *GEM* could originate from evaporation from melting ice.

Event H - The 20th of September

During the evening, just before reaching the dock in Longyearbyen at Svalbard 20th of August, a new period of elevated *GEM* measurements were observed. The peak reached a maximum value of 2.94 ng/m^3, see figure 4.7. At the time of the event, pressure and humidity were decreasing and the temperature was rather stable around 0°C. No data regarding visibility was available at this time, see figure 4.8. Neither data regarding solar radiation existed at this time of the expedition.

The 5-days trajectories for the event are found in figure 4.19. Trajectories created for 0.3 and $0.5 \cdot PBL$ follows each other and air masses seem to have originated from the north, somewhere around the North Pole, while the $0.7 \cdot PBL$ trajectory seem to originate from the Canadian side of the Arctic, see figure 4.19a. All of the three-level trajectories seem to have passed over all geographical regions before reaching the sampling point at 79.7°N and 9.0 °E. The cluster analysis for 5-days tracing supports that the air masses could have originated from an area close to the north pole, or possibly from the area north-east of Svalbard, see figure 4.19b. The majority of the winds seem to have originated from areas of continuous ice but also the MIZ could be a possible source since the measurements were taken in the end of the MIZ.

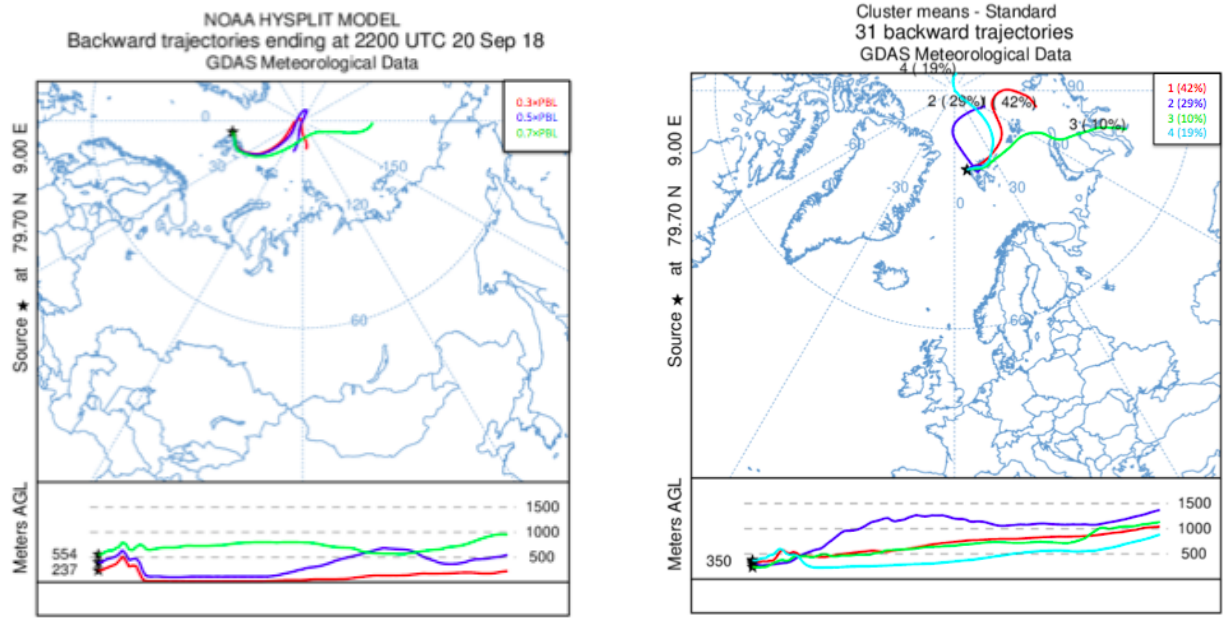

(a) (b)

Figure 4.19: *5-day backward trajectories and cluster analysis for the elevated GEM measurements the 20th of September. In (a), trajectories for 3 different heights, 0.3, 0.5 and 0.7*PBL, are shown, and in (b) cluster analysis is shown for the height of 0.5*PBL. Meters AGL refers to meters above ground level.*

Reasons for the observed elevated levels of *GEM* 20th of August are most likely found in the Arctic Region. Evasion of *GEM* from water within the MIZ or re-emission of earlier deposited mercury from snow- and ice-packs could be possible reasons to the high *GEM* concentrations. The observed decrease in pressure supports the idea that new air masses were introduced at this time at the sampling area.

28-days trajectories for the events A-H

For all the different events (**A-H**) long range transport of *GEM* was studied by creating 28-days backwards trajectories. Also these trajectories were created on three levels ($0.3, 0.5$ and $0.7 \cdot PBL$) and cluster analyses were preformed for the height of $0.5 \cdot PBL$. Figures of the generated trajectories for the events are found in Appendix A.2.

As explained in the theory section 2.8.2, the uncertainty in the trajectories created with *HYSPLIT* increases with the travelled distance, thus these trajectories contain a relatively high uncertainty. However, since mercury has a long residence time in the atmosphere, these long trajectories should be able to give indications of possible emission sources on a regional and global scale.

The majority of the created 28-days trajectories indicated that air masses, during the time of the expedition, frequently were circulating in the Arctic area or in the near surroundings. However, some of the trajectories generated for the events with elevated concentrations showed that air masses originated from, or were passing over, distant areas such as the the northern parts of United States (see figure A.3a, A.4b, A.7a). The 31st of

August, one of the three-level trajectories ($0.5 \cdot PBL$) indicated that air masses possibly could have originate from the central parts of Sweden and that air masses were passing over the northern parts of Russia before entering the Arctic region, see Figure A.8a. The 20th of September, one of the three-level trajectories showed that air masses possibly originated from areas around Japan (see figure A.10a).

The majority of the 28-days trajectories indicated that air masses could have originated from all different geographical regions including land. However, only the trajectories that passed over the United States, Sweden and the one that originated from Asia (Japan) originated from areas with high anthropogenic activity. These air masses could have contained elevated concentrations of GEM caused by human activity. Thus the elevated measurements seen 4th, 5th, 25th and the 31st of August and 20th of September could possibly be explained by long range transport of GEM, or by a combination of long range transport of air masses containing elevated GEM concentrations and re-emissions of GEM from oceans, ice or snow.

During 21st of August, event **C**, when depleted concentrations were observed. Both the 28-days three-level trajectories and the 28-days cluster analysis showed a possibility of that air masses could have originated from areas in the Northern Atlantic ocean, along the west coast of Norway and all the way down to Great Britain, see figure A.5a and A.5b. Depletion of GEM could thus possibly have taken place anywhere along the trajectories and travelled up to the North Pole with the air masses. However, depleted air masses of GEM are often explained by the phenomena AMDE, which is thought to depend on several conditions often found in the arctic environment. That depleted air masses would have travelled from warmer latitudes are however unlikely according to this theory. Further, BrO maps were studied to see if elevated levels possibly could be seen along the trajectories but no such observations could be made.

Summary of the observed trends for event A-H

As explained above several periods of elevated GEM concentrations reaching above 2 ng/m^3 (event **A-B, D-H**) were observed during the expedition. Meteorological data (air pressure, relative humidity, visibility air temperature and solar radiation) in combination with the events**B-H** supports the fact that there is a link between elevated concentrations of GEM and introduction of new air masses. The relative humidity was high during all the events, except for event **H** that took place on the final day of the expedition. During event **D**, the highest GEM peak during the expedition, as well as the highest humidity of the expedition were observed. Visibility varied largely during the expedition and no obvious trends for when elevated GEM measurements took place in regard to visibility could be seen. The air temperature was stable around 0°C for most of the time during the expedition and thus it was hard to see any relation between the GEM concentrations and the temperature. Solar radiation data were only available during the time when *IB Oden* was connected to the ice sheet (event **C-G**). During all of these events, except event **E**, a clear correlation between the events and increased solar radiation was observed. The increased solar radiation in combination with increased concentrations of GEM support the idea that mercury was evaporating from surfaces such as the ocean and the melting snow and ice. The introduction of new air masses caused by change in pressure and evaporation caused by increased solar radiation could both, respectively, or in combination be explanations to the elevated GEM concentrations. However, the observed peaks in solar radiation and the stable temperature indicate that melting of snow and ice took place at the sampling region and thus a lot of GEM could have evaded from melting the snow- and icepacks to the atmosphere causing the elevated GEM levels.

The increase in solar radiation during the depletion (event **C**) would support the general AMDE phenomena. However, since no elevated levels of BrO were observed, this phenomenon was not seen as a probable explanation. Therefore, the low GEM concentrations were believed to be caused by the introduction of new air masses that could have been depleted at another geographical location.

All of the 5-days trajectories, except the $0.7 \cdot PBL$ the 23rd of August (event **D**), stayed within the polar region. During event **D**, 0.7· the trajectory reached outside the polar region, through Finland and into the southern parts of Sweden. As a consequence the elevated measurements during event **D** could be explained by anthropogenic activity while the rest of the observed elevated measurements more likely could be explained by mercury that evades from Arctic surfaces. Regarding the 28-days trajectories, the majority of the trajectories were staying within the polar region. However, most of the events had some trajectory that passed over areas with higher anthropogenic activity. The uncertainty in these long trajectories make it hard to draw any conclusions. Since few of the trajectories indicated that air masses were likely to originate from areas with high

anthropogenic activity, the probability for the elevated GEM concentrations to be caused by human activity could be considered as low. However, during some of the events, a combination of evasion of mercury from the ocean, snow and ice and long range transport of GEM were considered as possible explanations. There is a probability that the re-emissions that are believed to taking place from oceans, snow and ice, originate from earlier deposited mercury that from the beginning have originated from anthropogenic activities. As mentioned in the theory part 2.3, 60 % of the global mercury is predicted to be caused by re-cycling of earlier deposited mercury.

4.2 GEM concentrations during the transit south

This section begins by presenting the result from the initial analysis of the data set obtained when *IB Odens* cruised south from Svalbard to Helsinborg. The initial evaluation intended to examine the data set and the risk of possible contamination. Thereafter, the results of the the final analysis are presented. Finally, the results from the analysis carried out for the specific events of interest (elevated concentration of GEM) will be presented. The parameters assessed in the analysis are air pressure, relative humidity and air temperature, in relation to GEM concentration.

4.2.1 Analysis of the initial GEM-data set during the transit south

The GEM measurements taken during the transportation route Svalbard to Helsingborg are seen in figure 4.20. It was observed that a majority of the data points reflect background concentration in the Northern Hemisphere, $1.5 - 1.7\ ng/m^3$. A trend in increased concentrations of GEM were observed from the 2nd of October, see figure 4.20. One potential explanation to the increased concentrations of GEM from the 2nd of October and forwards could be the increase in surrounding anthropogenic activities releasing mercury, located in Norway, Sweden and Denmark. Other European countries further south, for instance The United Kingdom and Germany also have activities releasing mercury that could have caused the elevated concentrations of GEM.

Several time periods with elevated concentrations were found in the data set, some of them had a gradual build up, meanwhile, at some periods the GEM concentrations suddenly peaked. For instance, the peak that lasted from 24th to 25th of September, had a gradual build up, meanwhile, the peak on the 27th of September had a gradual build up with a suddenly high peak within it, see figure 4.20. This suddenly high peak could possibly be caused by a change in the wind direction, which could have resulted in contamination. The risk of contamination could not be evaluated to the same extent as in the data set obtained during the expedition *Arctic Ocean 2018*. This was because no data were available regarding BC and particles during the cruise back to Helsingborg. Therefor, the contamination mask complied for the Arctic region data set was applied to this data set as well. The final data set will be evaluated and discussed in the next section (4.2.2).

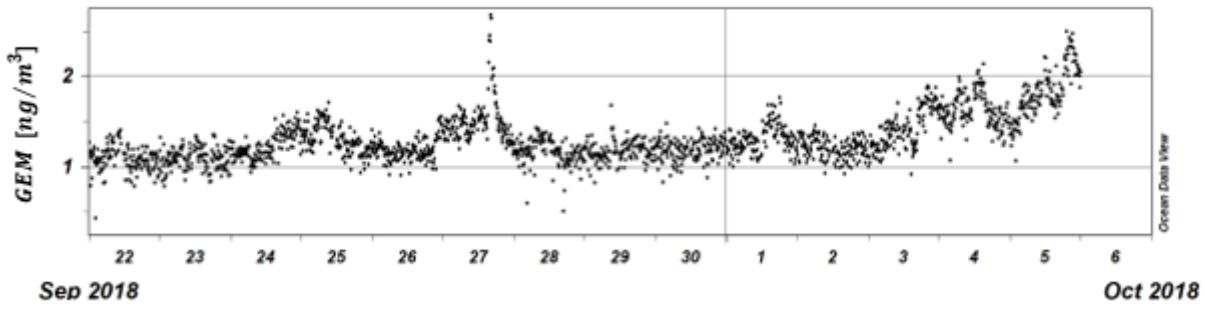

Figure 4.20: *GEM concentrations in the initial data set against time during the cruise from Svalbard to Helsingborg (22nd of September to the 5th of October).*

4.2.2 Analysis of final GEM-data set during the transit south

As can be seen in figure 4.21 below, a large amount of the data points were removed south of Svalbard when applying the contamination mask (the wind was entering the ship from the stern or at low speeds ($< 4\ m/s$)). After the removal of data points that possibly could have been influenced by contamination, during the transit Svalbard to Helsingborg, the remaining measurement reflects, to a large extent, background concentration of GEM in the Northern Hemisphere. Though, the GEM concentrations during the route outside the west coast of Norway (the 28th of September to 4th of October) seem to be slightly lower compared to the background concentration. When *IB Odens* passed the south of Norway (the 4th of October) and the west coast of Sweden (the 4th to the 5th of October), periods of elevated measurements of GEM were found.

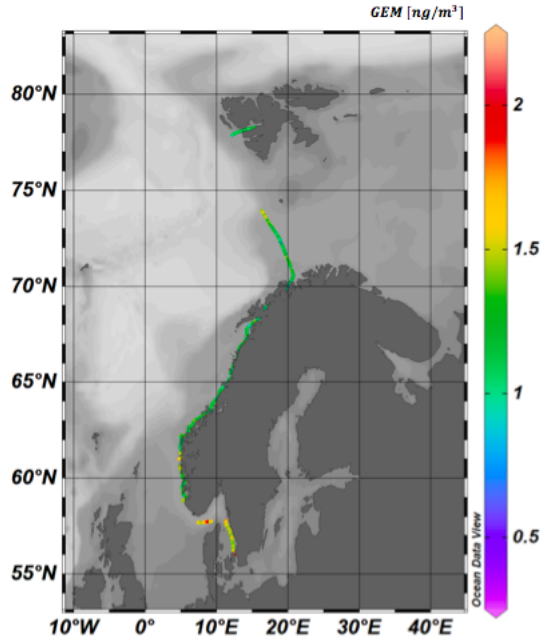

Figure 4.21: *GEM concentrations in the final data set against longitude and latitude during the transit south from Svalbard to Helsingborg (22nd of September to the 5th of October).*

The GEM concentrations in the final data set plotted against time during the cruise Svalbard to Helsingborg are seen in figure 4.22. The event that took place the 24th to 25th of September has been removed from the data set even though the peak had a gradual build up. Based on the character of the peak, it could be argued that this peak reflects elevated concentrations of GEM in the area rather then contamination, and should therefore be further evaluated. By using another method for evaluating the risk of contamination, the observed peak could still be present in the data set. Further discussion about the contamination mask is found in the section 4.5.3 below. The peak found the 27th of September with the suddenly high character have been removed. The final data set still contained measurements of elevated concentrations and these were further analysed in section 4.2.3. Furthermore, the data set consist of some single points reaching low concentrations around 0.4 ng/m^3. However, these were not further analysed in this study due to time constraints.

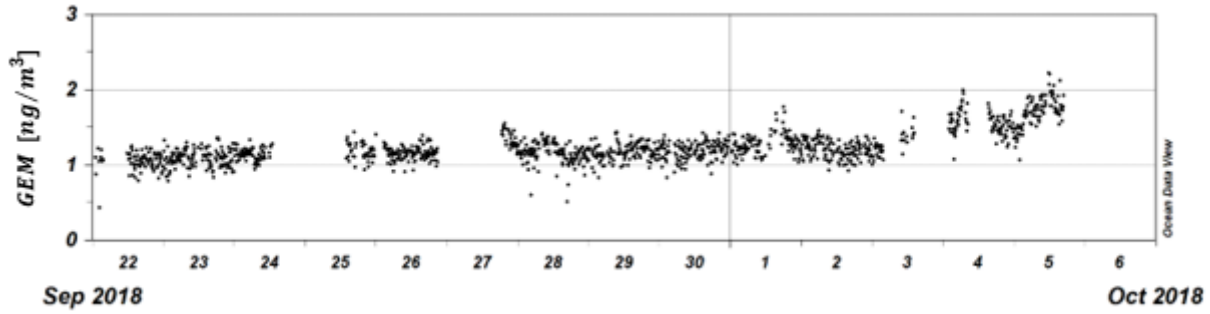

Figure 4.22: *GEM concentrations in the final data set against time during the cruise from Svalbard to Helsingborg (22nd of September to the 5th of October).*

4.2.3 Analysis of elevated GEM concentrations during the transit south

In figure 4.23, the *GEM* concentration plotted against time is shown, with the specific events of interest pointed out. The events of specific interest are named **I**-**K** in the figure. The events were evaluated in combination with the meteorological parameters, air pressure, relative humidity and air temperature.

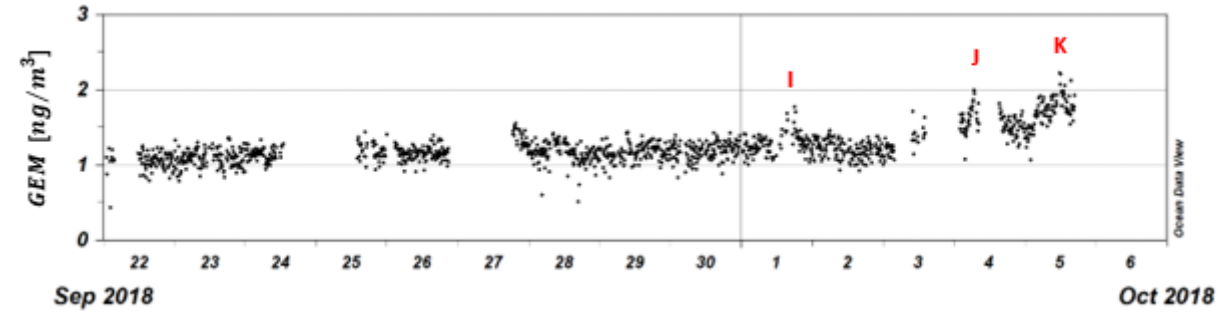

Figure 4.23: *GEM concentrations in the final data set, with the specific events of interest pointed out (**I**-**K**), against time during the cruise from Svalbard to Helsingborg (22nd of September to the 5th of October).*

Measurements of air pressure, relative humidity and air temperature taken during the transit south are found in figure 4.24. As can be seen in figure 4.24a, the air pressure changed multiple times, going from low-pressure- to high-pressure conditions, indicating that new air masses have been introduced multiple times during the cruise. The relative humidity varied significantly (ranged between 40 - 100 %), which can be seen in figure 4.24b. In the beginning of the transit south, the air temperature was stable around 0°C and from the 26th of September, the temperature then successively increased reaching temperatures above 10°C when cruising down the west coast of Sweden.

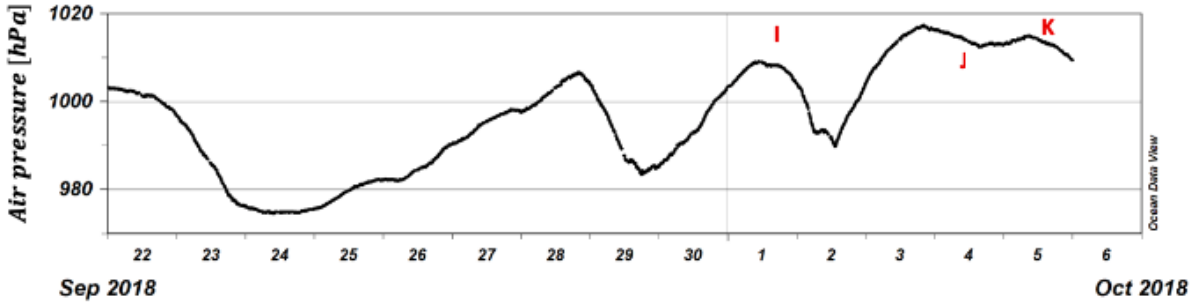

(a)

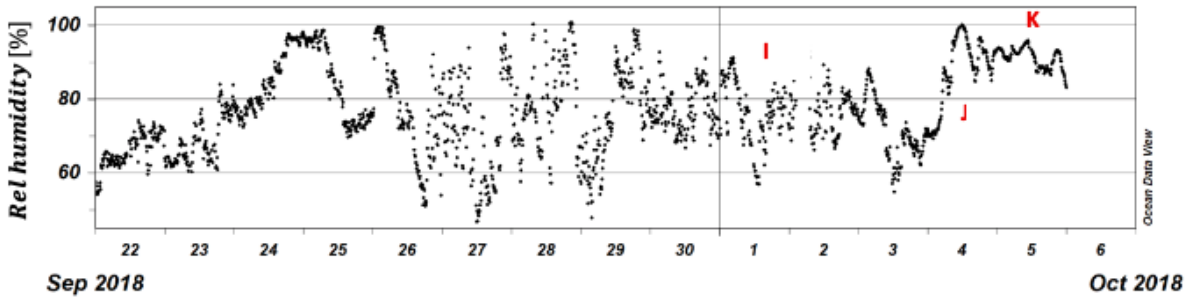

(b)

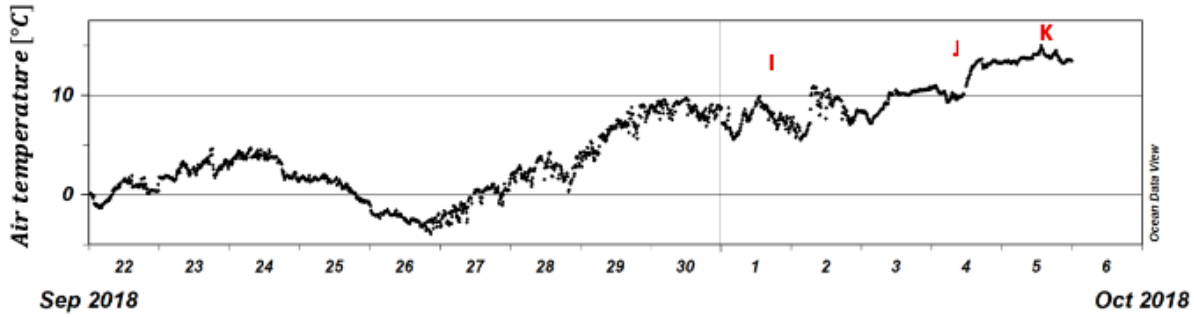

(c)

Figure 4.24: *Air pressure, relative humidity and air temperature plotted against time during the transit south from Svalbard to Helsingborg in 2018 (22nd of September to the 5th of October).*

The specific events considered to be of interest, **I-K**, have been studied in relation to the meteorological parameters and together with 5-days and 28-days backward trajectories. The results from the 5-day backward trajectories are presented in connection to each event. The 28-day backward trajectories are analysed and discussed in section *28-days trajectories for the events I-K* while the figures are found in appendix A.3.

Event I - The 1st of October

The first event of elevated *GEM* concentrations during the transit south were found in the evening the 1st of October with *GEM* concentration that reached a maximum of 1.77 ng/m^3. During this event, both the air pressure and the air temperature were decreasing and the relative humidity was increasing, see figure 4.24. These conditions could possibly indicate that new humid air masses were introduced to the sampling location at the time of the event.

In figure 4.25a, 5-day backward trajectories and cluster analysis are shown. At the three evaluated heights (0.3, 0.5, $0.7 \cdot PBL$), the 5-days backward trajectory showed that air masses originated from Greenland (see figure 4.25a). The three trajectories followed almost the same pathway. The air masses seem to have originated from Greenland and passed over open ocean before reaching the measurement point at the coast of Norway (60.51°N and 4.90°E). The cluster analysis performed at the height $0.5 \cdot PBL$, showed that the majority of the trajectories originated from Greenland. Greenland is mostly covered by snow and ice and has low anthropogenic activity.

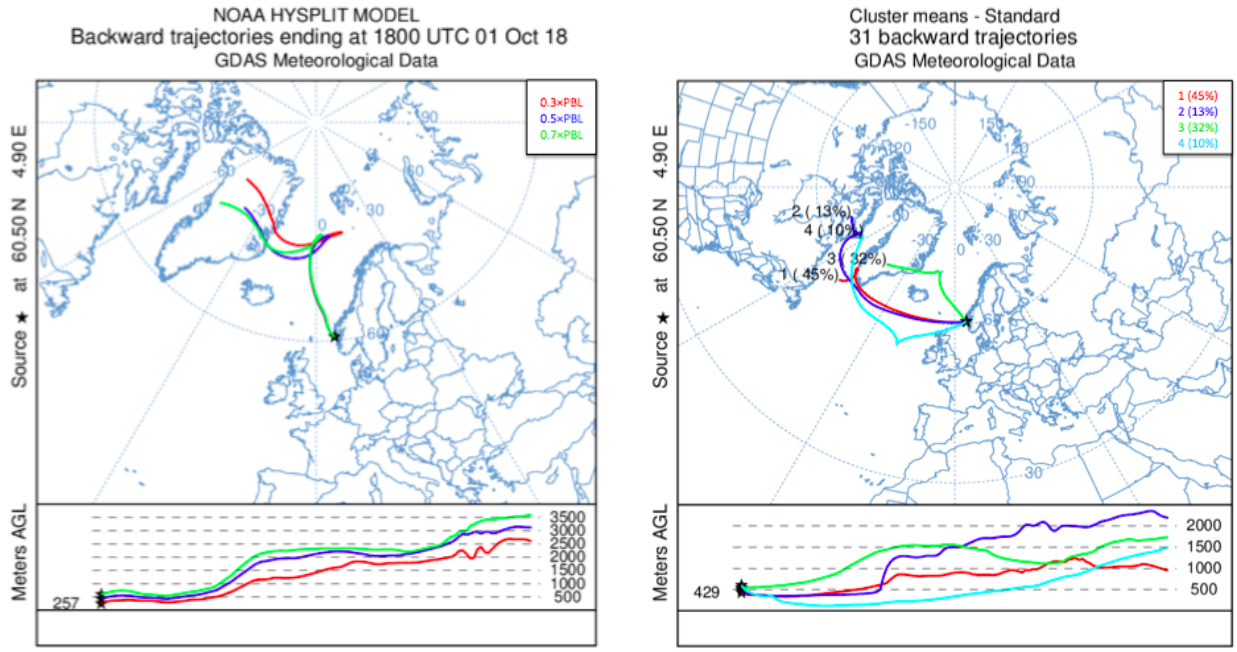

(a) (b)

Figure 4.25: *5-day backward trajectories and cluster analysis for the elevated GEM measurements the 1st of October. In (a), trajectories for 3 different heights are shown, and in (b) cluster analysis is shown for one height, 0.5*PBL. Meters AGL refers to meters above ground level.*

As presented above, Kamp et al. (2018) observed trends in how meteorological conditions changed when elevated *GEM* concentrations were found. The authors observed that when the concentration of *GEM* started to increase the pressure decreased and when the *GEM* concentration started to return back to previously observed levels, the pressure increased. This special pattern was observed during the event **I**, the 1st of October.

In Greenland, there are minor anthropogenic activities causing mercury emissions and the land masses are mostly covered by snow and ice and thus it can be concluded that the elevated concentrations most likely originated from evaporation of mercury from snow- and ice-packs on Greenland or from evasion from open ocean. However, anthropogenic activities located close to the measurement point, along the west coast of Norway, could possibly also be a potential source to the elevated *GEM* concentrations. Anthropogenic activities in Norway, such as oil refining and coal combustion, as well as natural activities such as forest fires, could be potential sources to the high concentrations observed.[58]

Event J - The 4th of October

During the morning on the 4th of October, a second peak of *GEM* concentrations during the transit south was identified reaching a maximum of 1.99 ng/m^3. During this period, the air pressure was slightly decreasing, meanwhile, the relative humidity and the air temperature were increasing, indicating that new humid air masses were introduced to the sampling location, outside the west coast of Sweden, see figure 4.24.

In figure 4.26, the 5-days trajectories and cluster analysis for event **J** can be found. As can be seen in figure 4.26a, the air masses seem to have originated from the Arctic area around Greenland. The trajetories on the $0.5 \cdot PBL$ and $0.7 \cdot PBL$ heights, passed over Island, open ocean and over the northern part of Great Britain before reaching the measurement point at 57.7°N and 8.80°E. The trajectory at $0.3 \cdot PBL$ passes over open ocean, Great Britain before reaching the measurement point. In the cluster analysis, it was observed that the majority of the trajectories originated from Greenland and passed over open ocean and the northern part of Great Britain. 42 % of the trajectories were extended further and seems to originate in the northern part of Canada.

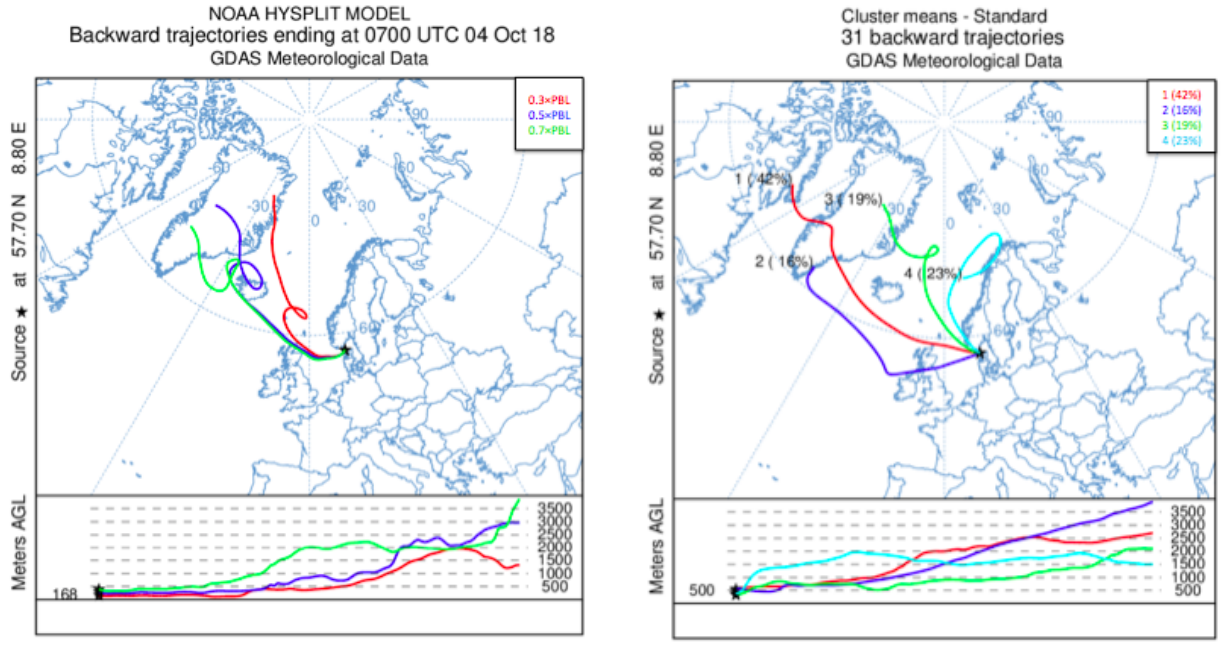

(a) (b)

Figure 4.26: *5-day backward trajectories and cluster analysis for the elevated GEM measurements the 4th of October. In (a), trajectories for 3 different heights are shown, and in (b) cluster analysis is shown for one height, 0.5*PBL. Meters AGL refers to meters above ground level.*

The meteorological condition observed during event **J**, the 4th of October, aligns with the temperature and pressure patterns observed by Kamp et al. (2018). During the event, the air pressure was slightly decreasing during the build up of the *GEM* concentration, followed by a small increase in the end of the event. However, a more rapid decrease and increase in the air pressure were seen by Kamp et al. (2018). Further, it was found that the temperature increased during the build up of the peak, followed by a small decrease. The observed temperature pattern matches the observation made by Kamp et al. (2018), even though they observed more clear changes in the air temperature.

Anthropogenic activities could hold the responsibility for the elevated *GEM* concentration observed on the 4th of October. The trajectories passed over Great Britain, where anthropogenic activities takes place and potential activities releasing mercury could be oil refineries, coal combustion, waste incineration but possibly also gold mining.[59][60] The air masses originated from Greenland, where few anthropogenic activities are located and the land area is mostly covered by ice and snow and thus *GEM* possibly could have evaporated from the ice- and snow-packs.

Event K - The 5th of October

The last period of elevated *GEM* concentration was observed during the 5th of October at around 12 am when *IB Oden* cruised the west coast of Sweden. The highest concentration of *GEM* measured was 2.22 ng/m^3. At

the time of the peak, the air pressure and the relative humidity were decreasing, while, the air temperature was somewhat increasing. The change in air pressure indicted that new air masses were introduced, and the decrease in humidity implied that the new air masses introduced were drier, see figure 4.24.

5-days backward trajectories and cluster analysis for the event the 5th of October are found in figure 4.27. In figure 4.27a, it was observed that all of the trajectories follow the same pathway resulting in a rather certain estimation. The air masses seem to have originated from open ocean in the North Atlantic Ocean passing over the south part of Great Britain, along the west coast of Germany and over Denmark before reaching the measurement point at 56.0°N and 12.7°E.

In the cluster analysis, see figure 4.27b, 42 % of the trajectories follows the same pathway as in the 5-days, three-level trajectories. Additionally, the trajectories seem to have originated from the Arctic area around Greenland and northern parts of Canada.

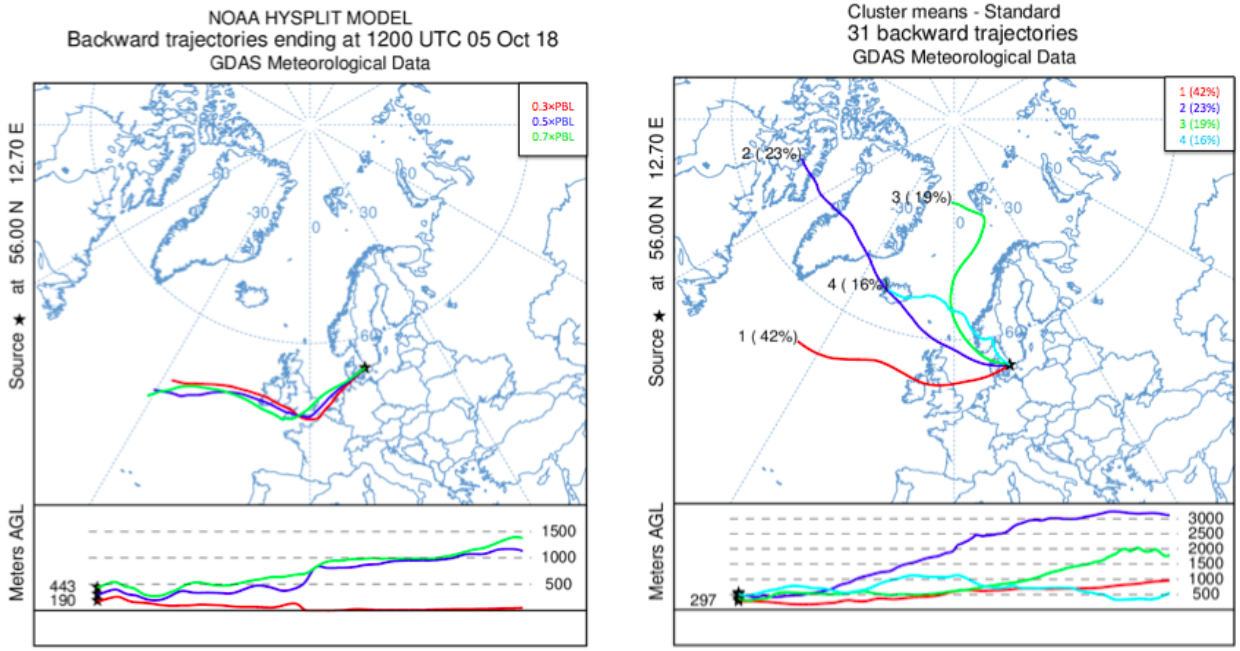

(a) (b)

Figure 4.27: *5-day backward trajectories and cluster analysis for the elevated GEM measurements the 5th of October. In (a), trajectories for 3 different heights are shown, and in (b) cluster analysis is shown for one height, 0.5*PBL. Meters AGL refers to meters above ground level.*

The meteorological conditions during the elevated *GEM* concentrations the 5th of October partly match the observation made by Kamp et al. (2018). During the event, air pressure was decreasing and at the same time, the air temperature was increasing. As mentioned above, Kamp et al. (2018) observed that the air pressure and the air temperature were decreasing and increasing, respectively, when *GEM* concentration suddenly peaked. Thus these observations align with what was observed during event **K**. However, they found that when *GEM* concentrations returned to previous observed concentrations, pressure increased and temperature decreased, this could not be seen in event **K**.

As presented above, the air masses passed over several countries that possibly could be responsible for the elevated *GEM* concentrations. In Denmark, Germany and Great Britain, oil refinery and coal combustion could be potential sources responsible for the high concentrations.[58][59] At the same time, gold mines are found in the southern parts of Great Britain and these could possibly also hold the responsibility for the elevated *GEM* concentrations.[60] Another potential sources to the observed elevated *GEM* concentrations could be waste incineration.

28-days trajectories for the events I-K

The 28-days trajectories, at three different heights ($0.3, 0.5$ and $0.7 \cdot PBL$), and the cluster analyses at one height ($0.5 \cdot PBL$), conducted for the events **I, J** and **K**) observed during the transit south are found in appendix A.3. The purpose of conducting 28-days long backward trajectories was to find regional and global sources of mercury releases. These kind of long trajectories are justified due to the long range transport of *GEM* and can be used for getting an indication of potential source. However, one should be aware of the uncertainty when tracing air masses using *HYSPLIT*. The 28-days backward trajectories for the specific events of interested showed that the majority of the air masses originated from the Arctic region and passed over Greenland. However, the trajectories for event **J** showed that air masses have been passing over Island, Greenland and originating from the Arctic region, see figure A.12. The 5th of October, event **K**, the majority of the trajectories passed over the northern part of Great Britain, Island and originating from Greenland and the Canadian Arctic.

In the cluster analyses, the majority of the air masses seem to have originated from the Arctic region and passed over the North Atlantic ocean, see figures A.11, A.12 and A.13. However, in event **K**, the air masses could have originated from areas with high anthropogenic activity, see figure A.13. Since, all of the trajectories indicated that the elevated *GEM* concentrations possibly could have originated from the Arctic environment thus the Arctic region could be a potential mercury releasing responsible for the elevated mercury levels found at the west coast of Norway and Sweden.

Summary of the observed trends for event I-K

The elevated concentrations of *GEM* during the transit south were observed along the west coast of Norway and Sweden. The highest concentrations observed during the transit was 2.22 ng/m^3 at the west coast of Sweden just before reaching dock in Helsingborg. It was observed that the concentrations of *GEM* became higher the further south *IB Odens* cruised, see figure 4.21.

The meteorological conditions changed multiple time during the transit south, but some similar patterns could be observed during the periods of elevated *GEM* measurements (event **I, J** and **K**). During all the events, a decrease in air pressure was observed indicating that new air masses were introduced. The air temperature was increasing during the peaks observed the 4th and 5th of October (event **J** and **K**). The relative humidity was increasing during the elevated peaks observed the 1st and 4th of October (event **I** and **J**).

Considering the 5-days trajectories and the cluster analyses conducted for the specific events of interest, it can be concluded that the majority of the trajectories originated from the Arctic region, passed over open ocean and over land masses with both high and low anthropogenic activity. In all of the events, the trajectories indicated that elevated *GEM* measurements possibly could originate from anthropogenic activities. Based on the observations from the 28-days, three-level trajectories and the cluster analyses, it can be concluded that the majority of the air masses originate from the arctic region but there is a possibility that air masses have passed areas with high anthropogenic activity.

The majority of the trajectories indicated that air masses likely originated from areas with high anthropogenic activity and thus a probable explanation to the elevated *GEM* concentrations. The Arctic region could also be a potential source to the elevated *GEM* concentrations found on the west coast of Norway and Sweden. There are few anthropogenic activities in the Arctic region and thus elevated *GEM* concentrations are likely to originate from evasion of mercury from snow- and icepacks. Therefore, the probability for the Arctic region to be a source to the elevated *GEM* concentrations found at the coast of Norway and Sweden is low compared to the probability that the elevated *GEM* concentrations originated from anthropogenic activity.

4.3 Analysis of GEM concentrations over geographical regions

Trends of *GEM* concentrations in regard to the geographical regions - MIZ in August (82.0 - 85.5°W), Contiguous ice (85.5 - 82.5°W), MIZ in September (82.5 - 82°W), open ocean (south of the MIZ) are seen in figure 4.28 and table 4.1. The different zones were determined from ice maps, which are found in appendix A.4. The *GEM* measurements obtained during the expedition *Arctic Ocean 2018* and during the transit south from Svalbard to Helsingborg were included in the evaluation. As can be seen in figure 4.28 and table

4.1, the periods with the highest and the lowest GEM concentrations and highest variability were found over continuous ice. The lowest variability of GEM concentration was observed during the period of open ocean in August, where the measurements mostly reflected the background concentration. The overall average GEM concentration and variability for the data set was 1.412 ± 0.38 ng/m^3.

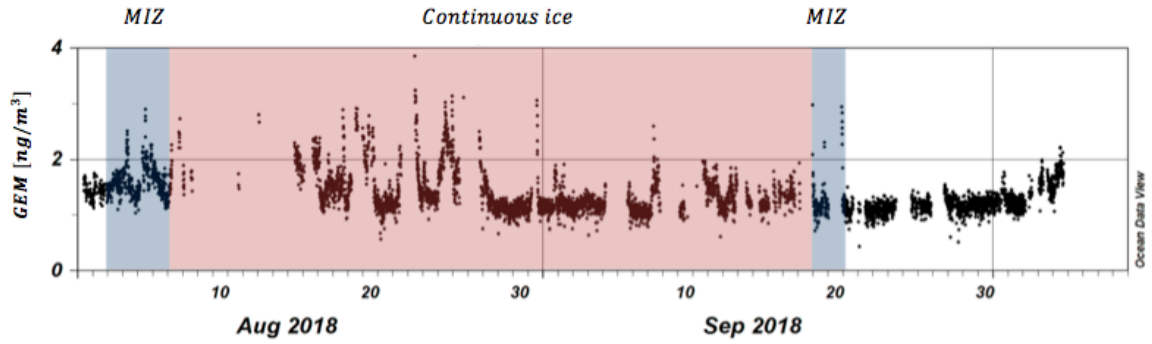

Figure 4.28: *GEM concentration plotted against time during the expedition Arctic Ocean 2018 (22nd of September to the 5th of October). Blue shading refers to the time when IB Oden passed through the MIZ in August (82.0- 85.5° W) and in September (82.5- 82° W) and red shading refers to when IB Oden travelled over continuous ice (85.5- 82.5° W). The white background refers to the time over open ocean (south of the MIZ). MIZ refers to marginal ice zone.*

In table 4.1, a summary of the average GEM concentrations and standard deviation over the three different geographical regions are found. The highest average GEM was found in August in the MIZ. One possible explanation for the highest average value could be releases of mercury from ice leads created by *IB Oden* when breaking the ice on the transit north. Sea ice on the ocean acts as a barrier and traps mercury under the ice sheet, and limits the mercury exchange between the ocean and the atmosphere. When a ship starts to break the ice in the MIZ, ice cracks are created followed by the establishment of ice leads, which are areas of open water. The newly formed ice leads can release mercury that had been trapped under the ice sheets. The average concentration of GEM over open ocean in August on the cruise north, and the period of continuous ice had similar values, 1.4 and 1.395 ng/m^3, respectively. The lowest averages of GEM were found in the MIZ at September and during the transit south.

Table 4.1: Summary of GEM concentrations and standard deviation over the geographical regions. MIZ refers to marginal ice zone.

Geographic Region	Time [ddmm]	GEM [ng/m^3]	Std [ng/m^3]
Open Ocean Aug	0108-0208	1.4	0.134
MIZ Aug	0208-0608	1.655	0.284
Contiguous ice	0608-1809	1.395	0.389
MIZ Sep	1809-2009	1.197	0.282
Open Ocean Sep-Oct	2209-0510	1.235	0.235

Analysis of GEM concentrations over the different geographical regions has been conducted in other studies. DiMento et al. (2018) analysed GEM concentrations in the Canadian Arctic and the authors found that the average concentration over the regions showed no clear trend, open ocean: 1.25 ± 0.1, MIZ: 1.24 ± 0.14, continuous ice: 1.26 ± 0.08 ng/m^3. The highest variability was observed in the MIZ.[61] Further, DiMento et al. (2018) measured dissolved Hg^0 in sea water during the expedition to be able to calculated a hypothetical air-sea flux of Hg^0. They found the highest concentration of dissolved Hg^0 over continuous ice and when they calculated a hypothetical air-sea flux value it was high. However, no significant increase in GEM concentration was found over continuous ice and thus the authors could confirm that sea ice acts as a barrier and limits the exchange of mercury between the ocean and atmosphere.[61]

Trends in *GEM* concentrations observed during *Arctic Ocean 2018* matches well with the observation made in the Arctic by Sommar et al. (2005). The measurements were sampled between July and September in 2005 during the *Beringia 2005 expedition*.[53] Summar et al. (2005) observed higher concentrations and variations of *GEM* over continuous ice, 1.81 ± 0.41 ng/m^3, compared to over open ocean, 1.55 ± 0.21 ng/m^3.[53] Similar trends were also found in the study by Aspmo et al. (2006).[54] In both of the articles, Sommar et al. (2005) and Aspmo et al. (2006), no measurements of *GEM* in the MIZ were conducted and thus no comparison was possible.

Nerentorp Mastromonaco et al. (2016) measured and analysed *GEM* concentrations in Antarctica. These observations showed higher concentrations over open ocean (1.2 ± 0.1 ng/m^3) than in the MIZ (1.0 ± 0.2 ng/m^3).[27] The trends observed by Nerentorp Mastromonaco et al. (2016), agrees well with the result of this study when *IB Oden* passed the MIZ in September and traveled into the open ocean in September until October. When *IB Oden* cruised from Svalbard to the MIZ, going north, lower concentrations of *GEM* were observed over open ocean compared to the concentrations measured in the MIZ. These difference could possible be explained by seasonality and spatial variations affecting the *GEM* concentrations at the two geographical regions.

Based on the observed trends made during the expedition *Arctic Ocean 2018* and trends found in earlier studies it can be argued that the higher concentrations of *GEM* found in the MIZ compared to over continuous ice are caused by the fact that the sea ice acts as a barrier and limits the exchange between the reservoirs. However, higher concentrations of *GEM* were found over continuous ice compared to over open ocean, indicating that ice and snow on ice, possibly are releasing mercury to the atmosphere during summertime. The increased solar radiation during the summer results in ice and snow melting and a reduction of *GOM* to *GEM* can take place in the reservoir, resulting in released/evaporated *GEM* to the atmosphere.

4.4 The Arctic region through time and the effect of climate change

Observations of *GEM* concentrations in the atmosphere, during the last 10-30 years, have shown a declining trend, however, both Cole et al. (2013) and Zhang et al. (2016) point out the fact that a much faster decrease is observed at temperate latitudes than at the northern high latitudes.[62][63] The decline at temperate latitudes seem to agree with the decreased anthropogenic emissions that have been observed especially in the Northern Hemisphere. *The Global Mercury Assessment (GMA) (2018)* have compiled anthropogenic mercury emissions to air at lower latitudes. The authors of the *GMA* found that emission in North America and Europe seemed to have declined between 1990 and 2010. After 2010 the emission appeared to have stayed stable, while in Asian regions like China, emissions increased until around 2007-2009, to then plateaued.[3]

The mercury cycling at the Arctic region is complex since it is largely influenced by spatial and seasonal variations. Meteorological and physical conditions changes considerably during the year and researches like Zhang et al. (2016) have earlier showed that trends in the Arctic region are complicated.[63] In table 4.2 the average calculated *GEM* value from the expedition *Arctic Ocean 2018* is presented together with average values presented in earlier studies conducted in the Arctic region.

Table 4.2: The average GEM concentration at the *Arctic Ocean 2018* expedition and *GEM* average from other studies performed in the Arctic region.

Location	Time Period	GEM (ng/m^3)	Reference
Arctic	Summer 2018	1.237 ± 0.217	This study
Arctic	Summer 2016	1.4 ± 0.2	Nerentorp Mastromonaco [12]
Arctic	Autumn 2015	1.2 ± 0.1	DiMento et al. [61]
Arctic	Summer 2005	1.72 ± 0.35	Sommar et al. [53]
Arctic	Summer 2004	1.5 ± 0.13	Aspmo et al. [54]

When comparing the average *GEM* value from the *Arctic Ocean 2018* to earlier observations made in the Arctic region (see table 4.2) it can be concluded that the declining trend in *GEM* concentrations observed in earlier research could not be seen. However, it should be noted that the different studies compared in the table

have been performed using different evaluation methods, and that the study by DiMento et al. (2015) was performed during autumn while the rest of the studies have been performed during summertime. Further, it can be concluded that the order of the average GEM value and the variation for the *Arctic Ocean 2018* is in line with what has been observed in earlier studies.

The implementation of new policies like *The Minamata Convention* should help to reduce anthropogenic mercury emissions to the environment. The effect the convention will have in remote areas like the Arctic region, is however hard to predict, and becomes even more complex due to the now present global warming. To be able to predict what effects climate change can have on the Arctic mercury cycle it is necessary to understand the effects climate change will have on the Arctic region and the Arctic weather, together with having an elaborated understanding for the flows and reactions that takes place in the Arctic mercury cycle. Today knowledge is lacking regarding many of the effects that are predicted to follow climate change, and at the same time there are several knowledge gaps in completely understanding the Arctic mercury cycling. These knowledge gaps together with the complexity of the mercury cycle makes the outcome of climate change on the mercury cycle ambiguous. However, some effects of climate change are known and have already been observed. The most obvious change is considered to be the loss of sea ice cover, multi-year ice is melting and replaced either by open water or first-year ice. These changes will result in more and longer periods of interactions between the atmosphere and the *Arctic Ocean*. The exchange between the atmosphere and the ocean is assumed to be the most important pathway for mercury cycling in the Arctic environment and is thought to regulate the transformation between different forms of mercury in the *Arctic Ocean*. Larger areas where the exchange of mercury between the air and the ocean can take place and longer periods with interactions can affect the mercury cycling in several diverse ways. For instance, increase the possibility for oxidised forms of mercury to deposit into the ocean, instead of at ice and snowpacks, should allow for more mercury to be removed from the atmosphere, bio-accumulate and biomagnify in the food chain or that mercury could be removed from the cycle by being transported to the deep ocean sediments. However, the decreased sea ice cover would at the same time make room for increased evaporation of mercury from the ocean to the atmosphere. Other effects predicted to take place are for instance linked to the temperature in the Arctic atmosphere. The rise in temperature is predicted to cause less oxidation of GEM into GOM, which will slow down the removal of GEM from the atmosphere. These are only a few examples of the effects that are predicted to follow climate change, basically, all meteorological parameters could change and observations like the intensified level of southerly winds have already been observed. Whether the GEM concentrations in the Arctic atmosphere will rise in the future due to climate change or decrease thanks to *The Minamata Convention* is hard to conclude with the present knowledge.

4.5 A comprehensive discussion about the results

In the following section, a summary of the main results and discussion are presented, followed by a section regarding the sampling uncertainty. Finally, suggestions regarding improvements of the contamination mask is presented.

4.5.1 General review of the final data set results

In this study, several periods of elevated GEM concentrations reaching far above background concentration ($1.5 - 1.7\ ng/m^3$) were observed. The highest GEM concentration observed reached $3.86\ ng/m^3$. One half atmospheric mercury depletion event was found, where the GEM concentration dropped to $0.57\ ng/m^3$. The overall average concentration of GEM was found to be $1.412 \pm 0.38\ ng/m^3$.

The GEM data were evaluated together with meteorological data and trajectories. A correlation between pressure and elevated and depleted GEM concentrations were found, where changes in pressure were observed for all but one of the events. A clear trend in the intensity of solar radiation was also observed for the events during the period when *IB Oden* was connected to a ice sheet. The solar radiation increased significantly during or just before the events. Regarding air temperature, relative humidity and visibility no specific patterns could be observed at the time of the events. However, the relative humidity was high (around 100 %) and the air temperature was stable (around 0°C) most of the time during the expedition. These stable conditions were not observed during the transit south.

The meteorological conditions observed, especially regarding the air pressure, supports the idea that the sampled air masses were exchanged several times during the expedition and during the transit south. The new air masses could have contained elevated and/or depleted GEM concentrations. The increased intensity in solar radiation observed in connection to elevated GEM concentrations strengthen the idea that evaporation of GEM from open ocean, continuous ice and snow have taken place. However, the rise in solar radiation could possibly also result in increased amount of photochemical reactions, which eventually will cause depleted GEM concentrations.

Considering the 5-days trajectories generated, the majority indicated that air masses originated from the Arctic region. Anyhow, one of the trajectories during the expedition, events **D**, showed that air masses possibly could have originated from Finland and/or the east coast of Sweden. During the transit south, it was found that trajectories generated for event **J** and **K** were passing over areas with high anthropogenic activity. Thus, the majority of the trajectories during the expedition *Arctic Ocean 2018* indicate that the source of the elevated concentration, more likely, are found in evaporation of earlier deposited mercury in the Arctic area rather than caused by direct release of mercury from anthropogenic activities. However, the trajectories generated during the transit south indicated that anthropogenic activities more likely were responsible for the elevated measurements sampled at the west coast of Norway and Sweden.

It was decided to create 28-days backward trajectories to find possible regional and global sources causing mercury releases. As far as observed, these kind of trajectories have not been created in previously conducted GEM studies. With regard to the long residence time of GEM in the atmosphere it should be justified to make these long trajectories. However, when making these long backward trajectories there is a risk that the specific elevated air mass have been mixed with other air masses and thus the mercury concentration could have been diluted. The uncertainty in these trajectories was also found to be high due to the large difficulties in modelling winds and the limited satellite data in the polar regions.

When tracing air masses backward in time, the height and the duration of the trajectories needs to be carefully chosen. When choosing a too low height, for instance the air sampling height, the backward trajectories could hit the ground and result in a inaccurate tracing. The number of days tracing backward in time is often chosen to be less than 10 and whether that is accurate or not should be further analysed. It is therefore suggested that future research, who intend to trace air masses backward in time, investigate the height and number of days in more detail. It would also ease future studies if research could be more transparent about their choices when tracing air masses.

Higher elevated GEM concentrations were observed over continuous ice compared to open water. The reason for this could possibly be found in releases of GEM from earlier deposited mercury in snow and ice or due to evaporation of GEM from newly created ice leads. Both the lowest and the highest observed concentrations of GEM were found over continuous ice when *IB Oden* was connected to an ice sheet. At the 21st of August (event **C**) several low measurements were observed. As discussed above, the typical conditions regarding halogens and ozone concentrations previously observed in relation to depletion events were not found. However, the phenomena of observing elevated concentrations of GEM, hours or within days, after the depletion event was found in this study. In order to fully understand the reason of the depletion, measurements of other possible oxidants would be helpful together with measurements of other forms of mercury. Anyhow, the cause of the depletion could possibly be explained by newly introduced air masses that contained depleted levels of GEM. The elevated measurements of GEM observed on the 23rd of August (event **D**) could be explained either by re-emission of the earlier deposited mercury observed 21st of August or by long range transport of elevated air masses created from anthropogenic activities. A combination of long range transport and re-emission could also be a possible explanation.

To be able to draw any conclusions regarding mercury trends over the geographical regions more consistent measurements would have been needed. In this study, the MIZ had the highest average GEM concentration on the way up to the North Pole, while on the way south the MIZ had the lowest average GEM concentration. This could be explained by several aspects, such as seasonal variations, temporal differences and due to the fact that less measurements where taken in the MIZ in September compared to in August. Similar aspects could have had effects on the averages of GEM concentrations over open ocean.

When evaluating trends of mercury in the Arctic region over time, several aspects needs to be considered, for instance the use of contamination masks, the amount of measurements taken, the evaluation method used. An option would be to use stationary data, for example at the station at Ny-Ålesund located on Svalbard,

this would make it easier to capture mercury trends over seasons and years due to the possibility of making continuous measurements. Further, continuous measurements taken at all of the seasons would be needed to see trends throughout the years and between different years. This is highly important to be able to capture the effects of climate changes.

4.5.2 Sampling uncertainty

The instrument, *Tekran 2537A*, have been used during several Arctic and marine expeditions. Signs of passivation in one of the goal cartridges was observed when evaluating the measurements. If the measurement would have been analysed continuously during the sampling period, the passivation on one of the goal cartridges could have been observed earlier and validated. According to Eric Prestbo at Tekran Instruments Corporation, the validation could have been conducted by switching place of the cartridges and to investigate if the passivation follows the cartridge. Leak check and heat control or cleaning of the valves are other ways of validating passivisation. However, none of these operations were performed since no one responsible for the sampling was on board *IB Oden*.

The passivation resulted in the measurements taken by cartridge A were removed from the data set. This resulted in 50 % less data points and larger gap between the measurements. If both cartridges would have worked, observations in the data set would have been more secure.

4.5.3 Suggestion regarding a more elaborated contamination mask

It could be discussed whether the contamination method used in this study is appropriate or not. During this expedition, a lot of effort was put into keeping the ships chimney smoke away from the air inlets. Therefore, it could be assumed that gradual build up peaks should not be caused by contamination, meanwhile, suddenly high peaks could still be created by contamination. When studying the final data set it could, at some points, look like the wrong data points were removed or kept. Instead of using the contamination mask used in this study, one option could be to evaluate the data set visually. Thus only suddenly high peaks could have been removed. Further, another alternative could have been to use so called quality flags, to mark the quality of the data. A flag with low quality could for example represent when the wind entered the ship from the stern and when the wind speed was low. While a higher quality flag could represent when the wind entered the ship from the fore and when the wind speed was higher than 4m/s.

5 Conclusions

Atmospheric measurements of mercury taken during the expedition *Arctic Ocean 2018* and the transit south from Svalbard to the west coast of Sweden, Helsingborg, has contributed to an increased understanding of the mercury cycling in the high Arctic and sub-Arctic regions. However, the complex interactions in the Arctic mercury cycle and the fact that only measurements of GEM were available in the evaluation limits the conclusions that could be drawn.

The evaluation of the GEM concentrations in this study suggests that high solar radiation and changes in air pressure are closely correlated to observations of elevated and depleted GEM concentrations. The majority of the observed elevated GEM concentrations found in the Arctic region are suggested to not be directly linked to anthropogenic activities, but rather originate from re-emission of earlier deposited mercury at Arctic surfaces. However, observed elevated GEM concentrations further south were considered to more likely be related to anthropogenic activities. The observed depleted concentrations of GEM, found on the 21st of August, were proposed to be caused by the introduction of new air masses containing already depleted GEM levels, rather than, depending on the presence of commonly know oxidant, such as BrO, at the sampling area.

The observed trends over the geographical regions showed that the largest variation in GEM concentrations were found over continuous ice. The observed average GEM concentration over continuous ice was both higher and lower than the averages observed over open ocean in August and September, respectively. The difference in the average GEM concentrations observed in open ocean, in August and in September, could result from the difference in the amount of measurements taken, less measurements were taken in August than in September. The magnitude of the measurements taken over open ocean in September are in the same order as the measurements taken over continuous ice and thus more appropriate to use when comparing trends over the geographical regions. When comparing these averages it can be suggested that higher concentrations of GEM are found at continuous ice than at open ocean.

When comparing GEM concentrations in the Arctic region over time, no obvious trends were observed and thus no conclusion regarding how the mercury cycle in the Arctic region has been affected by climate change could be drawn. The mercury cycling in the Arctic area is complex and climate change is likely to influence the mercury interactions in diverse and multidimensional ways. Thus, the implications of climate change will result in an even higher level of complexity in the Arctic mercury cycle. The result of this study highlights the importance of studying complex systems like the mercury cycle in combination with other research fields. Future research could increase the understanding of the mercury cycling and thus help to predict the outcome of challenges like climate change.

6 Future research

The outcome of this study indicates that there are many uncertainties regarding global mercury cycling and the cycling of mercury within the Arctic region. Above all, to overcome many of these uncertainties, more mercury sampling needs to be conducted at different geographical locations and regions. Additionally, the majority of the studies in the Arctic region have been conducted during summertime and because of that, knowledge about how mercury cycling in the Arctic region is affected by seasonality is lacking. It is therefore suggested that future research expeditions should be performed at other seasons than during the summer. More mercury measurements could help to model the mercury interactions between the atmosphere, ocean and the terrestrial reservoir within the polar ecosystem and it could also help to predict how the cycling is and will be affected by climate change.

Future research within the Arctic region should also focus on measure GEM, GOM and HgP in the atmosphere and in the ocean, as well as in the terrestrial reservoir. In this study, only measurements of GEM in the atmosphere were evaluated due to lack of additional data, which resulted in difficulties in understanding the mercury transformation and transportation in the Arctic region. Moreover, in order to fully understand the transformation of GEM to GOM measurements of other oxidants than BrO, for instance $Cl\cdot$ and $I\cdot$, would be needed alongside the mercury measurements.

Future research should also consider the potential risk of contamination more carefully, for example by measuring the concentration of mercury in the fuel used and to use a more elaborated contamination mask. As the result showed in this study, data points that were potentially not created by contamination were excluded from the evaluation causing a false picture of some of the elevated GEM concentrations.

In this study and in several previous studies that evaluates GEM, backward trajectories have been used for tracing air masses. In future studies the chosen heights and number of days tracing backward in time needs to be further analysed, to get a more representative picture of how mercury travels with air masses.

Continued evaluation of this data set could focus on what happened during the depletion event found the 21st of August. The depleted GEM concentrations can be further evaluated taking other oxidants and more parameters into consideration. It is important for the mercury researchers to cross boundaries and work together with researchers in other fields in the purpose of fully understand the mercury cycling on earth.

References

[1] Nationalencyklopedin. *Kvicksilver [Internet].* [cited 2019-01-28]. Available from: http://www.ne.se/uppslagsverk/encyklopedi/lång/kvicksilver.

[2] United States Environmental Protection Agency. Global Mercury Assessment: Source, Releases and Environmental transport [Internet]. Geneva, Switzerland: UNEP Chemical Branch; 2013. [cited 2019-01-24]. Available from: http://hdl.handle.net/20.500.11822/7984.

[3] United States Environmental Protection Agency. Global Mercury Assessment 2018 [Internet]. Geneva, Switzerland: UNEP Chemical Branch; 2018. [cited 2019-01-24]. Available from: https://wedocs.unep.org/bitstream/handle/20.500.11822/27579/GMA2018.pdf?sequence=1&isAllowed=y.

[4] Wängberg, I., Nerentorp Mastromonaco, M., Munthe, J., and Gårdfeldt, K. Airborne mercury species at the Råö background monitoring site in Sweden: distribution of mercury as an effect of long-range transport. *Atmospheric Chemistry and Physics* 2016;16:13379-13387. [cited 2019-03-09]. Available from: https://doi.org/10.5194/acp-16-13379-2016.

[5] United States Environmental Protection Agency. *Minamata convention on mercury.* [cited 2019-01-25]. Available from: https://www.epa.gov/international-cooperation/minamata-convention-mercury.

[6] United States Environmental Protection Agency. *Minamata convention on mercury.* [cited 2019-01-25]. Available from: http://www.mercuryconvention.org/Convention/Text.

[7] Arctic Monitoring and Assessment Programme. *AMAP Assessment 2011: Mercury in the Arctic [Internet].* Oslo: Arctic Monitoring and Assessment Programme; 2011. [cited 2019-02-02]. Available from: https://www.amap.no/documents/download/989/inline. 2011.

[8] Tekran Instruments Corporation. *Tekran Manual: Model 2537A Mercury Vapour Analyzer User Manual.* Toronto, Canada: Tekran Instruments Corporation; 2006.

[9] Mordechai, P., Valeri, M., Eran, T., Menachem, L., Valente, R., and Obrist, D. Mercury Depletion Events in the Troposphere in Mid-Latitudes at the Dead Sea, Israel. *Environmental Science and Technology* 2007;41(21):7280-7285. [cited 2019-03-23]. Available from: http://departments.agri.huji.ac.il/soils/tas/papers/Peleg_2007.pdf.

[10] Steffen, A., Douglas, T., Amyot, M., Ariya, P., Aspmo, K., Berg, T., Bottenheim, J., Brooks, S., Cobbett, F., Dastoor, A., Dommergue, A., Ebinghaus, R., Ferrari, C., Gardfeldt, K., Goodsite, M. E., Lean, D., Poulain, A. J., Scherz, C., Skov, H., Sommar, J., and Temme, C. A synthesis of atmospheric mercury depletion event chemistry in the atmosphere and snow. *Atmospheric Chemistry and Physics* 2008;8:1445-1482. [cited 2019-02-28]. Available from: https://doi.org/10.5194/acp-8-1445-2008.

[11] Horowitz, H. M., Jacob, D. J., Zhang, Y., Dibble, T. S., Slemr, F., Amos, H. M., Schmidt, J. A., Corbitt, E. S., Marais, E. A., and Sunderland, E. M. A new mechanism for atmospheric mercury redox chemistry: implications for the global mercury budget. *Atmospheric Chemistry and Physics* 2017;17:6353-6371. [cited 2019-04-29]. Available from: www.atmos-chem-phys.net/17/6353/2017/.

[12] Nerentorp Mastromonaco, M. Mercury cycling in the global marine environment [dissertation]. Gotheburg: Chalmers University of Technology; 2016.

[13] Bernhoft, R. A. Mercury Toxicity and Treatment: A Review of the Literature. *Journal of Environmental and Public Health.* 2012;2012. [Cited 2019 April 01]. Available from: https://www.ncbi.nlm.nih.gov/pmc/articles/PMC3253456.

[14] World Health Organisation. *Mercury and health.* [updated 2017-03-17; cited 2019-04-23]. Available from: https://www.who.int/news-room/fact-sheets/detail/mercury-and-health.

[15] Bakir, F., Damluji, S. F., Amin-Zaki, L., Murtadha, M., Khalidi, A., Al-Rawi, N. Y., Tikriti, S., Dhahir, H. I., Clarkson, T. W., Smith, J. C., and Doherty, R. A. Methylmercury Poisoning in Iraq. *American Association for the Advancement of Science* 1973;181(4096):230-241. [cited 2019-03-02]. Available from: https://www.jstor.org/stable/pdf/1736448.pdf?refreqid=excelsior%1d.

[16] Zhang, X., Siddiqi, Z., Song, X., Mandiwana, K. L., Yousaf, M., and Lu, J. Atmospheric dry and wet deposition of mercury in Toronto. *Atmospheric Environment* 2012;50:60–65. [cited 2019-03-03]. Available from: https://www.sciencedirect.com/science/article/pii/S1352231012000039.

[17] Krabbenhoft, D. P. and Sunderland, E. M. Global Change and Mecury. *Environmental Science* 2013;341(6153):1457-1458. [Cited 2019 April 15]. Available from: www.sciencemag.orgSCIENCEVOL.

[18] Obrist, D., Kirk, J. L., Zhang, L., Sunderland, E. M., Jiskra, M., and Selin, N. E. A review of global environmental mercury processes in response to human and natural perturbations: Changes of emissions,

climate, and land use. *Ambio* 2018;47. [cited 2019-03-14]. Available from: https://doi.org/10.1007/s13280-017-1004-9.

[19] PolarDiscovery. *Arctic: Location and Geography.* [cited 2019-03-22]. Available from: http://polardiscovery.whoi.edu/arctic/geography.html.

[20] National Snow and Ice Data Center. *All About Sea Ice - Characteristics.* [cited 2019-03-22]. Available from: https://nsidc.org/cryosphere/seaice/characteristics/index.html.

[21] Rachel Hauser. Polar Paradox. NASA Earth Observatory. [Updated 2000 January 31; Cited May 21]. Available from: https://earthobservatory.nasa.gov/features/PolarParadox?fbclid=IwAR1yt1Y0c1fwYKgTEIOWzcav4fjKRNPDbmWiJWoRqbVeI83F0JQf83ui2Mg.

[22] Wadhams, P. *The Geophysics of Sea Ice [Internet].* Boston: Springer; 1986. [cited 2019-03-12]. Available from: http://link.springer.com/10.1007/978-1-4899-5352-0$_1$5. 1986.

[23] National Oceanic and Atmospheric Administration. *ESRL Themes: Surface and Planetary Boundary Layer Processes [Internet].* USA: NOAA [cited 2019-03-13]. Available from: https://www.esrl.noaa.gov/research/themes/pbl/.

[24] Pielke, R. A. and Hayden, B. P. *Planetary boundary layer.* Encylopaedia Britannica. [updated 2018-07-03; cited 2019-04-01]. Available from: https://www.britannica.com/science/planetary-boundary-layer.

[25] National Snow and Ice Data Center. *All About Arctic Climatology and Meteorology - Factors Affecting Arctic Weather and Climate.* [cited 2019-03-22]. Available from: https://nsidc.org/cryosphere/arctic-meteorology/factors_affecting_climate_weather.html.

[26] PolarDiscovery. *Arctic, the Frozen Ocean - Introduction.* [cited 2019-04-01]. Available from: http://polardiscovery.whoi.edu/arctic/index.html.

[27] Nerentorp Mastromonaco, M., Gårdfeldt, K., Jourdain, B., Abrahamsson, K., Granfors, A., Ahnoff, M., Dommergue, A., Mejean, G., and Jacobi, H.-W. Antarctic winter mercury and ozone depletion events over sea ice. *Elsevier* 2016;129:125-132. [cited 2019-04-02]. Available from: https://doi.org/10.1016/j.atmosenv.2016.01.023.

[28] Steffen, A., Lehnherr, I., Cole, A., Ariya, P., Dastoor, A., Durnford, D., Kirk, J., and Piloteg, M. Atmospheric mercury in the Canadian Arctic. Part I: A review of recent field measurements. *Elsevier* 2015;322(509-510):3-15. [cited 2019-01-24]. Available from: https://doi.org/10.1016/j.scitotenv.2014.10.109.

[29] Douglas, T. A., Sturm, M., Simpson, W. R., Blum, J. D., Alvarez-Aviles, L., Keeler, G. J., Perovich, D. K., Biswas, A., and Johnson, K. Influence of Snow and Ice Crystal Formation and Accumulation on Mercury Deposition to the Arctic. *Environmental Science and Technology* 2008;42(5):1542-1551. [Cited 2019 Mars 2]. Available from: https://pubs.acs.org/doi/10.1021/es070502d.

[30] Brown, S. S. and Stutz, J. Nighttime radical observations and chemistry. *Chemical Society Reviews* 2012;41:6405-6447. [Cited 2019 May 16]. Available from: https://pubs.rsc.org/en/content/articlepdf/2012/cs/c2cs35181a.

[31] Obrist, D., Agnan, Y., Jiskra, M., Olson, C. L., Colegrove, D. P., Hueber, J., Moore, C. W., Sonke, J. E., and Helmig, D. Tundra uptake of atmospheric elemental mercury drives Arctic mercury pollution. *Nature* 2017;547(7662):201-204. [cited 2019-03-15]. Available from: http://www.nature.com/articles/nature22997.

[32] Phys.org. *A better understanding of the high levels of mercury pollution in the Arctic tundra.* [updated 2018-02-12; cited 2019-04-23]. Available from: https://phys.org/news/2018-02-high-mercury-pollution-arctic-tundra.html.

[33] Winner, C. *How Does Toxic Mercury Get into Fish?* Woods Hole Oceanographic Institution. [updated 2010-10-01; cited 2019-05-12]. Available from: https://www.whoi.edu/oceanus/feature/how-does-toxic-mercury-get-into-fish/.

[34] Holmes, C. D., Jacob, D. J., and Yang, X. Global lifetime of elemental mercury against oxidation by atomic bromine in the free troposphere. *Geophysical Research Letters* 2006;33(20). [Cited 2019 May 6]. Available from: http://doi.wiley.com/10.1029/2006GL027176.

[35] Skov, H., Christensen, J. H., Goodsite, M. E., Heidam, N. Z., Jensen, B., Wåhlin, P., and Geernaert, G. Fate of Elemental Mercury in the Arctic during Atmospheric Mercury Depletion Episodes and the Load of Atmospheric Mercury to the Arctic. *Environmental Science and Technology* 2004;38(8):2373—2382. [cited 2019-03-27]. Available from: https://pubs.acs.org/doi/full/10.1021/es030080h.

[36] Spicer, C. W., Plastridge, R. A., Foster, K. L., Finlayson-Pitts, B. J., Bottenheim, J. W., Grannas, A. M., and Shepson, P. B. Molecular halogens before and during ozone depletion events in the Arctic at polar sunrise: concentrations and sources. *Elsevier* 2002;36:2721-2731. [cited 2019-03-20]. Available from: https://ac.els-cdn.com/S1352231002001255/1-s2.0-S1352231002001255-main.pdf?$_tid = 5f53d7ca - 6cab - 4227 - 91a2 - c04b3e68ff44acdnat = 1553075539$.

[37] Bottenheim, J. W., Fuentes, J. D., Tarasick, D. W., and Anlauf, K. G. Ozone in the Arctic lower troposphere during winter and spring 2000 (ALERT2000). *Atmospheric Environment* 2002;36(15-16):2535-2544). [Cited 2019 May 16]. Available from: https://www.sciencedirect.com/science/article/pii/S1352231002001218.

[38] Nymand Larsen, J., Anisimov, O. A., Constable, A., Hollowed, A. B., Maynard, N., Prestrud, T. D., and Stone, J. M. Polar regions. In: Climate Change 2014: Impacts, Adaptation, and Vulnerability [Internet]. Cambridge: Cambridge University Press; 2014. [Cited 2019 April 24]. Available from: https://www.ipcc.ch/site/assets/uploads/2018/02/WGIIAR5-Chap28$_FINAL.pdf$.

[39] Ferdinand, B. *What Is Biodilution? [Internet].* World Atlas. [updated 2018-07-03; cited 2019-04-01]. Available from: https://www.worldatlas.com/articles/what-is-biodilution.html.

[40] Prestbo, E. Private Communication. [Cited 2019-02-26]. 2019.

[41] Hawkins, L. *Model 2537X Training Course.* [PowerPoint Presentation]. 2015. [Cited 2019-04-17].

[42] *Ocean Data View.* [cited 2019-04-16]. Available from: http://odv.awi.de/.

[43] Schlitzer, R. Ocean Data View User's Guide Version 5.1.7 [Internet]. 2019. [cited 2019-04-16]. Available from: https://odv.awi.de/fileadmin/user$_upload/odv/misc/odvGuide.pdf$.

[44] Cohen, M. *HYSPLIT Cheat Sheet. The National Oceanic and Atmospheric Administration.* [Fact Sheet Received via Private Communication]. 2018. [Cited 2019-04-17].

[45] Cohen, M. Private Communication. [Cited 2019-03-20].

[46] Stein, A. F., Draxler, R. R., Rolph, G. D., Stunder, B. J. B., Cohen, M. D., and Ngan, F. NOAA's HYSPLIT Atmospheric Transport and Dispersion Modeling System. *Bulletin of the American Meteorological Society* 2015;96(12):2059-2077. [Cited 2019 April 16]. Available from: http://journals.ametsoc.org/doi/10.1175/BAMS-D-14-00110.1.

[47] Sjöfartsverket. *Isbrytaren/Forskningsfartyget Oden.* [updated 2019-01-22; cited 2019-03-22]. Available from: http://sjofartsverket.se/oden.

[48] Ziegler, P. and Karlsson, L. Private Communication. [Cited 2019-04-10].

[49] Schmale, J. Private Communication. [Cited 2019-03-04].

[50] National Oceanic and Atmospheric Administration. [cited 2019-02-23]. Available from: ftp://arlftp.arlhq.noaa.gov/pub/archives/gdas1.

[51] Radke, L. F., Friedli, H. R., and Heikes, B. G. Atmospheric mercury over the NE Pacific during spring 2002: Gradients, residence time, upper troposphere lower stratosphere loss, and long-range transport. *Journal of Geophysical Research - Atmospheres* 2007;112(D19). [cited 2019-03-02]. Available from: http://doi.wiley.com/10.1029/2005JD005828.

[52] Cohen, M. *The National Oceanic and Atmospheric Administration.* [Internet/PowerPoint presentation on the Internet]. USA: NOAA Air Resources Laboratory; 2016. [Cited 2019-03-19]. Available from: https://www.arl.noaa.gov/documents/reports/Trajectory_Starting_Heights_ver_01.pdf.

[53] Sommar, J., Andersson, M. E., and Jacobi, H. Circumpolar measurements of speciated mercury, ozone and carbon monoxide in the boundary layer of the Arctic Ocean. *Atmospheric Chemistry and Physics* 2010;10(11):5031-5045. [cited 2019-03-01]. Available from: http://www.atmos-chem-phys.net/10/5031/2010/.

[54] Aspmo, K., Temme, C., Berg, T., Ferrari, C., P.A., G., Fain, X., and Wibetoe, G. Mercury in the Atmosphere, Snow and Melt Water Ponds in the North Atlantic Ocean during Arctic Summer. *Environmental Science and Technology* 2006;40(13):4083-4089. [cited 2019-03-06]. Available from: https://pubs.acs.org/sharingguidelines.

[55] Kamp, J., Skov, H., Jensen, B., and Sorensen, L. L. Fluxes of gaseous elemental mercury (GEM) in the High Arctic during atmospheric mercury depletion events (AMDEs). *Atmospheric Chemistry and Physics;* 2018;18(9):6923-6938. [Cited 2019 Mars 15]. Available from: https://www.atmos-chem-phys.net/18/6923/2018/.

[56] Brooks, S. B., Saiz-Lopez, A., Skov, H., Lindberg, S. E., Plane, J. M. C., and Goodsite, M. E. The mass balance of mercury in the springtime arctic environment. *Geophysical Research Letters;* 2006;33(7). [Cited 2019 Mars 19]. Available from: http://doi.wiley.com/10.1029/2005GL025525.

[57] Pokki, J. *Metals and minerals production 2016-2017.* Geological survey of Finland. [updated 2018-03-27; cited 2019-05-09]. Available from: http://en.gtk.fi/_system/print.html?from/informationservices/mineralproduction/finmipr1117.html.

[58] International Energy Agency. *Statistics - Global energy data at your fingertips.* [Cited 2019 May 9]. Available from: https://www.iea.org/statistics/?country=WORLD&year=2016&category=Energy%20supply&indicator=TPESbySource&mode=chart&dataTable=BALANCES.

[59] Department of Business, Energy and Industrial Strategy. UK Energy Statistics, Q1 2018. [Cited 2019 May 9]. Available from: www.gov.uk/government/statistics/total-energy-section-1-energy-trends.

[60] *Current activities.* Minerals UK - Centre for sustainable mineral development. [cited 2019-05-09]. Available from: https://www.bgs.ac.uk/mineralsUK/exploration/current.html.

[61] DiMento, B. P., Mason, R. P., Brooks, S., and Moore, C. The impact of sea ice on the air-sea exchange of mercury in the Arctic Ocean. *Elsevier* 2018;144:28-38. [cited 2019-05-01]. Available from: http://doi.org/10.1016/j.dsr.2018.12.001.

[62] Cole, A. S., Steffen, A., Pfaffhuber, K. A., Berg, T., Pilote, M., Poissant, L., Tordon, R., and Hung, H. Ten-year trends of atmospheric mercury in the high Arctic compared to Canadian sub-Arctic and mid-latitude sites. *Atmospheric Chemistry and Physics* 2013;13(3):1535-1545. [Cited 2019 May 16]. Available from: https://www.atmos-chem-phys.net/13/1535/2013/.

[63] Zhang, Y., Jacob, D. J., Horowitz, H. M., Chen, L., Amos, H. M., Krabbenhoft, D. P., Slemr, F., Louis, V. L. S., and Sunderland, E. M. Observed decrease in atmospheric mercury explained by global decline in anthropogenic emissions. *National Academy of Sciences* 2016;113(3):526. [Cited 2019 May 16]. Available from: https://www.ncbi.nlm.nih.gov/pmc/articles/PMC4725498/.

[64] Angot, H., A. Dastoor, A., Simone, F., Gårdfeldt, K., Gencarelli, C., and Hedgecock, I. Chemical cycling and deposition of atmospheric mercury in polar regions: review of recent measurements and comparison with models. *Atmospheric Chemistry and Physics* 2016;16:10735-10763. [cited 2019-01-24]. Available from: https://doi.org/10.5194/acp-16-10735-2016.

[65] Brooks, I. *Odens rutt från Svalbard [photography].* 2018 [cited 2019-01-28]. Available from: https://polarforskningsportalen.se/arktis/expeditioner/arctic-ocean-2018/galleri#&gid=1&pid=56.

A Appendix A

A.1 Time-plots of particles and BC concentration

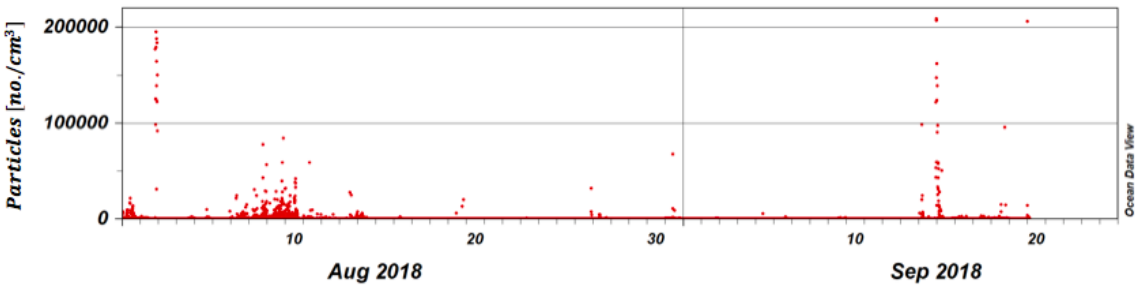

Figure A.1: *Concentration of particles against time, during the expedition Arctic Ocean 2018. The data were obtained from Paul Zieger and Linn Karlsson.*

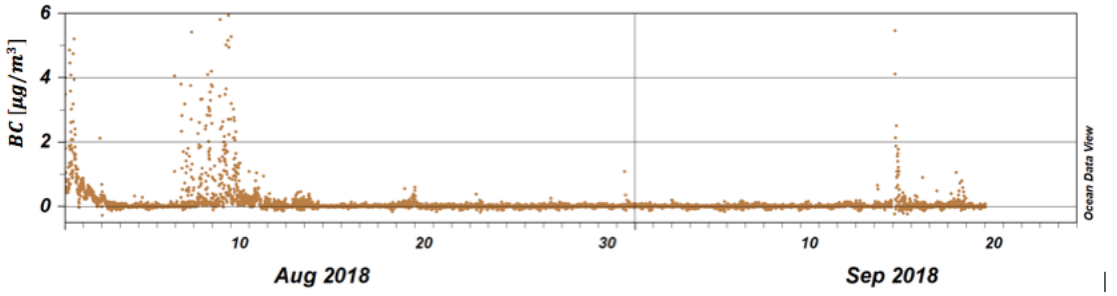

Figure A.2: *Concentration of black carbon against time, during the expedition Arctic Ocean 2018. The data were obtained from Paul Zieger and Linn Karlsson.*

A.2 28-days backward trajectories and cluster analysis during the expedition Arctic Ocean 2018

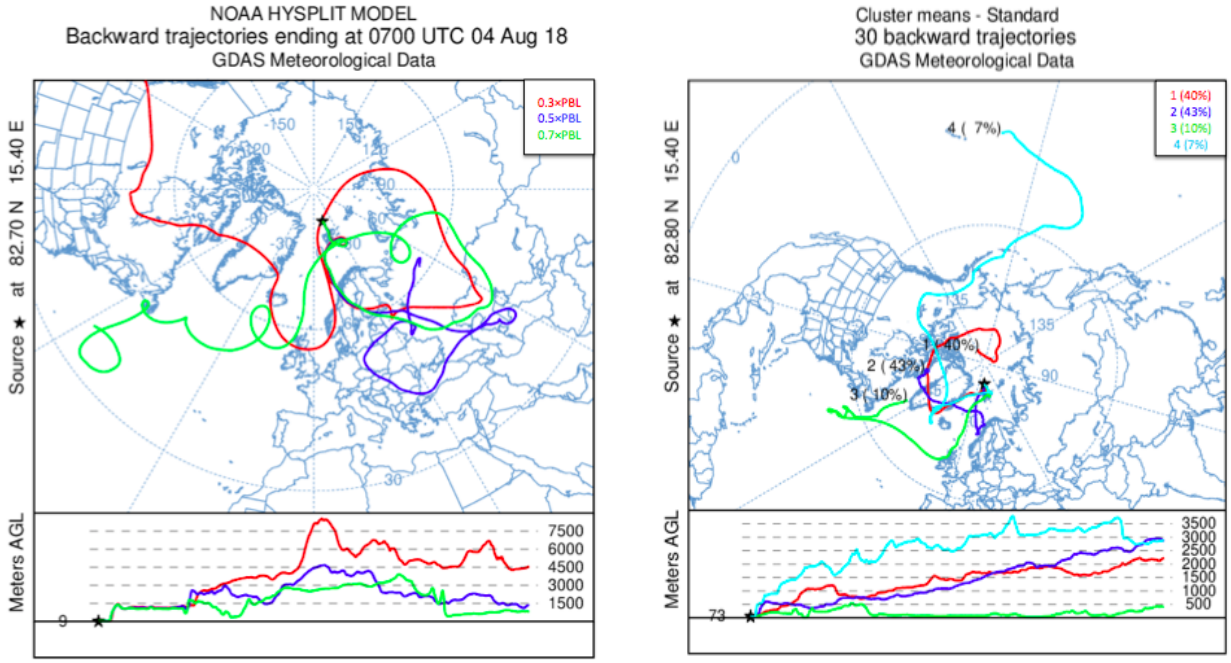

(a) (b)

Figure A.3: *28-day backward trajectories and cluster analysis for the 4th of August. In (a), trajectories for 3 different heights, 0.3, 0.5 and 0.7*PBL, are shown, and in (b) cluster analysis is shown for one height, 0.5*PBL. Meters AGL refers to meters above ground level.*

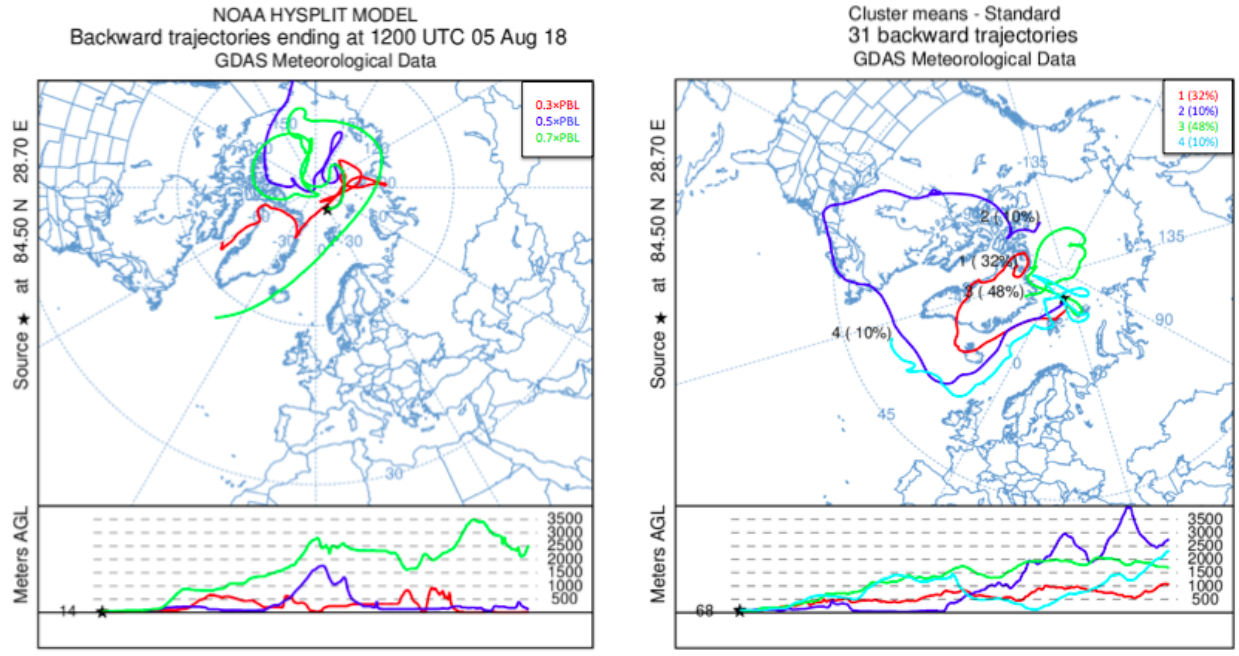

(a) (b)

Figure A.4: *28-day backward trajectories and cluster analysis for the 5th of August. In (a), trajectories for 3 different heights, 0.3, 0.5 and 0.7*PBL, are shown, and in (b) cluster analysis is shown for one height, 0.5*PBL. Meters AGL refers to meters above ground level.*

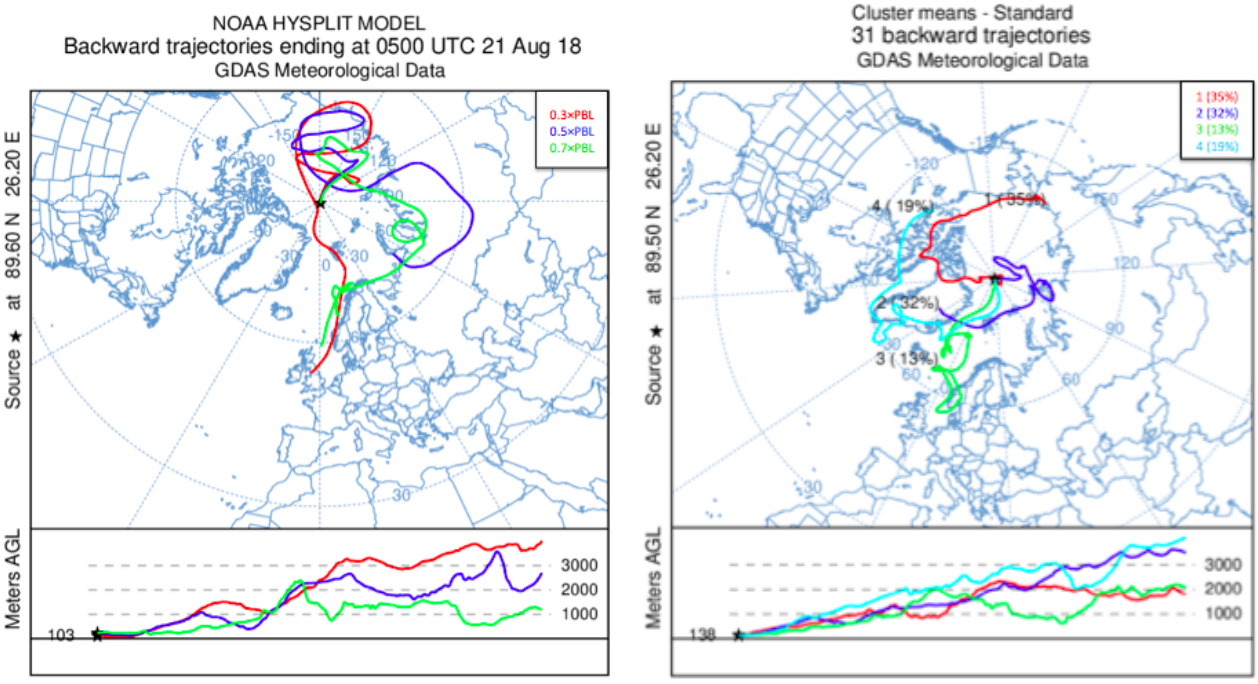

(a) (b)

Figure A.5: *28-day backward trajectories and cluster analysis for the 21st of August. In (a), trajectories for 3 different heights, 0.3, 0.5 and 0.7*PBL, are shown, and in (b) cluster analysis is shown for one height, 0.5*PBL. Meters AGL refers to meters above ground level. The percentages in the cluster analysis does not add up because of round-off error.*

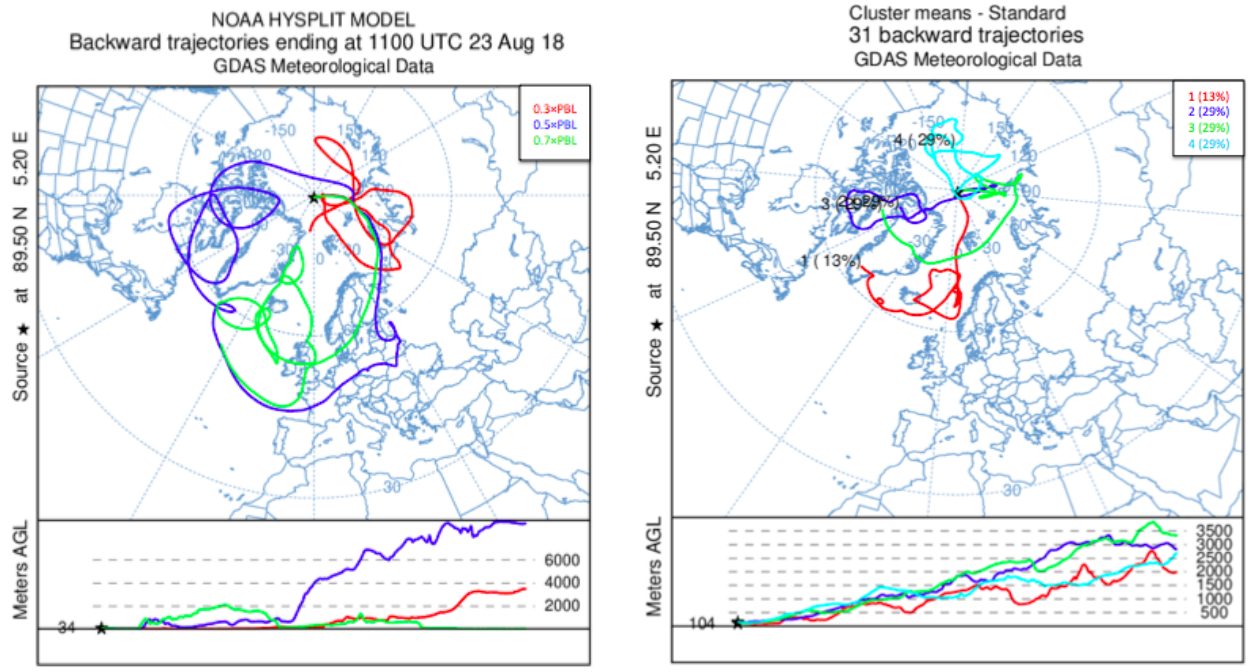

(a) (b)

Figure A.6: *28-day backward trajectories and cluster analysis for the 23ed of August. In (a), trajectories for 3 different heights, 0.3, 0.5 and 0.7*PBL, are shown, and in (b) cluster analysis is shown for one height, 0.5*PBL. Meters AGL refers to meters above ground level.*

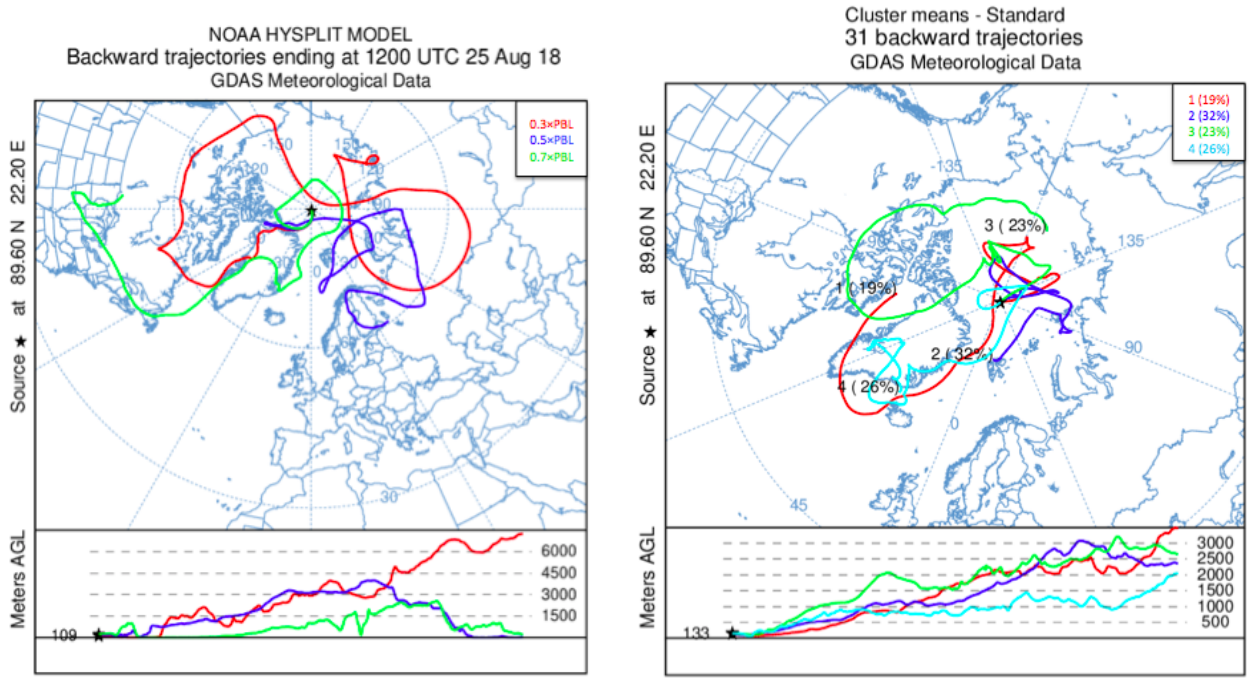

(a) (b)

Figure A.7: *28-day backward trajectories and cluster analysis for the 25th of August. In (a), trajectories for 3 different heights, 0.3, 0.5 and 0.7*PBL, are shown, and in (b) cluster analysis is shown for one height, 0.5*PBL. Meters AGL refers to meters above ground level.*

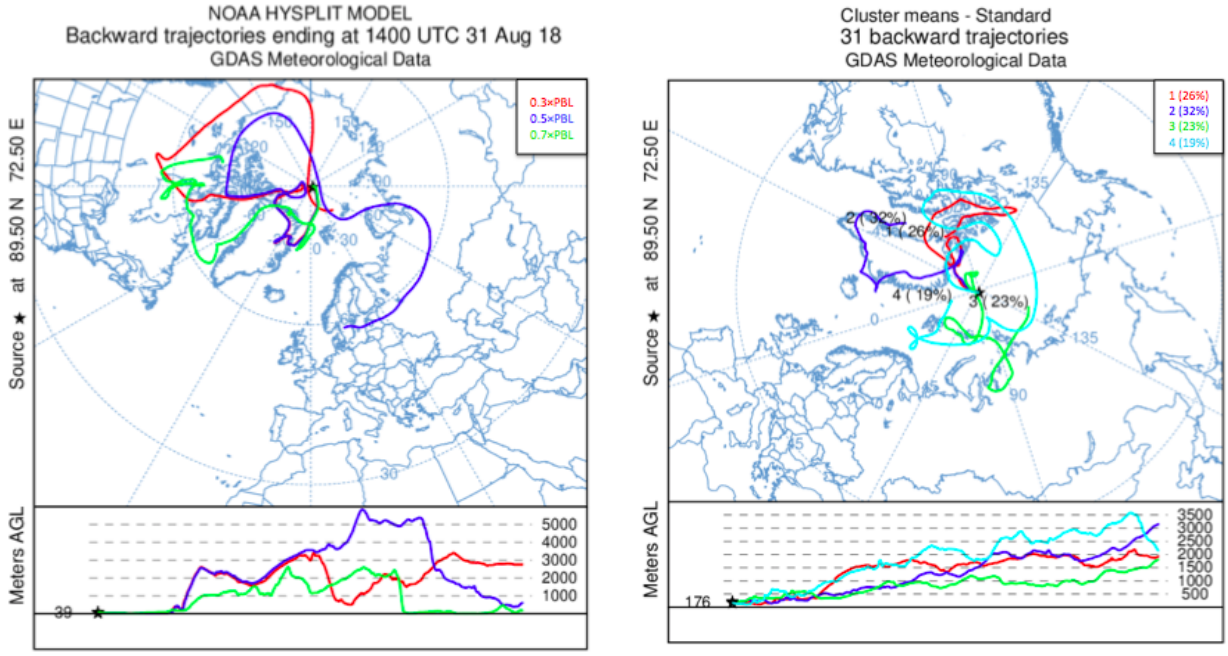

(a) (b)

Figure A.8: *28-day backward trajectories and cluster analysis for the 31st of August. In (a), trajectories for 3 different heights, 0.3, 0.5 and 0.7*PBL, are shown, and in (b) cluster analysis is shown for one height, 0.5*PBL. Meters AGL refers to meters above ground level.*

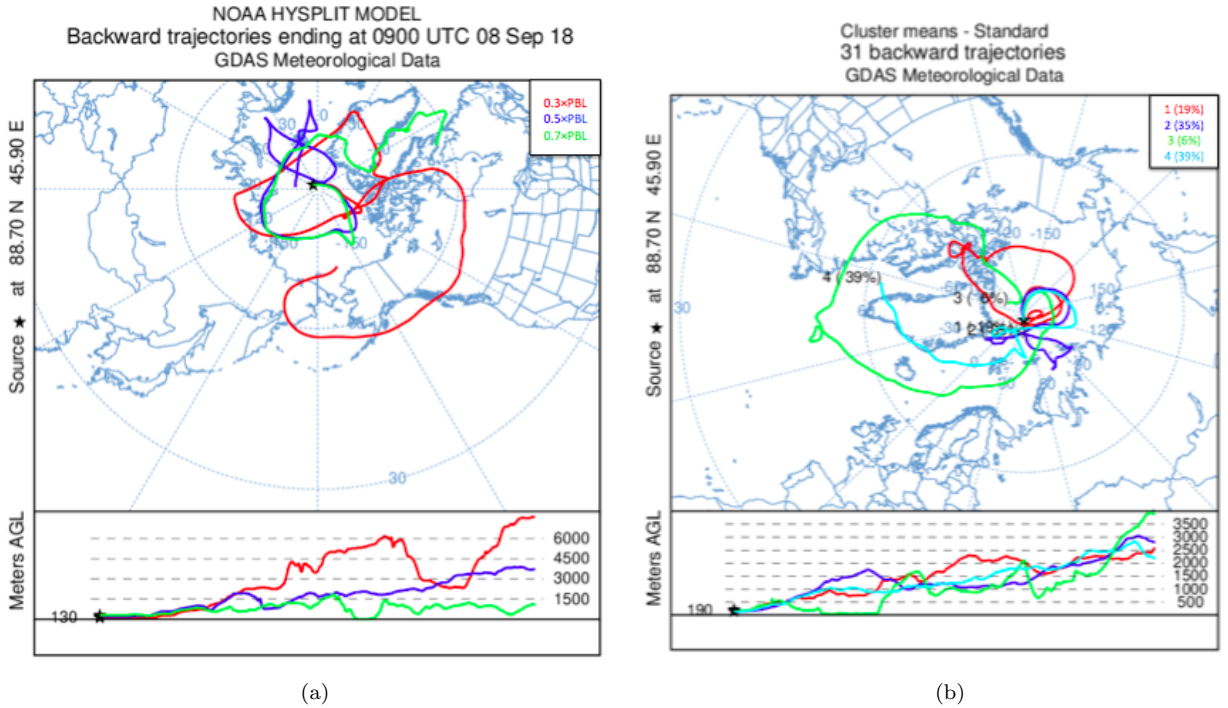

(a) (b)

Figure A.9: *28-day backward trajectories and cluster analysis for the 8th of September. In (a), trajectories for 3 different heights, 0.3, 0.5 and 0.7*PBL, are shown, and in (b) cluster analysis is shown for one height, 0.5*PBL. Meters AGL refers to meters above ground level. The percentages in the cluster analysis does not add up because of round-off error.*

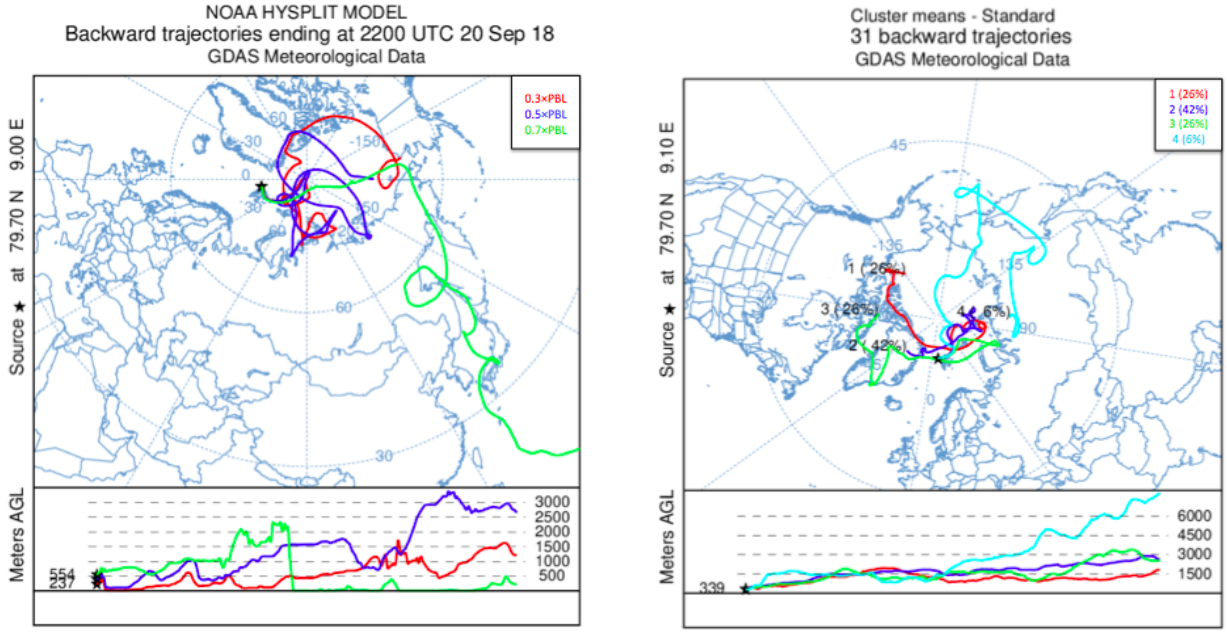

(a) (b)

Figure A.10: *28-day backward trajectories and cluster analysis for the 20th of September. In (a), trajectories for 3 different heights, 0.3, 0.5 and 0.7*PBL, are shown, and in (b) cluster analysis is shown for one height, 0.5*PBL. Meters AGL refers to meters above ground level.*

A.3 28-days backward trajectories and cluster analysis for the cruise Svalbard to Helsingborg

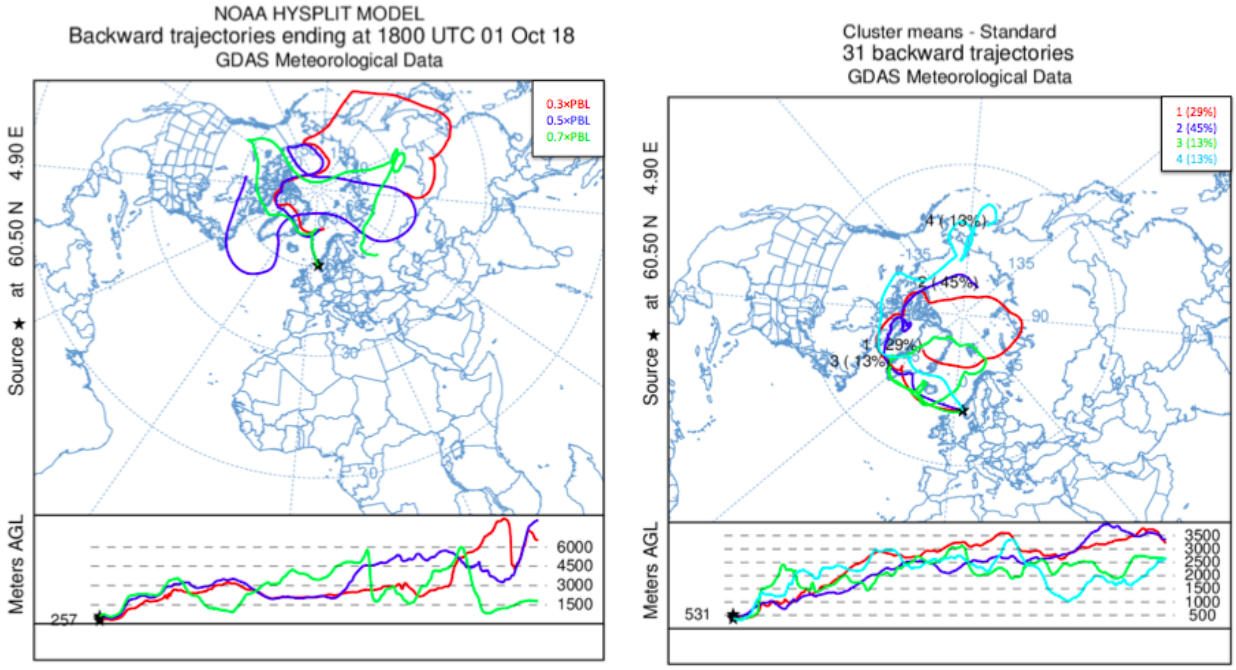

(a) (b)

Figure A.11: *28-day backward trajectories and cluster analysis for the 1th of October. In (a), trajectories for 3 different heights are shown, and in (b) cluster analysis is shown for one height, 0.5*PBL. Meters AGL refers to meters above ground level.*

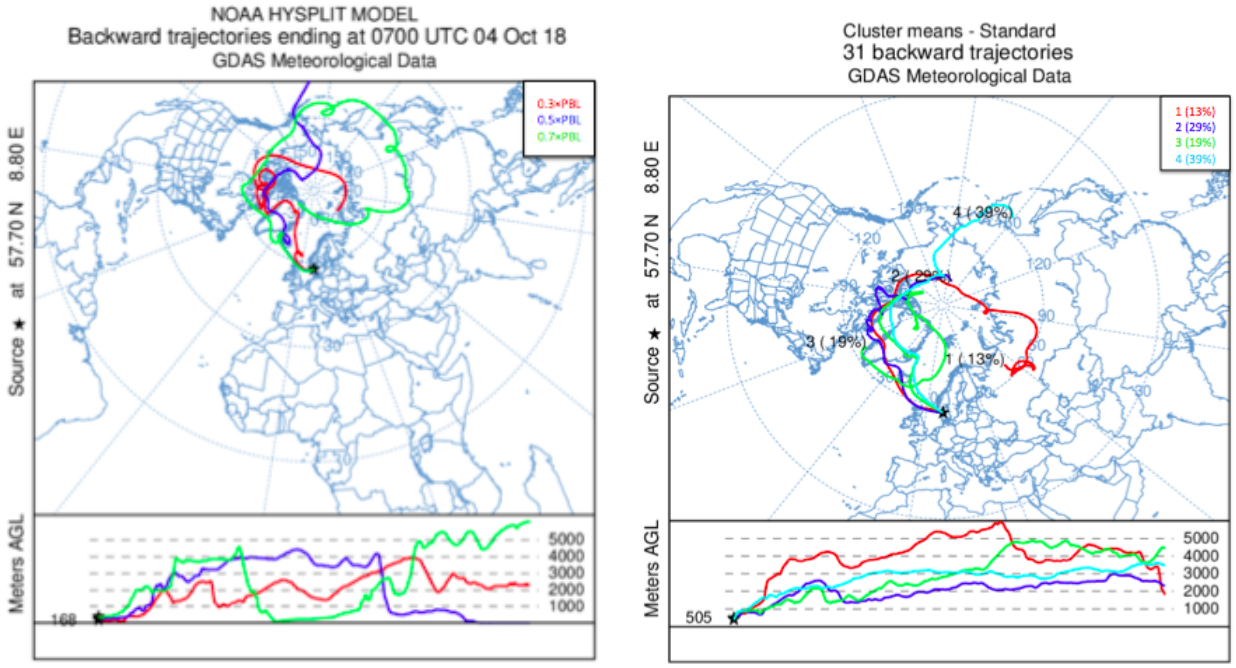

(a) (b)

Figure A.12: *28-day backward trajectories and cluster analysis for the 4th of October. In (a), trajectories for 3 different heights are shown, and in (b) cluster analysis is shown for one height, 0.5*PBL. Meters AGL refers to meters above ground level.*

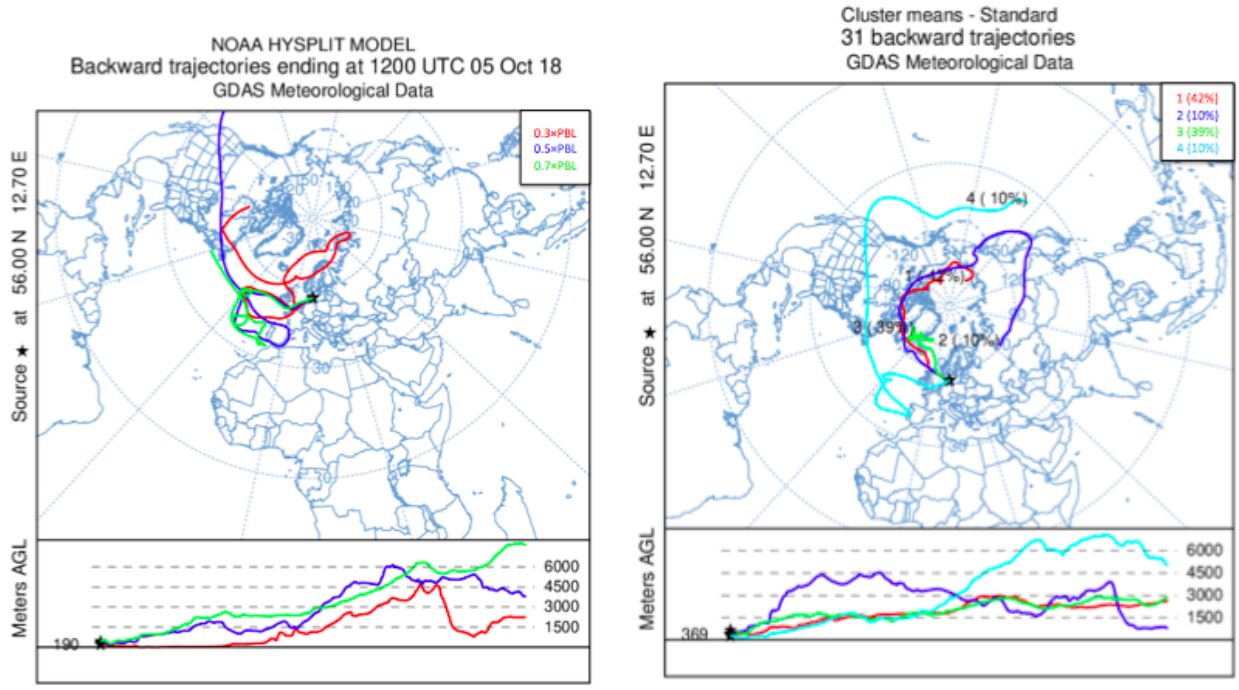

(a) (b)

Figure A.13: *28-day backward trajectories and cluster analysis for the 5th of October. In (a), trajectories for 3 different heights are shown, and in (b) cluster analysis is shown for one height, 0.5*PBL. Meters AGL refers to meters above ground level. The percentages in the cluster analysis does not add up because of round-off error.*

A.4 Ice maps

In figure A.14, the sea ice concentration (%) in the Northern Hemisphere during two time episodes are illustrated. The pictures are obtained from European Organization for the Exploitation of Meteorological Satellites (EUMETSAT) (reference). In figures A.14a and A.14b, the sea ice concentration during the 2nd of August and 20th of September are pictured, respectively. The longitude and latitude grid is 3 °, meaning going from one line to another the degrees changes with 3 in both directions.

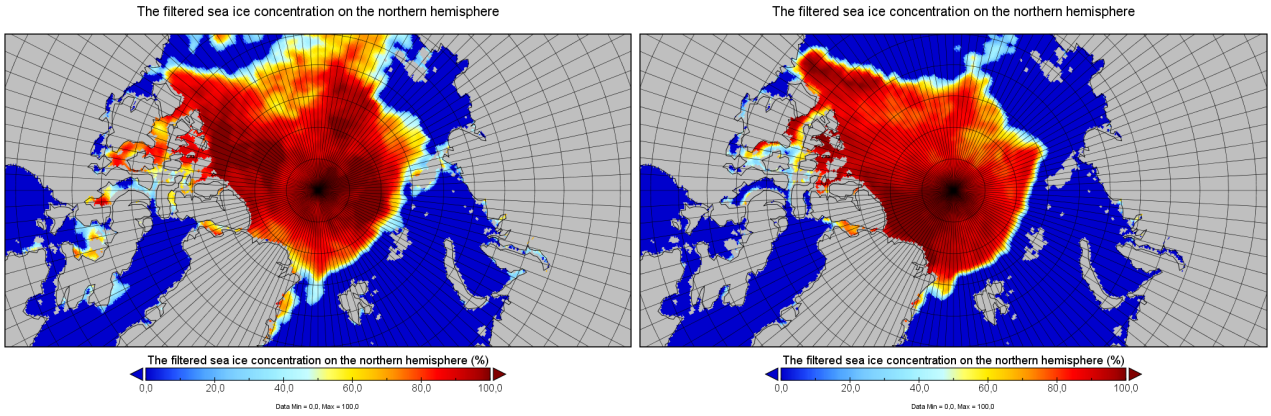

(a) *Sea ice concentration the 2nd of August 2018* (b) *Sea ice concentration the 20th of September 2018*

Figure A.14: *Sea ice concentration in percentage on the northern hemisphere*

A.5 BrO maps

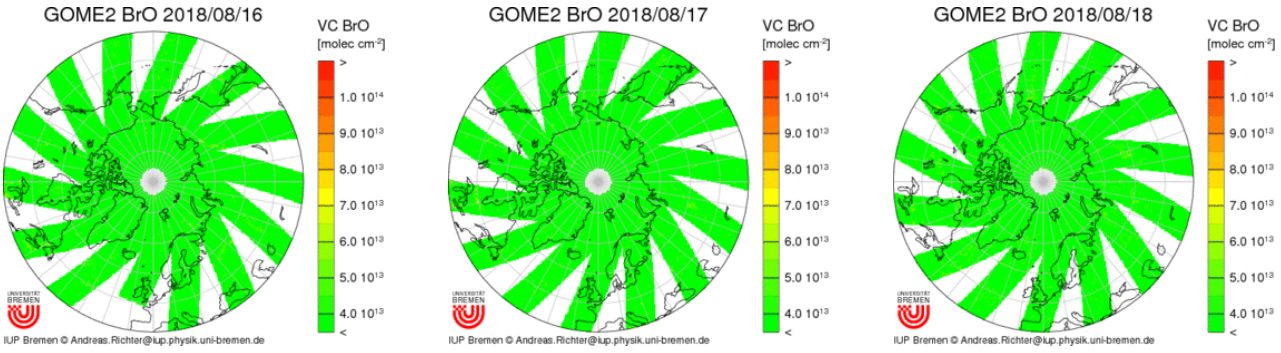

(a) (b) (c)

Figure A.15: *Illustration of the BrO concentration present during the 16th, 17th and 18th of August in the Arctic Environment. The pictures were obtained from the University of Bremen.*

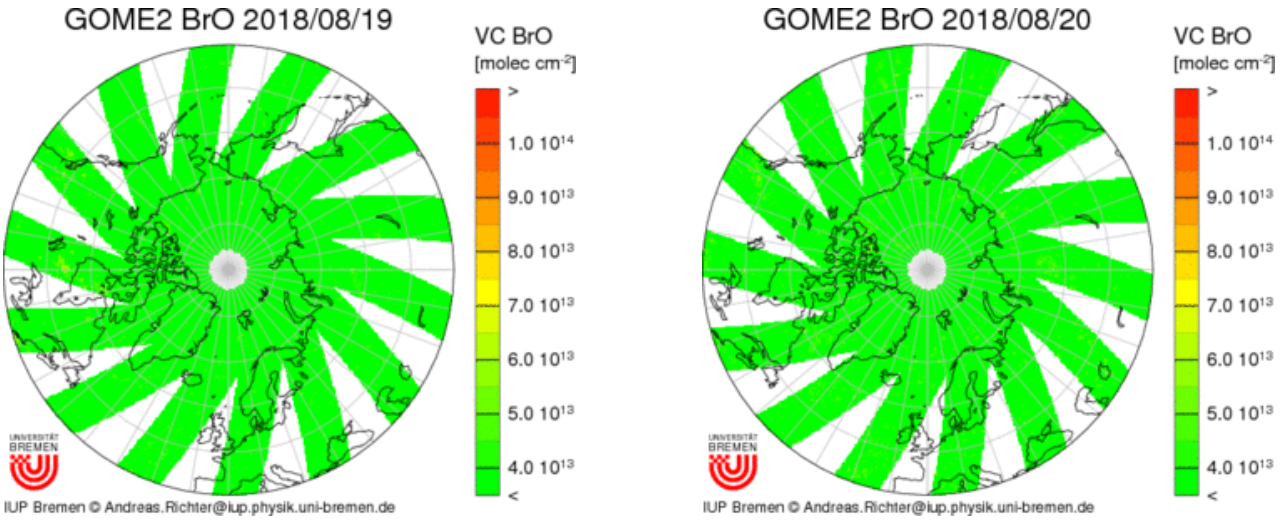

(a) (b)

Figure A.16: *Illustration of the BrO concentration present during the 19th and 20th of August in the Arctic Environment. The pictures were obtained from the University of Bremen.*